Characterisation of Human Bronchial Epithelial Response to Injury and Identification of Potential Resident Progenitor Cells *in vitro*

By
Hala S. Nijmeh, BSc.

Thesis Submitted to the University of Nottingham for the degree of Doctor of Philosophy

February 2009

“Most of the fundamental ideas of science are essentially simple, and may, as a rule, be expressed in a language comprehensible to everyone.”

Albert Einstein

Abstract

As the first line of defence against external stimuli, the airway epithelium undergoes frequent injury during an adult life. This is countered by repair mechanisms that ensure the integrity of the epithelium. It has been established that there are resident stem/progenitor cells localized within specific niches throughout the respiratory tract. Stem/progenitor cells are activated according to the severity of the insult and are thought to be responsible for repairing the airway epithelium. It has been difficult to isolate those stem cells.

In this study, an *in vitro* human bronchial epithelial model was adapted and characterised. In culture, a pseudostratified epithelium was observed, with basal, ciliated, and secretory cells. Mucus production was also seen in this model. A scrape-wound of the model was employed to study the responses of the airway epithelium to injury. It was observed that migration and then proliferation, of CD44 expressing basal cells, are the first events that take place after scrape-wounding. Up-regulation of CD44 was also observed at the edge of the wounds early post-wounding. This suggested a key role for CD44-expressing basal cells in migration and proliferation after wounding, also suggesting this population may contain a progenitor cell population.

Investigation of the secretory profile of the airway epithelium post-wounding revealed an increase in a number of cytokines and growth factors. In particular, IL-6, IL-8, ENA-78, and RANTES were all elevated compared with unwounded cultures.

A side population (SP) was identified in differentiated and undifferentiated human bronchial epithelial cells in at least some cultures accounting for 0.1-1.15% of cells present.

In summary, the epithelium is important in airway wound repair with basal cells appearing to contain the progenitor population in this human bronchial epithelial cell (HBEC) model. Moreover, SP studies suggested the presence of SP in at least some cultures, which might contribute to airway regeneration. The secretory profile of the airway epithelium post-wounding indicates up-regulation of specific cytokines, which may be important in the pathogenesis of lung diseases such as asthma and COPD. This model should prove useful to assess wound repair pathways and may be of use in the future for proof of concept studies on novel therapeutic agents.

Publications

Wadsworth, S., H. Nijmeh, I.P.Hall (2006). "Glucocorticoids Increase Repair Potential in a Novel in vitro Human Airway Epithelial Wounding Model." Journal of Clinical Immunology **26**(4): 376-387.

Sharp, T. V., A. Al-Attar, D. E. Foxler, *et. al.* (2008). "The chromosome 3p21.3-encoded gene, LIMD1, is a critical tumor suppressor involved in human lung cancer development." Proceedings of the National Academy of Sciences **105**(50): 19932-19937.

Abstracts

Nijmeh, H.S., Hall, I.P., Wadsworth, S.J. (2007). "Basal Cells and a Hoecsht Effluxing Side Population of Cells: Role in the Repair of Mucociliated Bronchial Epithelial Cultures." In: American Thoracic Society (ATS). San Francisco, USA, 2007. Published in: American Journal of Respiratory and Critical Care Medicine, Volume 175, Abstracts Issue page A120, April 2007.

Nijmeh, H.S., Hall, I.P. (2008). "An *In Vitro* Model of Epithelial Cells from Human Lung Biopsies: Differentiation Potential and Side Population Studies." In: American Thoracic Society (ATS). Toronto, Canada, 2008. Published in: American Journal of Respiratory and Critical Care Medicine, Volume 177, Abstracts Issue page A720, April 2008.
.

Nijmeh, H.S., Sayers, I., Hall, I.P. (2009). "Secretory Profile of Human Bronchial Epithelial Cell (HBEC) *In Vitro* Post-Injury." In: American Thoracic Society (ATS). San Diego, USA, 2009. Submitted, in press.

Acknowledgements

I cannot begin to adequately thank Mom and Dad, for their support financially, emotionally, and every other aspect possible. Without you guys I would not have been able to start this PhD, nor finish it, so I hope I made you proud.

I am especially indebted to the following: my supervisor, Prof. Ian Hall, for his constant support and invaluable guidance over the course of my PhD, and for always making time for me in his very busy schedule. Dr. Samuel Wadsworth, thank you for everything from starting me off in the lab and then constantly having the patience to help me in whatever I needed. It goes without saying as well, thank you for the support over a few beers here and there. Dr. Ian Sayers, thanks for first helping me throughout the analysis and then reading the whole thesis with no obligation, and teaching me to be very organized in preparing it.

I would like to thank everyone in Therapeutics and Molecular Medicine, from admin, to PhD students. You all contributed to me finishing this, whether it was advice on lab work, or chilling outside work hours (or in between) over a few beers. Special thanks to Dr. Claudia Ceresa and Dr. Mark Roberts for their supply of biopsies, and help in cell culture. Dr. Adrian Robin and Julie Swales for their help using the FACS machine. Dr. Ian Spendlove for his help in Luminex assays.

Of course, “thank yous” should also go to all my friends in Amman and in England. You guys were there for me all the time. Thank you Matt, as well, for helping me through this in every possible way. I got some good advice from you through it all, and you kept up with me ranting on many occasions, and put up with the constant computer failures. Finally, thank you to my 3 great sisters, Raja, and the rest of my family, simply for being there in case I needed anything. I have done it!

Table of Contents

List of Figures

List of Tables

Abbreviations

Δ	Delta
°C	Degree Celsius
A	Absorbance
ABCG2	ATP-binding cassette, sub-family G (WHITE) member 2
ALI	Air liquid interface
AQP3	Aquaporin 3
ASC	Adult stem cells
ASMC	Airway smooth muscle cells
ATP	Adenosine triphosphate
ATS	American Thoracic Society
BADJ	Broncheoalveolar duct junction
BAL	Broncheoalveolar lavage
BASC	Broncheoalveolar stem cells
Bcrp1	Breast cancer resistance protein 1
BEBM	Bronchial epithelial basal media
BEDM	Bronchial epithelial differentiation media
BEGM	Bronchial epithelial growth media
BLAST	Basic Local Alignment Search Tool
BM	Basement membrane
bp	Base pair
BPE	Bovine pituitary extract
BrdU	Bromodeoxyuridine (5-bromo-2-deoxyuridine)
BSA	Bovine serum albumin
$CaCl_2$	Calcium chloride
CC-26	Clara cell 26
CCSP	Clara cell secretory protein
cDNA	Complimentary DNA
CF	Cystic fibrosis
CFTR	Cystic fibrosis transmembrane receptor
CGRP	calcitonin gene-related peptide
CK	Cytokeratin
CO_2	Carbon monoxide

COPD	Chronic obstuctive pulmonary disease
Ct	Threshold cycle
DAPI	4,6-diamidino-2-phenylindole
DEPC	Diethylpyrocarbonate
DMEM	Dulbecco's modified eagle's media
DMSO	Dimethyl Sulfoxide
DNA	Deoxyribonucleic acid
Ebr	Ethedium bromide
ECM	Extracellular matrix
EDTA	Ethylenediaminetetraacetic acid
EGF	Epidermal growth factor
EGFP	Enhanced green fluorescent protein
EGFR	Epidermal growth factor receptor
ELISA	Enzyme linked immunosorbent assay
EMTU	Epithelial-mesenchymal trophic unit
ENA-78	Epithelial derived neutrophil activator 78
ERK1/2	Extracellular-regulated kinase 1 and 2
ESC	Embryonic stem cells
FACS	Fluorescent activated cell sorter
F-actin	Filamentous actin
FCS	Fetal calf serum
FGF	Fibroblast growth factor
FRET	Fluorescence resonance energy transfer
FSC	Forward scatter
GA	Gentamycin and amphotericin-B
GAPDH	Glyceraldehyde-3-phosphate dehydrogenase
G-CSF	Granulocyte colony stimulating factor
GM-CSF	Granulocyte macrophage colony stimulating factor
GPTEC	Guinea pig tracheal epithelial cells
GSI-B_4	Griffonia simplicifolia isolectin B_4
H_2O	Water
HA	Hyaluronic acid
hASM	Human airway smooth muscle
HBEC	Human bronchial epithelial cells
HBSS	Hank's balanced salt solution

hEGF	Human recombinant epidermal growth factor
HEPES	N-2-Hydroxyethylpiperazine-N'-2-ethanesulfonic acid
HGF	Hepatocyte growth factor
HIF-1α	Hypoxia-inducible factor 1 α
HLA	Human leukocyte antigen
Hoechst 33342	bisBenzimide H 33342 trihydrochloride
HPRT	Hypoxanthine ribosyltransferase
hrs	Hours
HSC	Hematopoietic stem cells
hTERT	Human telomerase reverse transcriptase
IF	Immunofluorescence
IFN	Interferon
IL	Interleukin
IP-10	Interferon-inducible protein 10
JNK	c-jun N-terminal kinase
K14	Keratin 14
KGFR	Keratinocyte growth factor receptor
KO	Knockout mouse
LRC	Label retaining cells
LPS	Lypopolysaccharides
MAPK	Mitogen-activated protein kinase
MCP	Monocyte chemoattractant protein
$MgCl_2$	Magnesium chloride
min	Minutes
MIP	Macrophage inflammatory protein
MKP1	MAP Kinase Phosphatase 1
MMP	Metalloproteinases
MSC	Mesenchymal stem cells
MT1-MMP	Membrane type 1 MMP
mRNA	Messenger ribonucleic acid
NaOH	Sodium hydroxide
NEB	neuro-epithelial bodies
NGF	Nerve growth factor
NO	Nitric oxide
PBS	Phosphate buffered saline

PCR	Polymerase chain reaction
PGP	Protein gene product
PI	Propidium Iodide
PNEC	Pulmonary neuroendocrine cells
Q	Quencher
qPCR	quantitative real time PCR
R	reporter
RA	Retanoic acid
RANTES	Regulated on activation, normal T-cell expressed
RNA	Ribonucleic acid
rpm	revolutions per minute
RT-PCR	reverse transcriptase PCR
SCID	Severe combined immuno-deficient
SCID-hu	Humanized SCID
sec	Seconds
SEM	Scanning electron microscopy
SEM	Standard error of mean
SP	Side population
SPC	Surfactant protein C
SSC	Side scatter
STPE	Streptavidin Phycoerythrin
TA	Transient amplifying
TAE	Tris-acetate-EDTA
TF	Tissue factor
TGF	Transforming growth factor
TIMP	Tissue inhibitors of metalloproteinases
UV	Ultraviolet
vCE	variant CCSP-expressing cells
VEGF	Vascular endothelial growth factor
α	Alpha
β	Beta
γ	Gamma

Chapter 1. **Introduction**

1.1 The respiratory system and airway epithelium

The respiratory tract consists of upper and lower airways. The nose, followed by the sinuses, mouth, and the throat, make up the upper airways, while the trachea, bronchi, and lungs and their internal structures are contained in the lower airways. The bronchi branch into smaller bronchi and then the bronchioles, ending with air sacs called the alveoli where gas exchange takes place. These are all contained inside lobes of the lungs (see Figure 1-1). The entire respiratory system is lined with epithelial cells containing a number of different cell types with specific structure and function, and this airway epithelium is the focus of this study.

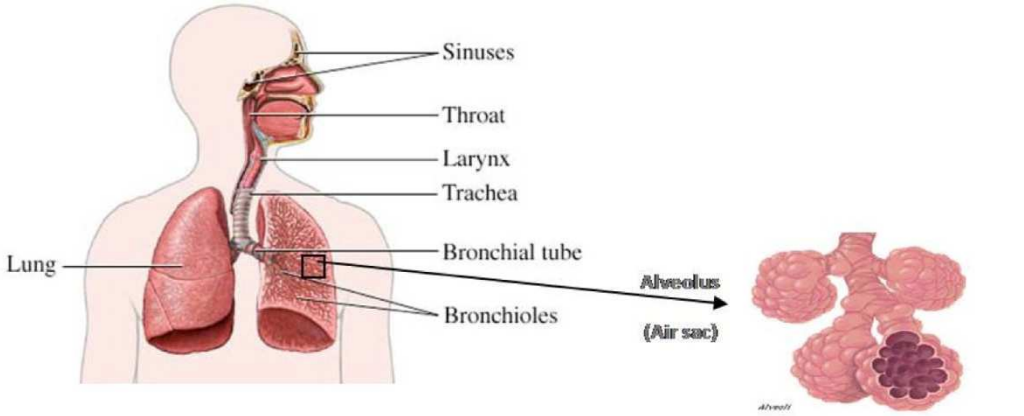

Figure 1-1: The anatomy of the respiratory tract.

This chapter gives an overview of the airway epithelial functions and structure as well as the role and potential applications of stem/progenitor cells, with more detailed information in the chapters following. Chapter 3 describes a human bronchial epithelial cell (HBEC) wound repair model, where the cell types involved in wound repair are investigated. Chapter 4 investigates the secretory profile of the bronchial epithelium post wounding. Finally, chapter 5 investigates the potential progenitor sub-populations present in the bronchial epithelium post-wounding. In this chapter, the general aspects of lung disease, epithelial and stem cell biology, are discussed, and each following results chapter contains details of my relevant research in specific areas.

1.1.1 Anatomy of the airway epithelium

The respiratory tree is lined with several specialized epithelial cell types that fulfil a number of functions to ensure lung homeostasis. There are at least 8 morphologically unique epithelial cell types, which can be classified into three categories: basal, ciliated columnar and non-ciliated secretory columnar cells (Knight and Holgate 2003) depending on the region in which they are found in the respiratory system. Immune and inflammatory cells are also seen to migrate to and remain in the airway epithelium through the basement membrane to aid in epithelial cell function. Figure 1-2 is a cross-section through the airway wall showing the different epithelial cell types present and the underlying mesenchyme, and are discussed further in the following sections.

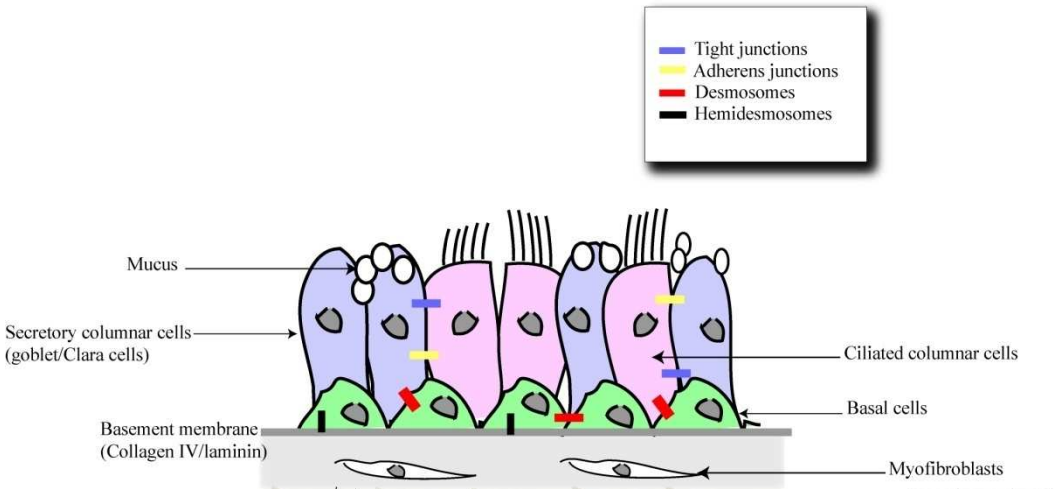

Figure 1-2: Schematic cross-section of the airway wall.
The airway is lined with an epithelium, anchored together with several different junctions. The underlying mesenchyme is also shown consisting of (myo) fibroblasts, smooth muscle cell bundles, blood vessels, and afferent nerve endings positioned deep into the airway. Drawing is not to scale.

As the first site of contact with the outer environment, the airway epithelium is susceptible to damage, during adult life, from various insults including: toxic pollutants and chemicals, bacteria and viruses, and smoke particles. However, the cells in this layer are arranged in an adhesive mechanism to ensure three dimensional structure and normal function is maintained. Basal cells are strongly attached to the basement membrane *via* specialized cell-extracellular matrix (ECM) junctions, termed hemidesmosomes, which confer additional mechanical integrity in the tissue (Green and Jones 1996). Similarly, basal-columnar interactions are ensured *via* the intercellular adhesion molecules that belong to cadherin family (desmosomes), which also create trans-cellular networks throughout the tissue giving it the ability to resist mechanical stress (Green and Jones 1996). As for columnar-columnar interactions, these depend upon belt like tight junctions (zona occludens), responsible for cellular transport regulation, and adherence is also maintained *via* E-cadherin adherens junctions (Roche 1993).

Figure 1-2 shows the adhesive mechanisms between epithelial cells and basement membrane. It is thought that the airway epithelium is pseudostratified in large airways, becoming columnar and cuboidal as it progresses through the airways to the lower airways (Crystal, Randell, Engelhardt *et al.* 2008). .

1.1.1.1 Basal cells

Basal cells are abundant in the conducting airways although their number decreases according to the size of the region (Wang C. Z. 1992), since cell types' present in the different regions of the airways vary, and as mentioned before basal cells are important for attaching other epithelial cells to the BM *via* hemidesmosomes (Figure 1-2). They have pyramidal shape with low cytoplasm to nucleus ratio (Evans MJ 2001). Historically, basal cells were thought to be the origin of stem cells in the airway epithelium, giving rise to ciliated and secretory columnar cells in larger airways (Boers, Ambergen and Thunnissen 1998). In addition to their possible progenitor role and attachment of superficial cells to the basement membrane, basal cells also secret a number of active molecules including cytokines, chemokines, and growth factors.

1.1.1.2 Columnar secretory cells

These cells are present at the apical surface of the epithelial layer. In large airways, mucus-secreting goblet cells are the predominant secretory cells and the main source of airway mucus. They are characterized by membrane-bound electron-lucent acidic mucin granules (Jeffery and Li 1997). Mucus is secreted to trap any toxin and foreign molecules that the airway epithelium comes into contact with and thus these are the epithelial cell type involved in the mucociliary

clearance function of the airway epithelium (section 1.1.2). The number of mucus-secreting cells has been observed to be elevated in chronic inflammatory diseases, such as asthma and COPD, and these cells are thought to contribute to the productive cough associated with these diseases (Lumsden, McLean and Lamb 1984). These mucus goblet cells are seen in larger airways (trachea and bronchi); while Clara cells are found in smaller airways (terminal bronchioles). Mucous and Clara cells also contain electron dense granules (Jeffery and Li 1997). Clara cells are believed to metabolize xenobiotic compounds by the action of p450 mono-oxygenases, and they produce bronchiolar surfactant (Joan Gil 1971) as well as having ion absorbing and secreting properties (Van Scott, Hester and Boucher 1987). Moreover, Clara cell populations are thought to contain the stem or progenitor cells of the small airway epithelium where mucus goblet cells and basal cells are sparse (Hong, Reynolds and Giangreco 2001). Another type of secretory cell is the serous cell, resembling mucus goblet cells with a difference in granule content where it is seen to be electron-dense. These cells have only been found in rodent airways, but two populations of these rare cells have been observed in small airways of human lung (Rogers, Dewar, Corrin *et al.* 1993).

1.1.1.3 Columnar ciliated cells

Ciliated cells account for over 50% of all epithelial cells within the airways (Knight and Holgate 2003). It is thought that these cells arise from secretory or basal cells and were initially thought to be terminally differentiated. However, they were observed to undergo trans-differentiation when mice epithelium was exposed to naphthalene injury (Lawson, Van Winkle, Toskala *et al.* 2002) (Park, Wells, Zorn *et al.* 2006) suggesting their potential involvement in bronchiolar

epithelial repair. Their primary role is the directional transport of mucus, or any foreign object, from the lung to the throat.

1.1.1.4 Alveolar type I cells

Covering 90-95% of the alveolar surface, alveolar type I cells are one of the two types of alveolar epithelial cells (Crapo JD 1982). They are squamous thin cells that are very susceptible to injury. Alveolar type I cells are unable to divide, and form a thin blood-gas barrier where gas exchange occurs. They are important in maintaining the normal cellular composition and function of the alveolar epithelium (Williams 2003). Compared to their type II neighbours, these cells have received little attention due to the lack of specific molecular markers and reproducible methods of isolation *in vitro*. Recently, it has been clear that alveolar type I cells are involved in maintaining homeostasis in the alveolar epithelium (Berthiaume, Voisin and Dagenais 2006).

1.1.1.5 Alveolar type II cells

Type II cells are cuboidal in shape covering 5% of the distal lung. They serve as stem or progenitor cells for type I cells after alveolar injury and play a major role in gas exchange (Sugahara, Tokumine, Teruya *et al.* 2006). One other major function of type II cells is their surfactant protein (SP) production (especially SPC), and phospholipids production which line the alveoli differentially reducing surface tension at different volumes contributing to alveolar stability (Witherden, Vanden Bon, Goldstraw *et al.* 2004; Mason 2006).

1.1.1.6 Pulmonary neuroendocrine cells (PNEC)

In addition to the above main epithelial cell types, pulmonary neuroendocrine cells (PNEC) are present throughout the bronchial tree either clustered in neuro-epithelial bodies (NEB) or as individual cells (Gosney, Sissons and Allibone 1988). These cells are thought to be very rare, increasing in number in chronic bronchitis. PNEC are thought to be involved in the secretion of a number of amines and peptides vital for foetal lung growth and airway function (Reynolds, Giangreco and Power 2000) and may play role in localized epithelial cell regeneration.

1.1.1.7 Other cell types surrounding the airway epithelium

As shown in Figure 1-2, the airway epithelium is underlined by (myo) fibroblasts, smooth muscle cells, blood vessels, afferent nerve endings, and immune cells. Briefly, immune cells including mast cells, lymphocytes, dendritic cells, and macrophages, migrate and reside in the epithelium in response to external insults, and are involved in airway remodelling and inflammation present in a number of lung diseases including asthma and COPD (Rennard, Rickard, Spurzem *et al.* 1992). The bronchial epithelium is rich with intra-epithelial nerves, penetrating the basement membrane where they spread along the epithelial side of the basal lamina extending between epithelial cells and the ending of the airway lumen. This was shown by immunoreactivity for the pan-neuronal marker protein gene product (PGP) 9.5 at the sub-epithelial level (Dirk Adriaensen 1993). Fibroblasts are present beneath the basement membrane where the epithelium rests. They play a role in tissue repair and airway remodelling by secreting growth and attachment factors (Pollak, Huynh and Lefebvre 1992) and chemotactic cytokines

stimulating the bronchial epithelium to migrate following injury and thus contributing to the repair mechanism (Shoji, Rickard, Ertl *et al.* 1989). Surrounding the airway wall are airway smooth muscle cells (ASMC) from the trachea down to the alveolar duct controlling contraction and relaxation of the airway walls. These responses are regulated by intracellular signalling pathways (Hall 2000) achieved *via* a series of homeostatic mechanisms though phospholipase C, adenyl cyclase, and ion channel pathways. ASMC are important in the pathology of airway diseases including asthma, a disease characterised by airway inflammation and increased mass of bronchial SMC (described in more detail in section 1.2.1.1). Hence it has been proposed that ASMC abnormality could cause airway hyperresponsiveness in patients with asthma (Borger, Tamm, Black *et al.* 2006). ASMC seem to have an immune function as well by displaying the ability to cytokines which in turn have a bi-directional effect on ASM constrictor and relaxant responses (Hakonarson, Kim, Whelan *et al.* 2001).

1.1.1.8 Basement membrane (BM)

Basement membrane (BM), also called the basal lamina, is a thin sheet-like membrane (40-120 nm thick), upon which basal epithelial cells adhere, consisting of ECM proteins, anchoring filaments of laminin 5, collagen IV, and proteoglycans including perlecan (Altraja, Laitinen, Virtanen *et al.* 1996). BM consists of a lamina lucida and a lower lamina densa. Below the BM, the reticular basement membrane – a layer of collagenous matrix – is found where fibroblasts are embedded. Collagen, proteoglycans, and glycoproteins, are present in all layers of the BM in differing combinations. BM plays a role in holding all the epithelial cells together and also in epithelial-mesenchymal interactions. In

addition to its structural support role, BM facilitates adhesion and migration of epithelial cells through ECM protein interactions and acts as a reservoir for growth factors. It is also required for the establishment of correct epithelial polarity (Howat, Holmes, Holgate *et al.* 2001). Recently, pores which traverse the whole BM thickness have been observed, wide enough to allow the cells from the lamina propria to cross into the epithelium without matrix degradation (Howat, Holmes, Holgate et al. 2001).

1.1.2 Functions of the airway epithelium

1.1.2.1 Epithelial barrier function and adhesion mechanisms

The primary role of the airway epithelium is protecting the airways, by acting as the continuous first line of contact with the outside environment. It protects the respiratory tract from inhaled toxins such as toxic gases and metals, pathogens such as viruses and bacteria, and inflammatory substances such as dust mite antigen and pollen. This defence is mediated by the adhesion mechanisms discussed above in section 1.1.1 and presented in Figure 1-2.

1.1.2.2 Mucociliary clearance and protective factors secretions

In addition to its role as a protective barrier, the airway epithelium is capable of trapping foreign particles in the mucus that is produced by secretory epithelial cells, which in turn are transported out of the respiratory tract by the coordinated beating of cilia (Bals, Beisswenger, Blouquit *et al.* 2004). Moreover, the airway epithelium serves as a rich source of anti-oxidants and anti-bacterial agents including lactoferrin, lysozyme, and opsonins (Velden and Versnel 1998). It also

produces anti-proteases such as tissue inhibitors of metalloproteinases (Velden and Versnel 1998).

1.1.2.3 Epithelial inflammatory potential

When the airway epithelium is injured, pro-inflammatory responses are activated, producing mediators such as arachidonic acid products, TGF-β, cytokines and chemokines including IL-8 and IL-6. This particular function of the airway epithelium is discussed in more detail in Chapter 4.

1.1.2.4 Epithelial regeneration and role in repair mechanism

Another major function of the airway epithelium, which is under much recent focus, is its regenerative potential and role in wound repair. The prevailing view is that the airway epithelium contains resident stem or progenitor cells which may be activated after injury and are responsible for maintaining a healthy and functional epithelium. These stem cells are thought to reside in specific niches along the respiratory tract and home to the site of injury when necessary (see Figure 1-7). This regenerative function of the epithelium is discussed further in Chapter 3.

1.2 Epithelial damage in respiratory disease

Asthma and chronic obstructive pulmonary disease (COPD) are both inflammatory conditions of the lung involving abnormal structural remodelling which interferes with normal maintenance and function of the lung. Remodelling in this context, refers to an alteration in mass and size of tissues and their

components as a response to injury and/or inflammation. This becomes inappropriate when the alteration takes place repeatedly leading to chronic diseases. Distinctions have been made between asthma and COPD reflected in differences in the severity, origin and nature of the remodelling process, as well as differing patterns in the expansion of inflammatory cells and cytokines (Jeffery 2000). However, similarities are also emerging between these two clinical conditions, especially concerning the presence of damaged epithelium in both, albeit to varying levels. The following sections summarize the remodelling processes in both asthma and COPD, focusing on the epithelial dysfunction occurring in both.

1.2.1 Inflammation and its relationship to airway remodelling

The main histologic features of asthma and COPD are epithelial alterations (discussed in the next sections), sub-mucosal hyperplasia, smooth muscle cell hyperplasia and hypertrophy, sub-epithelial fibrosis, microvascular proliferation, airway wall edema, and inflammatory cell permeation (Bergeron and Boulet 2006). The magnitude of these features, however, differs in each condition, and is discussed in the following sections with emphasis on the epithelial role in both disorders.

1.2.1.1 Epithelial dysfunction in asthma

Asthma can be defined, according to the American Thoracic Society (ATS) in 1963, and revised in 1987 [ATS 1987] as: “a clinical syndrome characterised by increased responsiveness of the tracheobronchial tree to a variety of stimuli. The major symptoms of asthma are paroxysms of dyspnoea, wheezing, and cough,

which may vary from mild and almost undetectable to severe and unremitting (status asthmaticus). The primary physiological manifestation of this hyperresponsiveness is variable airways obstruction. This can take the form of spontaneous fluctuations in the severity of obstruction, substantial improvements in the severity of obstruction following bronchodilators or corticosteroids, or increased obstruction caused by drugs or other stimuli" (M. R. Sears 1993). Irreversible airway obstruction can be a result of airway remodelling, making it difficult to treat asthma patients. According to statistics from Asthma UK, 5.2 million people in the UK are currently under treatment for asthma (last updated on 04 July 2006). One of the hallmarks of asthma is remodelling of virtually every tissue present leading to structural alterations (Figure 1-3).

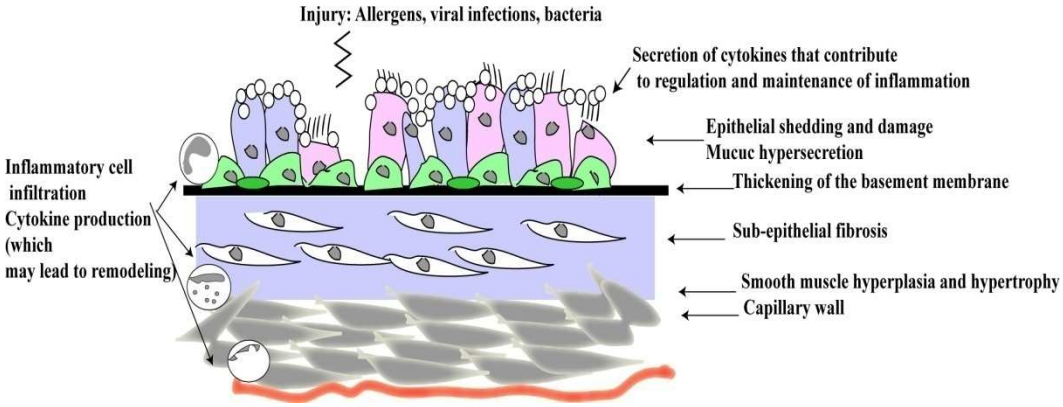

Figure 1-3:Remodeling in asthma.
A schematic section through an airway showing structural alterations seen in asthma

Loss of epithelial integrity is evident in asthmatic patients (**Naylor** 1962). Moreover, sub- epithelial fibrosis, leading to thickening of the basement membrane, has been observed in all severities of asthma (Elias, Zhu and Chupp 1999). An increase in macromolecules, including: collagen I, III, and V, fibronectin, tenascin, lumican, and biglycan (reviewed in (Bergeron and Boulet

2006)) could also perpetuate inflammation by storing inflammatory mediators including cytokines and chemokines (discussed further in Chapter 4). Mucus overproduction is considered one effect of asthma in adult and child airways, related to goblet cell and submucosal gland hyperplasia (Aikawa, Shimura, Sasaki *et al.* 1992). Another observation in asthma is smooth muscle dysfunction and remodelling, with altered expression of cytokines, chemokines and cellular adhesion molecules, leading not only to broncho-constriction, but also sub-mucosal inflammation and airway hyper-responsiveness (Fixman, Stewart and Martin 2007). Wall stiffness and loss of integrity can also be seen in asthma as a result of decrease cartilage volume and increased proteoglycan degradation (Bergeron and Boulet 2006). Finally, change in the microvasculature of the airway wall can result in airway wall edema, with an increased expression of vascular endothelial growth factor (VEGF) (Hoshino, Takahashi and Aoike 2001).

Structural changes could, in part, be explained as a result of airway wall inflammation where inflammatory exudates and infiltrates are present characterised by the presence of eosinophils and their secreted products. Increased numbers of activated mast cells, neutrophils, macrophages, lymphocytes, and spontaneous release of histamine have also been reported in broncheoalveolar lavage (BAL) collected from patients suffering from mild asthma (Foresi, Bertorelli, Pesci *et al.* 1990; Jeffery 1992). A list of some factors seen to be produced in airways of patients suffering from asthma is presented in

Table 1-1.

Recently the concept has emerged that the damaged epithelium incompletely repairs causing chronic wound events, and secretion of secondary mediators; which may play a role in the structural changes and inflammatory responses seen in asthma (reviewed in section 1.2.1.1 below) (Holgate 2007). Another concept involved with asthma biology is that of the epithelial-mesenchymal trophic unit (EMTU), which when activated is thought to activate the characteristic Th2 related inflammation, seen in asthma (Holgate 2008).

EMTU has been recently described in the upper airways of the lung consisting of mesenchymal and epithelial layers separated by the BM. It facilitates attachment of the epithelium to the ECM, binding of growth factors, communication between cells, and separates the airway lumen from the subepithelial layer. It has also been observed that EMTU is essential for epithelial development *via* a number of signalling mechanisms of the underlying mesenchymal cells (Knight, Lane and Stick 2004). The intimate communication of the epithelial and mesenchymal cells has led to believe that during certain lung diseases, epithelial mesenchymal transition (EMT) occurs during tumour invasion or following wound repair (Kalluri and Neilson 2003). This relates to the observation that epithelial cells undergo molecular reprogramming and lose their adherence and polarity, and gain mesenchymal properties (Knight, Lane and Stick 2004).

Table 1-1: List of selected factors produced in asthmatic airways

Factor	Source	Function
Lymphokines		
IL-4	Th2 cells, mast cells	Cofactor for IgE synthesis Increase in Th2 cells and decrease in Th1 cells Eosinophils maturation
IL-5	Th2 cells, mast cells	Eosinophill maturation Increase in Th2 cells Decrease in Apoptosis BHR
Pro-infalmmatory cytokines		
IL-1	Mast cells, macrophages	Growth factor for Th2 cells Neutophil chemoattractant Epithelial activation BHR
IL-6	Mast cells, macrophages, epithelial cells	T cell and B cell growth factor Epithelial activation Increase in IgE synthesis
IL-8	Macrophages, epithelial cells	Neutrophil chemoattractant
IL-9	Th2 cells	Mucus gene expression in epithelial cells
TNF-α	Mast cells, macrophages	Epithelial and macrophage activation
RANTES	Epithelial cells	Eosinophil chemoattractant Lymphocyte activation
GM-CSF	Mast cells, epithelial cells	Leukotriene release Eosinophil apoptosis and activation Proliferation of haematopoeitic cells BHR

IL: interleukin, TNF: tumour necrosis factor, RANTES: Regulated on Activation Normal T Cell Expressed and Secreted, GM-CSF: granulocyte macrophage colony stimulating factor, BHR: bronchial hyperresponsiveness.

1.2.1.2 Epithelial dysfunction in chronic obstructive pulmonary disease (COPD)

Chronic obstructive pulmonary disease (COPD) can be defined, according to the new American Thoracic Society (ATS) guidelines as: “a preventable and treatable disease characterized by airflow limitation that is not fully reversible. The airflow limitation is usually progressive and is associated with an abnormal inflammatory response of the lungs to noxious particles or gases, primarily caused by cigarette smoking. Although COPD affects the lungs, it also produces significant systemic consequences." (ATS 2008). It has been ranked amongst the most common causes of death in western countries (De Boer 2002). There are two conditions thought to be responsible for the level of COPD severity: mucus hypersecretion, also known

as chronic bronchitis, characterised by presence of a chronic cough, and a constant increase in sputum production (Bergeron and Boulet 2006), and emphysema which is characterized by the loss of lung parenchyma and an increase in airspace size (Jeffery 1998). Remodelling of the airway wall, as seen in asthma, also takes place in COPD, with differences in the anatomic sites and the structures affected (Figure 1-4). The single major risk factor of COPD is smoking. Increased numbers of neutrophils (higher than in asthma depending on the severity), macrophages, T-cells, and mast cells have been observed in the airway wall of COPD patients, alveolar compartments and vascular smooth muscle (Di Stefano, Capelli, Lusuardi *et al.* 1998), with the presence of eosinophils being observed when obstruction is partially reversible.

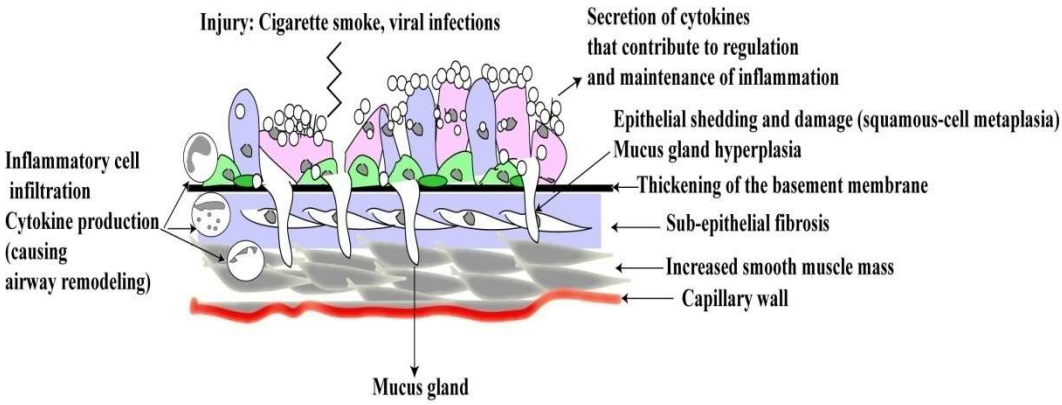

Figure 1-4:Remodeling in COPD.
A schematic section through the airway wall of a patient suffering from COPD showing structural tissue alterations and inflammation.

As mentioned previously migration and activation of inflammatory cells are mostly controlled by cytokines and chemokines (discussed in detail in Chapter 4), secreted by various structural cells (Tetley 2005). Monocyte chemoattractant protein (MCP)-1, macrophage inflammatory protein (MIP)-1α, TNF-α, IFN-γ, IL-1β, IL-6, and IL-8 are all associated with COPD (Chung 2001). GM-CSF and/or

IL-4 but not IL-5 is also found in the inflamed COPD lung. Neutrophils are thought to be the main cause of tissue damage in COPD through the release of mediators including metalloproteinases (MMPs), and neutrophil elastase (Chung 2001). Secretion of epithelial-derived neutrophil activator (ENA)-78, as well as IL-8, from the alveolar macrophages, is enhanced (Morrison, Strieter, Donnelly *et al.* 1998). RANTES mRNA expression has also been shown to be up-regulated in patients with chronic bronchitis (Chung 2001; Chang, Summer and Sun 2005). Thus it can be seen that whilst there are some common features present in asthma and COPD, the cytokine profiles of both are different.

1.3 Stem cells of the airway epithelium

1.3.1 What are stem cells?

Stem cells are the basic cellular unit needed to produce embryos, and regenerate adult tissues. For a cell to be termed a stem cell, it has to possess two fundamental characteristics. First, it must be unspecialized and have the ability to self renew indefinitely. Second, it must be able to differentiate under appropriate conditions into any type of cell in the body. There are three main classes of stem cells identified depending on their multilineage differentiation potential: firstly, totipotent stem cells, that can give rise to an entire embryo and placenta, characterized by unlimited capacity; secondly, pluripotent stem cells, that have a more restricted developmental potential and have the ability to produce most, but not all, tissues of an organ; and finally, multipotent stem cells, which give rise to the three germ layers: endoderm, mesoderm, and ectoderm, as well as organ specific cell lineages, and have a commitment to producing cells with a specific

function (Borok, Li, Liebler *et al.* 2006). As for their developmental potential, stem cells can be divided into two major types: adult and embryonic stem cells, described in the following sections.

1.3.1.1 Embryonic stem cells (ESC)

Embryonic stem cells (ESC) come from the inner cell mass of the 4-5 days old embryo, the blastocyst. ESCs are pluripotent long-term self renewable cells with normal karyotype, and can differentiate into any cell type of the three germ layers. The internal layer, the endoderm, gives rise to the lung, respiratory epithelium, thyroid, liver, and pancreas. The external layer, the ectoderm, gives rise to the skin, neural tissues, adrenal medulla, pituitary glands, and the connective tissues of the head and face, eyes, and ears. Finally, the middle layer, the mesoderm, gives rise to the bone marrow (blood), adrenal cortex, lymphatic tissues, skeletal, smooth, and cardiac muscles, connective tissues including bone and cartilage, urogenital system, and heart and blood vessels. ESC can be induced to differentiate into various cell types in the body under the correct conditions. One such example comes from the work of Coraux *et. al.*, whereby murine ESC were generated into airway epithelial tissue *in vitro* (Coraux, Nawrocki-Raby, Hinnrasky *et al.* 2005). Briefly, they were able to culture murine ESC cells into embryoid bodies, and they observed growth of Clara cells (determined by clara cell secretory protein (CCSP) mRNA expression). They then tested the potential of Clara cells to differentiate further by growing them on porous membranes at an air liquid interface condition, and finally they observed a fully differentiated pseudostratified epithelium (Coraux, Nawrocki-Raby, Hinnrasky et al. 2005).

1.3.1.2 Adult stem cells (ASC)

On the other hand, adult stem cells (ASC) are undifferentiated cells found in any organ of the adult body. They reside in specialized niches in the body, and are observed to be directed to differentiate into the specified type of tissues in response to the necessary environmental signal sent by the niche, contributing to the repair and maintenance of that organ (Borok, Li, Liebler et al. 2006). Figure 1-5 shows the traditional hierarchy of adult renewing tissues such as the epithelium. One good example of a well-defined niche is the small intestinal and colonic crypts (Korinek, Barker, Moerer *et al.* 1998). A new concept has recently been proposed for ASC, termed trans-differentiation or plasticity, which is the ability of a stem cell of one type of tissue to differentiate into another type of cell in another type of tissue, contrary to what was historically believed, that organ specific stem cells were lineage restricted. This was first shown when bone marrow derived cells were shown to be able to differentiate into muscle tissues (Ferrari, Cusella, Angelis *et al.* 1998).

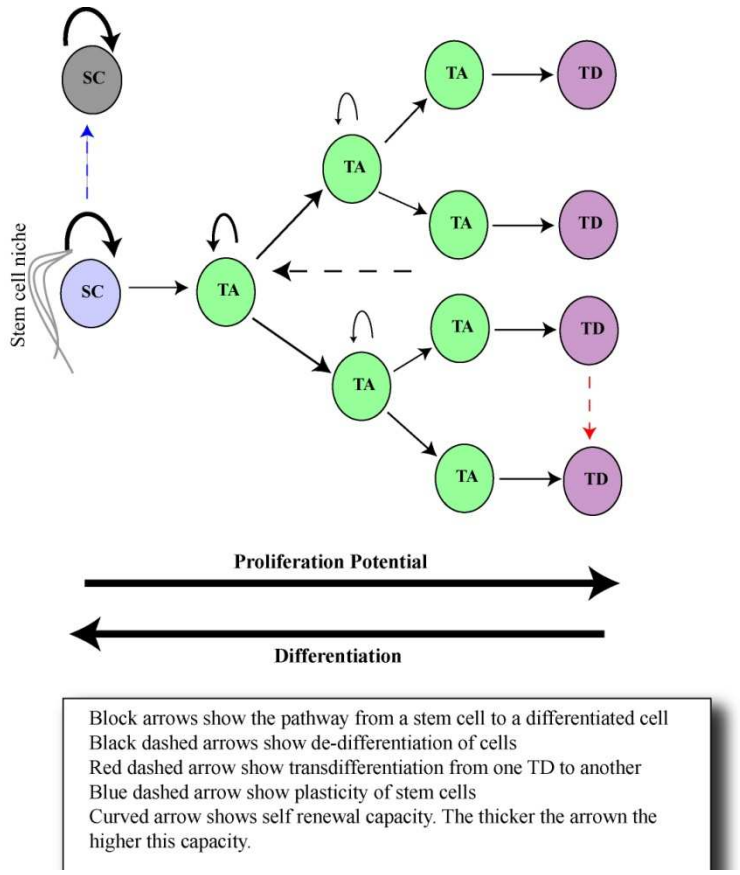

Figure 1-5:Traditional stem cell hierarchy in adult renewing tissues.

1.3.2 Stem cells involved in regeneration of the airway epithelium

As mentioned earlier, the airway epithelium is in permanent contact with the outer environment and thus may be injured frequently. There is a definite repair system seen after injury ensuring the restoration of a normal healthy epithelium. The severity of injury could vary from loss of impermeability to partial shedding or complete denudation of the basement membrane (Puchelle 2000) and involves a series of cellular events that are discussed in more detail in section 3.1.2 and presented in Figure 3-1 . The prevailing view is that stem or progenitor cells play a role in repair mechanism (Neuringer and Randell 2004) either involving resident stem cells in the airway epithelium (discussed in section 1.3.2.1), or circulating

stem cells, the latter being much more controversial and discussed in section 1.3.2.2 below. Figure 1-6 below summarizes the possible roles and types of stem cells involved in lung development and regeneration during adult life.

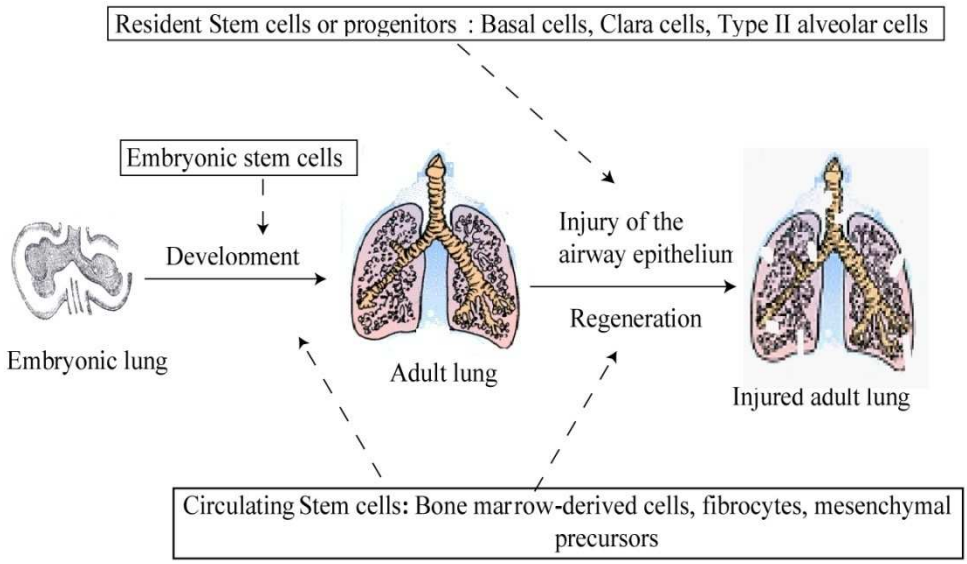

Figure 1-6:Schematic diagram of stem cell involvement in lung development and regeneration.

1.3.2.1 Resident epithelial stem cells

Until recently, due to the complexity of the respiratory tree and the lack of appropriate models, only limited information has been available about differentiation and regulatory mechanisms of resident respiratory stem cells. As discussed above, the lung consists of multiple cell types from different germ layers. Another limitation is the slow turnover and low regeneration potential of the airway epithelium compared to some other organs such as the liver. However, when the airway epithelium is injured, proliferation and regeneration rates tend to dramatically increase. A general idea was that each lung subdivision contains its own supply of stem cells, thus local repair of the trachea and bronchus is thought

to occur by mucus and secretory cells (Borthwick, Shahbazian and Krantz 2001), whereas Clara cells are responsible for the bronchiolar regeneration (Reynolds, Giangreco and Power 2000). Alveolar type II cells are thought to regenerate the alveolus (Mason 2006). Figure 1-7 below shows the cell types suspected to be the stem cells at different areas in the respiratory tree.

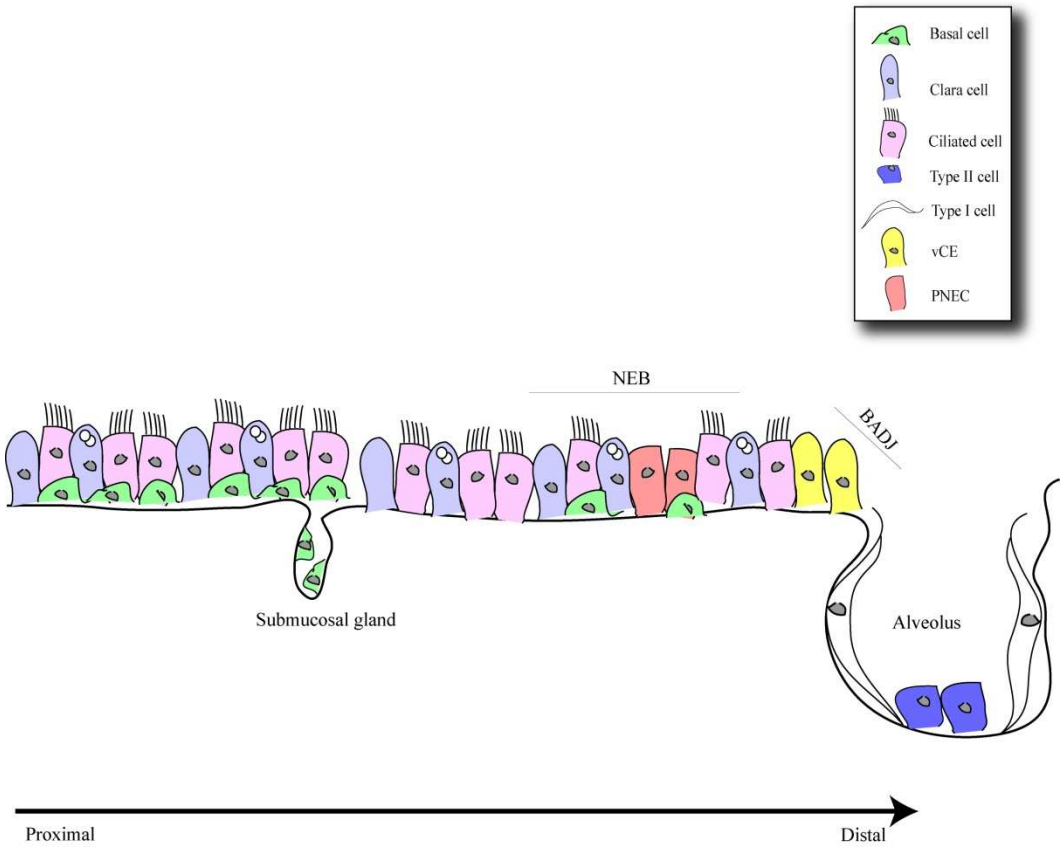

Figure 1-7:Resident epithelial stem cells and their niches.
Basal cells are suspected to contain the stem cells of the trachea and proximal airways (green cells) with the major stem cell compartment possibly residing in sub-mucosal glands. Further down the respiratory tree, where basal cells are scarce, Clara cells (grey cells) are suspected to acquire stemness possible residing in neuroepithelial bodies (NEB). Some investigators have proposed that variant Clara cell secretory protein (CCSP)-expressing (vCE) cells reside in broncheoalveolar duct junctions (BADJ) and co-express CCSP and surfactant protein C (SPC) (yellow cells) and that these cells are the main stem cell compartment at this end. Moving down to the alveolus, type II cells are thought to contain the stem cell population (blue cells).

Two origins have been reported for the tracheal epithelial stem cells: some suggested that it is the tracheal gland ducts (Duan, Sehgal and Yao 1998), while others think it is tracheal lining epithelial cells (Boers, Ambergen and Thunnissen

1998) mostly located at or near the basement membrane. The latter are thought to be more the transient amplifying (TA) cells rather than the more primitive stem cells. Clara cells, however, are said to be TA cells if not the stem cells of the bronchioles (Hong, Reynolds and Giangreco 2001). Most recent research has shown that a subset of Clara cells achieved the criteria of adult, niche-specific stem cells. This subset was described as expressing the Clara cell secretory protein (CCSP) mentioned earlier (Hong, Reynolds and Giangreco 2001). Hong *et. al.* and other studies have demonstrated that there was a pollutant resistant subpopulation of Clara cells (variant CCSP-expressing cells or vCE cells) and calcitonin gene-related peptide (CGRP)-expressing PNEC in the neuroepithelial bodies (NEB) microenvironment which serve as a location of pluripotent regenerative cells in naphthalene treated mice (Hong, Reynolds and Giangreco 2001) (Reynolds, Giangreco and Power 2000).However, PNEC could not repopulate the epithelium after CCSP expressing population depletion, concluding that the CCSP positive Clara cells must contain the stem cell population rather than PNEC. Finally, alveolar stem cells are thought to be contained within the type II cell population: these have been reported to express CD44 that mediates matrix adhesion in the lung. This feature is shared with basal cells of the tracheal and bronchial epithelium (Wadsworth, Nijmeh and Hall 2006). In addition, the vCE cell population residing within NEB , have also been shown to reside at the broncheoalveolar duct junctions (BADJ) in mice airways, and are able to repair the epithelium after naphthalene injury (Giangreco, Reynolds and Stripp 2002). These have been termed broncheoalveolar stem cells (BASC) and were observed to be expressing both CCSP and surfactant protein C (SPC).

One strategy to identify organ stem cells is based upon the capacity of hematopoietic stem cells (HSC) to efflux Hoechst dye, *via* ATP-binding cassette transporter (ABCG2), also called breast cancer resistance protein (Bcrp1) (Goodell, Brose, Paradis *et al.* 1996). These cells were termed the side population (SP) cells because they could be isolated by dual-wavelength flow cytometry where Hoechst staining was absent. This is discussed in more detail in Chapter 5. In the adult lung, SP was seen to comprise 0.03-0.07% of total mouse lung cell suspensions (Summer, Kotton, Sun *et al.* 2003).

Recently, mouse lung airway digests were found to contain SP cells, with a phenotype of vCE of NEB (Giangreco, Shen and Reynolds 2004). Although the role of SP cells in tissue regeneration is the subject of much current research, there are no conclusive functional studies thus far to show that these cells are lung stem cells.

1.3.2.2 Circulating stem cells

A series of studies have argued against the original hypothesis which states that adult tissues are thought to be renewed only by progenitor cells originating from the same germ layer. Circulating cells derived from bone marrow and from the mesoderm, can directly regenerate a number of non-hematopoietic tissues, such as neurons which come from the ectoderm (Eglitis and Mezey 1997), and hepatocytes which come from the endoderm (Petersen, Bowen, Patrene *et al.* 1999). When the lungs of chimeric mice were analyzed after a single bone-marrow-derived HSC was transplanted there, 20% of type II alveolar epithelial cells and 4% of the airway epithelial cells were derived from that donor marrow cell (Krause, Theise, Collector *et al.* 2001). However, because transplantation

experiments are inevitably to some extent artificial, investigators have employed a parabiotic mouse model, where two mice were joined together by stitching their flanks so that their circulation is gradually merged (Wagers, Sherwood, Christensen *et al.* 2002). They found that trans-differentiation of circulating HSC and their progeny is an extremely rare occurrence, if it exists at all. Moreover, one study showed no evidence of epithelial reconstitution of tracheal xenografts when HSC purified from mouse bone marrow by the Hoechst efflux method was delivered. However, these cells may require factors *in vivo* to enable them to acquire the characteristics of this tissue (Macpherson, Keir, Webb *et al.* 2005). There is thus considerable controversy regarding whether cells from bone marrow contribute to regeneration of the lung epithelium. The predominant view is that local cells within the lung are responsible for repairing the lung epithelium, while bone-marrow derived cells contribute very few cells directly to the airway or alveolar epithelium structure (Kotton and Fine 2008).

Despite this controversy, it is agreed that bone-marrow-derived cells may have some role during lung repair. One proposal for this role was immune modulation of mesenchymal stem cells (MSC), whereby Aggarwal *et. al.*examined culture-expanded hMSC and different immune cells. They observed that hMSC have the ability to control or inhibit inflammatory responses and activate the anti-inflammatory pathways (Aggarwal and Pittenger 2005), which in theory could aid in the reduction of transplantation complications such as rejection, as one example. In addition, functional rescue has also been seen after infusion of bone marrow cells into the right and left main bronchi of rabbit lungs suffering from emphysema, by reducing inflammation and apoptosis, as well as enhancing the proliferation of alveolar cells (Yuhgetsu, Ohno, Funaguchi *et al.* 2006). The

mechanism of this protective effect is not fully known but was suggested to involve paracrine effects (Shigemura, Okumura, Mizuno *et al.* 2006). Moreover, following HSC transplantation, studies on humans have shown proof of chimerism in the lung, where 2% and 6% of Y-chromosome-positive epithelial cells were seen in female recipient lung tissue sections, suggesting a possibility that circulating stem cells can differentiate into lung epithelial cells (Mattsson, Jansson, Wernerson *et al.* 2004). One other example came from work of Spencer *et. al.* to asses long term lung engraftment following sex-mismatched lung transplantation (Spencer, Rampling, Aurora *et al.* 2005). In one study, following female lung transplantation into male donors, transbronchioal biopsy specimens were examined from two boys with cystic fibrosis (CF). Median of 8.2% of all lung cell nuclei were positive for Y-chromosome, with 1.4% of those being inflammatory cells. 3.6% Y-chromosome-positive epithelial cells were located in the alveolar region and 1.4% in the bronchial region (Spencer, Rampling, Aurora et al. 2005), detected as early as 3 weeks following engraftment and were seen to be constant till up to 37 months. This suggested long term chimerism in lung epithelium.

1.4 Potential applications of stem cells in lung diseases

Intense research over the last decade has focused on studying development, morphological and physiological mechanisms of organ formation, maintenance, regeneration, and repair after injury. A recent focus has also been on the investigation of stem cells and their role in the above processes. But, how could these stem cells be of potential value in relation to therapeutic opportunities?

The first possible application of stem cells could be providing novel methods to assess wound repair pathways, which are central to the functions of the airways. As described previously, loss of normal airway integrity can be seen in a number of airway diseases including asthma and COPD. Many attempts have been carried out to try and develop appropriate models of the airway wall *in vitro* and *in vivo*, using human and animal tissues (discussed in detail in chapter 3). Stem cells are characterised by self-renewal and undifferentiated capabilities, and thus if airway stem cell populations can be identified, they could be induced *in vitro* to differentiate into physiologically relevant (non-transformed) models of airway tissue which would be valuable *in vitro* models.. These models could lead to better understanding of the cellular and molecular events of cellular repair and wound healing processes. More in-depth knowledge is needed about the specific cell types involved in wound repair, and the inflammatory processes and airway remodelling, such as those seen in asthma and COPD. In addition, these models might prove useful in the investigation of resident lung stem cells and their role in tissue regeneration. Thus far, a lack of specific stem cell markers has been an obstacle in respiratory research, due to the fact that it is thought that different stem cell populations are involved in regenerative responses in different regions of the respiratory tract.

The second possible application of stem cells, following the development of such models, could be to assess the toxicity of environmental and therapeutic agents. These models can be exposed to various toxins, such as those thought to be responsible for the development of lung diseases (e.g. cigarette smoke). This would potentially allow *in vitro* assessment of the mechanisms underlying the injury and repair responses to such agents in physiologically relevant models.

These injury models (discussed in chapter 3) could also be used to assess efficacy of existing and novel therapeutics agents to study their potential use in the management of airway diseases.

The third possible use of stem cells could be to manipulate them directly as a novel therapeutic approach. They could either involve inhibition of cell proliferation, or the use of stem cell for tissue regeneration. As an example: one hallmark of COPD is mucus over-production, possibly due to proliferation of mucin-producing epithelial cells. If mucin-producing epithelial cell differentiation was clearly understood, inhibition of proliferation could potentially be used in order to manage this feature of COPD. However, this might prove difficult as suppressing differentiation of these cells might lead to suppression of differentiation of other epithelial cell types needed for re-epithelisation. Another potential approach would be the use of BASC (as previously identified by Kim *et. al.*, located in the BADJ) (Kim 2007) to try and aid repair of the severely destroyed alveoli seen in emphysema after prolonged periods of inflammation and tissue damage. If BASC could be stimulated to migrate over the BM to replace the damaged cells and efficiently repair the alveolar epithelium, at least potentially lung regeneration might be observable. This could prove difficult however, if the injury was severe to an extent where the underlying cell scaffolds was damaged.

A fourth potential application of stem cells is that they could be tissue-engineered into complex tissues in order to reconstitute the lung. Tissue-engineering refers to the formation of a manmade functional organ by autologous cells introduced into biologic carrier structures, referred to as matrices. This possibility may seem far from reality since the respiratory system is very complex involving multiple cell

types and tissues interacting with the surrounding vasculature, in order to ensure a functioning gas exchange unit. However, expansion of stem cell pools *in vivo* or *ex vivo*, and differentiation into functional cell lineages capable of regenerating damaged tissues, have been described previously. Certain adult stem cells including the bone marrow (BM)-derived stem cells (described in section 1.3.2.2), have been observed to circulate under appropriate conditions in the blood and home to distant tissues promoting repair of sites of damage, including the liver, heart, lung, skin, eyes, and gastrointestinal tract (reviewed in (Mimeault, Hauke and Batra 2007)). A recent development was from a group of German researchers, where patients with myocardial infraction were injected with autologous bone marrow into their coronary arteries (Strauer, Brehm, Zeus *et al.* 2001). Although improvement in the myocardial function was noted, the study did not carry out morphological analysis, and thus it was not conclusive that the bone marrow had trans-differentiated into cardiomyocytes. More relevantly to this thesis, recently, a cellular, tissue-engineered airway functionally normal and free from host rejection, was produced and transplanted back into a 30-year old female suffering from end-stage bronchomalacia after severe tuberculosis infection (Macchiarini P. 2008). In bronchomalacia, a deficiency in tracheal or bronchial cartilaginous wall is observed, which may lead to obstructive emphysema. A trachea obtained from a deceased subject was denuded of all epithelial cells and human leukocyte antigen (HLA), and seeded with the recipient's epithelial cells and chondrogenic mesenchymal stem cells. This was introduced into a bioreactive device where the airway construct was rotated in culture medium tailored to suite the requirements of both medium and gas phases. The graft was then shaped according to the patients requirements and after dissecting the old damaged trachea, was

introduced to the patient. The patient was then monitored for 4 months, and a functional airway was observed with normal appearance. If it became possible to expand alveolar tissues *ex vivo*, as well as appropriate surrounding vasculature, these could also, in theory, be transplanted into the lungs, as a novel approach in the management of emphysema and COPD. However, gas exchange units are very complex, and would be much more difficult to engraft than the trachea due to their location in the lungs.

Fifthly, recent research has identified potential cancer stem cells. These cells were observed to have a defect in their self renewal regulation. This concept provides potential tools that could be used in cancer therapy. This could be facilitated by identifying the cell types that produce tumours, and whether or not those actually originate from stem cell pools. For example, in a report by Kannan *et. al.*, the type II cell marker SPC and the proliferation marker Ki-67 were seen in human adenocarcinoma cells and squamour cell carcinoma (Ten Have-Opbroek, Benfield, van Krieken *et al.* 1997). Stem cells could potentially be useful as a therapeutic modality in cancer if carrying and delivering specific genes and drugs to the malignancies were achievable. The alternative approach would be to attempt and inhibit amplification of stem cell derived populations in tumours by cell-based therapeutic strategies.

Finally, the ultimate aim is not only to identify stem cells, but to understand where they go and how they recreate the alveolar septal architecture to be able to understand how restoration of a functional three dimensional relationship amongst the alveoli, airways and surrounding vessels, occurs, since they are all vital for an appropriate gas exchange unit. In conclusion, stem cell biology holds promise in regenerative medicine, cell-based therapies, and tissue engineering. A

greater in-depth knowledge of the respiratory system, tissue damage, lung disease environment, and stem cell niches and fate, needs to be available in order to investigate all the potential therapeutic applications and manipulate them successfully in the clinic.

Chapter 2. **Materials and Methods**

To investigate the airway epithelial wound repair mechanism and the potential role of stem or progenitor cells in repair, an *in vitro* model of primary human differentiated bronchial epithelial cells (HBEC) was used. The method in which cells are grown at an air liquid interface (ALI), which mimics the airway epithelium *in vivo*, was adapted from Danahay *et. al.* (Danahay, Atherton, Jones *et al.* 2002). The following sections describe the general techniques used, further specific details can be found within the relevant chapters. Suppliers of chemicals and media are listed in Appendix A.

2.1 Cell culture

2.1.1 Human bronchial epithelial cells (HBEC)

2.1.1.1 Recovery of preserved cells

Primary human bronchial epithelial cells (HBEC) were obtained commercially from Lonza, Clonetics™ frozen in cryovials and these were assigned as passage (p) 0 in this study. Frozen cells were introduced back into culture by rapidly thawing the cryovials at 37º C. Once completely thawed the cell suspension was diluted in the appropriate volume of media and mixed gently. The cells were seeded into T-25 flasks (5 ml per flask unless stated otherwise), when purchased (p0), in specialized bronchial epithelial growth medium (BEGM, section 2.1.1.5) and media was changed after 24 hrs to remove Dimethyl sulphoxide (DMSO)

which was used to cryopreserve the cells (section 2.1.1.4). Two HBEC donors have been used in this study and the details of the number of subjects for each experiment it mentioned in the specific section. Table 2-1 describes the details of the donors.

Table 2-1: HBEC donor information

Donor	Age	Sex	Race
4F0507 (Donor 1)	51	Female	Asian/Oriental
5F0750 (Donor 2)	8	Female	Caucasian

2.1.1.2 Harvesting cells

Cells were cultured in T-25 cell culture flasks during p1 and p2 and were then grown in T-75 cell culture flasks up to p3 in specialized BEGM (section 2.1.1.5). When cells reached confluency, they were dissociated by rinsing with 500 µl of 0.5 mg/ml warm 10x trypsin-EDTA solution (5 g porcine trypsin and 2 g EDTA) diluted to 1x in 1x PBS, for 30 seconds and was aspirated off. This was followed by re-incubation with 5 ml per T-75 flask or 2 ml per T-25 flask of fresh trypsin for 5 min at 37ºC until cell-substrate attachments are loosened. Trypsin was then neutralized (1:1 volume) with 0.5 mg/ml soybean trypsin inhibitor in 1x PBS; and cells were re-suspended in fresh media and collected by centrifugation at 1200 rpm for 8 min at 37 ºC. The cell pellet was then re-suspended in the desired media at the appropriate cell density required and seeded into new cell culture flasks or plates. All cells were incubated at 37 ºC in humidified 5% CO2 incubators.

2.1.1.3 Determination of cell counts

Cell counts were routinely determined prior to seeding cells into fresh media as required in order to maintain a constant cell number for each experiment. After harvesting and re-suspending, 10 µl aliquots of cells were placed in the chambers of a hematocytometer. Cells in each corner quadrant of the grid were counted and multiplied by 10^4 to give the number of cells per ml since the area of the 4 corner squares is 1 mm^3 (0.1 mm^3 x 10^4 = 1 ml). Volumes of cells were then adjusted to give the desired seeding densities.

2.1.1.4 Cryopreservation of cells

Approximately $4x10^6$ cells per ml were harvested as in section 2.1.1.2 and the cell pellet was re-suspended in cold 10% dimethyl sulphoxide (DMSO, diluted in 1ml of the desired media). Cell suspensions were placed in a sterile cryovial and immediately stored at -80°C for freezing for four hours then transferred to liquid nitrogen (-179°C).

2.1.1.5 Maintenance of HBEC in culture

Routine culturing of HBEC was performed in T-75 cell culture flasks in specialized bronchial epithelial growth medium (BEGM), prepared by adding the supplements provided in singlquots® bulletkits containing: 5.0 µg/ml insulin, 52 µg/ml bovine pituitary extract (BPE), 0.5 ng/ml human recombinant epidermal growth factor (hEGF), 0.5 µg/ml hydrocortisone, 0.5 µg/ml epinephrine, 10.0 µg/ml transferrin, 0.1 ng/ml retinoic acid (RA), 6.5 ng/ml triiodo-L-thyronine, and 50.0 µg/ml gentamycin and amphotericin-B (GA), (all final concentrations), to bronchial epithelial basal media (BEBM). GA can affect the growth of cells

and since it is stable for 3 days at 37ºC, it was not used for more than 3 passages. HBEC were passaged when the cells reached 80-90% confluency. The cells were then harvested as explained in section 2.1.1.2 and seeded into appropriate plates depending on the experiment to be carried out. These cells were either used directly as undifferentiated HBEC or differentiated as explained in the next section.

2.1.1.6 Differentiation of HBEC into a pseudostratified airway epithelium

The method of Danahay *et. al.* was used to generate a multi-cellular layered culture representative to that *in vivo* (Danahay, Atherton, Jones et al. 2002). Bronchial epithelial differentiation media (BEDM) is a 1:1 mixture of BEBM and Dulbecco's modified eagle's medium (DMEM) with the singlequot bulletkit supplements as above (section 2.1.1.5) but omitting triiodo-L-thyronine and the GA mix. RA was also not added and substituted by a higher final concentration of 50 nM. It has been shown previously that the airway epithelium becomes squamous without RA and mucin secretionfalls dramatically (Gray, Guzman, Davis *et al.* 1996). Figure 2-1 is a schematic diagram explaining the technique of HBEC differentiation *in vitro*.

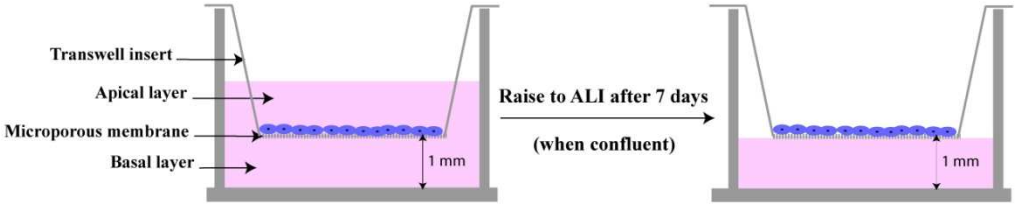

Figure 2-1: Differentiation of HBEC *in vitro*.
Primary human bronchial epithelial cells (HBEC) were cultured *in vitro* on microporous polyster membranes in submerged culture using bronchial epithelial differentiation media (BEDM) for 7 days (left) after which they were raised to air liquid interface (ALI) for a further 21 days to differentiate (right).

P4 HBEC were seeded at 0.8-1.7 x 10^5 cells per transwell insert in 500 µl BEDM onto polyester tissue culture inserts (0.4 µm pore size) in 12-well cell culture plates. These were cultured at 37ºC, 5% CO2 for 7 days, changing the media every 48 hrs. 500 µl of cell suspension in BEDM was added to the apical layer per insert and 1 ml per insert BEDM only was added to the basal compartment. The cells were maintained in submerged cultures for 7 days. After the cells had reached complete confluency, they were raised to air liquid interface (ALI) by adding media only to the basal compartment and the apical compartment was briefly rinsed with 250 µl per well fresh sterile phosphate buffered saline (PBS) to remove any mucus build-up, and differentiated for a further 21 days. Every 48 hrs, the media was replaced and the apical compartment was washed as above.

2.1.1.7 Wound repair model of HBEC

The wounding process explained below was adapted from a previously published method (Kim, McKinnis, Nawrocki *et al.* 1998) (Wadsworth, Nijmeh and Hall 2006)(White *et. al.*, 1999).

For wounding experiments with undifferentiated HBEC, when cells reached confluency in 24-well plates, they were wounded in two parallel lines using a sterile p200 Gilson pipette tip making sure the cells at the site of the wound were completely denuded down to the surface of the plate. The cell layer was wounded after aspirating off old media and adding 250 µl per well sterile PBS. PBS was then aspirated off to remove any cell debris and fresh BEGM was then added. Similarly, for wounding experiments with differentiated HBEC, the cell layers on the inserts were carefully wounded in two parallel lines as above. Again, this was done after aspirating off the old media and adding 250 µl per well fresh PBS; which was then aspirated off and fresh BEGM was added to the basal compartment only. Wounding experiments for both differentiated and undifferentiated HBEC were done on donor 1 only.

Images of the wounds were captured using an inverted Nikon Diaphot 300 microscope with a Plan PhL x2.5 objective (Nikon) and a digital camera (Insight QE model 4.2). Analysis of wound healing quantification was carried out using SpotCam Advanced software , Image solutions, diagnostic instruments Inc., Chorley, Lancashire, UK) by measuring the area of the wound. Examples of wound images and area measurements are provided in section 3.4.2.

2.1.2 Epithelial cells from lung biopsies:

Biopsies were acutely derived from bronchial tissue obtained at bronchoscopy with full local ethical approval from healthy, non-smoking subjects. This was carried out by Dr. Claudia Ceresa and Dr. Mark Roberts. Briefly, at the time of bronchoscopy the endobronchial samples were taken at first division subcorina (i.e proximal part of the airway). The biopsies were then placed into a 5ml bijou

tube with approximately 3 ml of sterile PBS without antibiotics, at room temperature. The bijou should be sealed inside a 'Blood Form Bag' and placed inside a second, sealed container. The sample was then transferred from the endoscopy suite directly to the laboratory and placed in a petri-dish and dissected under the microscope using fine dissecting tools and needles where the epithelial cells were carefully separated from the rest. The sample was then placed in a 6-well plate using 1 ml BEGM per well and the media was replaced every 7 days. Cells generally reached confluency within approximately 10-14 days. Cells were harvested as in section 2.1.1.2. Cells (from each biopsy) were then seeded into T-25 flasks (p1) until confluent after which they were split again into T-75 flasks. When they reach p4, differentiation of the epithelial cells was carried out as described in section 2.1.1.6. Undifferentiated and differentiated cells were characterised for epithelial and differentiation markers to determine the type and the purity of the cells grown, as well as their differentiation potential (refer to section 5.4.4 for more details). Cells were maintained at 37ºC in a 5% CO2, incubators at all times.

2.1.3 Isolation of single cells

To investigate the clonogenic potential of the various cell types present in cell populations obtained during this project, two methods for single cell isolation were used: dilution cloning and fluorescence-activated cell sorting (FACS). First, dilution cloning was carried out after cells were harvested as described in section 2.1.1.2. Dilution cloning is the process of obtaining a monoclonal cell population starting from a polyclonal one and this is achieved by sequentially diluting the cells until 1 cell per well is obtained. Starting from $2x10^6$ cells per ml,

the cell suspension was diluted to 2000 cells per ml and then 5 cells per ml in BEGM. 200µl of the diluted cell suspension was added to each well of a 96-well plate. Wells were then checked for cells under a phase-contrast microscope for colonies every 3-4 days and the media was changed after 10-14 days.

Another method of serial dilution, known as limiting dilution, was carried out by counting then diluting the cells to 1000 cells per ml suspension. Figure 2-2 gives a summary of the 96-well plate layout .96-well plates were prepared by adding 200 µl of the desired media in wells A1-H8 and 100 µl in the rest of the well. 100 µl of the diluted cell suspension was added to A1 with gentle mixing after which 100 µl was removed from A1 and added to B1 with mixing to give a 1:2 dilution, another 100 µl was removed from B1 and placed into C1 and so on until H1 (serial dilution 1). Dilution across the plate was then carried out in an analogous way using a multichannel pipette (serial dilution 2). This was carried out in 96-plates to study HBEC clonogenic potential (section 5.4.1). These studies only included donor 1.

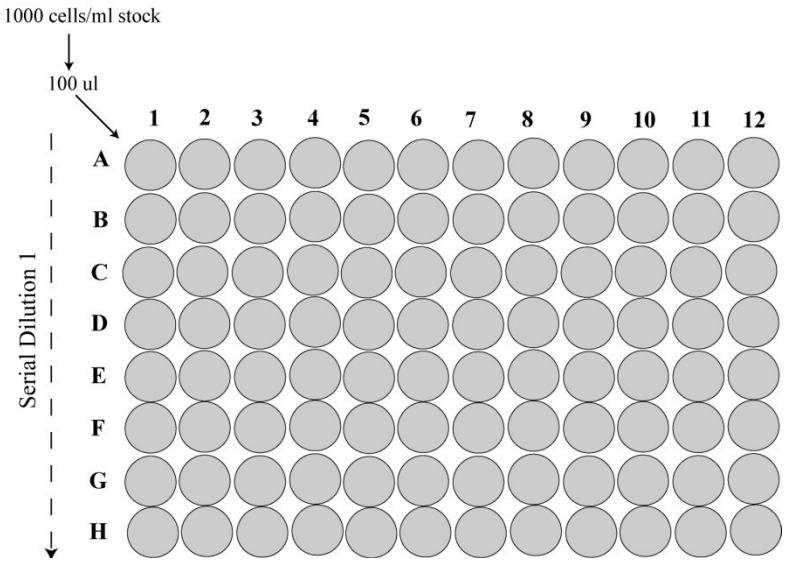

Figure 2-2: Cloning of HBEC using limited diltution.
Serial dilution 1 was first carried out down A1-H1 starting from A1 (containing 1000 cells/ml) removing 100µl and placing it into B1 with mixing and so on. Then serial dilution 2 was done across the plate using a multichannel pipette replacing 100 µl in each well.

Finally, single cell sorting was also carried out using a fluorescent-activated cell sorter (FACS, Coulter Altra Flow Sorter, Beckman Altra) using a blue UV laser. The cells from donor 1 were harvested as described above, centrifuged and re-suspended in fresh media at $1x10^6$ cells per ml and then sorted using the FACS machine into 150µl of fresh media per well.

2.2 Protein analysis

2.2.1 Immunofluorescence (IF)

To carry out immunofluorescence staining on undifferentiated HBEC, the procedure explained below was carried out on cells grown on plastic 24-well plates. However, for differentiated HBEC, microporous membranes were cut out carefully from the transwells, after the staining procedure was completed, using a

sterile blade and placed on glass slides with cells facing down on one drop of mounting media to preserve the cells on slides. Another drop was added over the membrane placed on the slide and a cover slip was then put on top, ensuring no bubbles were produced.

To visualize the expression and/or the cellular distribution of proteins of interest, antigens were detected using specific primary antibodies and dye-coupled subsequent secondary antibodies. The following is a summary of the protocol used to immunostain undifferentiated and differentiated HBEC.

250 µl per well of any of the solutions used in the protocol was added to undifferentiated HBEC unless stated otherwise. When handling differentiated HBEC, 250 µl per well of solution was added to both apical and basal compartments. Cells were washed with PBS three times (5 min each time) between each step to remove any residual solution from the previous step. Moreover, solutions were aspirated off in-between steps using an aspirator.

Fixation:

Cells were fixed by incubation with 4 % formaldehyde in PBS for 15 min at room temperature or overnight at 4 ºC.

Permeabilization:

To expose the intra-cellular antigens to the antibodies, cells were incubated with 0.15% triton X-100 in PBS for 10 min at room temperature

Blocking step and antibody addition:

To avoid non-specific antibody binding, cells were incubated with10% goat serum in 1% bovine serum albumin (BSA)/PBS for 15 min at room temperature or can be stored at 4 ºC until staining.

Primary antibody (diluted in 1% BSA/PBS at the desirable working concentration) was added to the fixed cells either for 1 hr at 37ºC or overnight at 4ºC. The primary antibody was subsequently detected using a suitable secondary fluorophore at 1:250 dilution 1%BSA/PBS and incubated for 30-45 min at 37ºC in the dark to minimize photo bleaching. Most steps from this point onwards were carried out in the dark by wrapping the samples with aluminium foil. The appropriate primary and secondary antibodies used, the working concentrations, and their sources are mentioned in the relevant chapters where IF was carried out

Fluorescence and confocal microscopy:

Immunofluorescent-labelled samples were imaged and analyzed using fluorescence and confocal microscopy. For fluorescence microscopy, a Nikon Diaphot 300 epifluorescence microscope (Surrey,UK) with a mercury lamp was used with a SPOTCam software to capture images. For confocal microscopy, a laser scanning Zeiss Axiovert 100 inverted microscope, with a Zeiss LSNM510 UV combi spinning disk attached (Carl Zeiss Ltd, Hertfordshire, UK) was used to capture Z-sections through the cultures for three dimensional images. Further

details can be found in specific sections where characterisation of epithelial cells was carried out.

All immunofluorescence was carried out on donor 1.

2.2.2 Luminex assays

The Luminex® system was employed to investigate cytokines, chemokines, and growth factors secreted by differentiated HBEC, grown at ALI, before and after injury. The principle of this technology is the ability to measure multiple analytes simultaneously in single-reaction well (see Figure 2-3). Molecular reactions on the surface of colour-coded microspheres, using different fluorescent intensities of two dyes, take place. The fluorescently-labelled microspheres, tagged to a reporter tag, capture the sample. The microspheres are then applied to the instrument by focusing them in a single file, where they pass two lasers. One illuminates the microsphere identifying the read bead, and the second excites the colour on the surface. Colour signal is captured, translated digitally into real time and the data is then quantified. The technology has the ability to detect at least 1 pg/ml of analyte in as small a volume as 25 µl per well.

This multiplex immunoassay is based on xMAP® detection technology, combining a flow cytometer, a fluorescent-dyed beads, lasers and digital signal processing. The assay was carried out according to the manufacturer's protocol using a pre-mix human Procarta® Cytokine Assay kit, 28-plex (cat # 1PC1028), a vacuum filtration system, Millipore (P/M MAVM0960R and WP6111560), a microplate shaker, labline model 4625 with 3mm orbit, and a Bioplex® plate reader (luminex machine) with a Bioplex manager version 2, BioRad.

Pre-mixed standards were reconstituted in 125 µl of cell culture media (BEDM) gently vortexed for 10 sec and incubated on ice for at least 10 min. Serial dilutions of the premixed antigen standards were prepared in cell culture media.

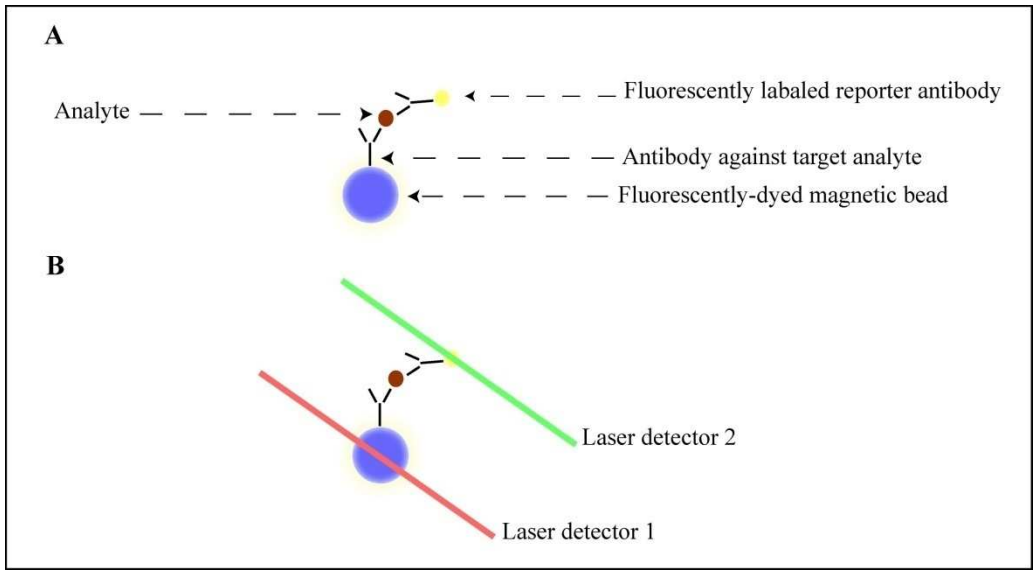

Figure 2-3: Basic Principle of Luminex System.
(A) shows the magnetic beads with an inner fluorescent dye, bound to antibodies against target proteins to be measured in the sample. A fluorescently labeled reporter antibody then binds to the target analyte. The beads are run through the luminex machine in a single file where one laser identifies the bead itself (laser detector 1) and another laser identifies the fluorescent detector antibody (laser detector 2)(B).

2.2.2.1 Luminex assay

Standards and samples were placed in 96-well plate with filter bottoms in duplicates and any unused wells were sealed before starting the assay. At the end of each step, solutions were removed by vacuum, and the samples were washed three times with 150 µl 1x wash buffer per well (salts were dissolved by vortexing 10x wash buffer, then 20 ml of 10x wash buffer was mixed with 180 ml deionised water). The bottom of the filter plate was then blotted thoroughly to remove excess buffer and returned to the filter plate holder. All reagents mentioned in the protocol are provided with the kit. Two subject samples were used for these

studies (donor 1 and donor2). Each included two replicates and the Luminex assay was carried out in duplicate.

Filter plate pre-wetting:

150 µl of reading buffer was added to each well and incubated for 5 min.

Antibody beads addition: Premixed antibody beads were vortexed for 30 sec at and 50 µl of antibody beads were added to each well.

Samples/standards loading:

75 µl Assay buffer and 25µl of standards or samples were added to each well and the plate was sealed, completely wrapped with aluminium foil, shaken for 30 sec at 500 rpm at, and the plate seal was carefully removed.

Detection antibody addition:

25µl of detection antibody was added to each well and the plate was again sealed, completely wrapped with aluminium foil, shaken for 30 min at 500 rpm at, and the plate seal was carefully removed.

Streptavidin-PE (STPE) addition:

STPE beads were vortexed to re-suspend and 50 µl was added to each well. The filter plate was again sealed, completely wrapped with aluminium foil, shaken for 30 min at 500 rpm, and the plate seal was carefully removed.

Plate reading: 120 µl of reading buffer was added to each well and the plate was sealed, completely wrapped with aluminium foil, shaken for 5 min at 500 rpm at, and the plate seal was carefully removed before analyzing on the Bioplex luminex machine. A standard curve for each analyte, using the 5PL-(parametric logistic) regression fit, was created from the standards, and this was used to determine the final concentration (pg/ml) in the samples. This was done using Bioplex manager

version 2 software (BioRad). An example standard curve is presented in Figure 2-4. Finally, the data was plotted as time points post wounding vs. cytokine observed concentration (pg/ml) and statistical analysis was done using Prism 5.0 software.

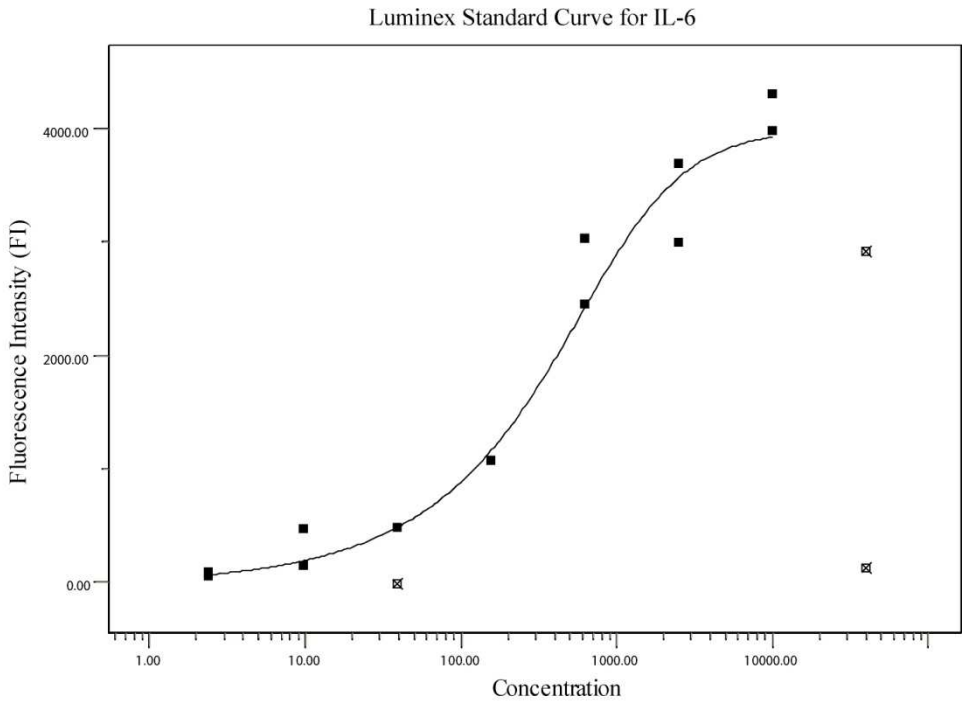

Figure 2-4: A representative standard curve created after luminex experiment (IL-6). A standard curve was created from the standards included, using 5PL-(parametric logistic) regression fit. Outliers as determined by the software (shown as x) were excluded from the fit . Samples were measures as duplicates at each concentration.

2.3 FACS-based Hoechst efflux method of stem cell purification

Flow cytometry is used to analyze the expression of cell surface markers and intracellular molecules, as well as characterising different cell types in heterogeneous cell populations. This is achieved by measuring the fluorescence intensity produced by fluorescent-labelled antibodies detecting proteins bound to specific cell-associated molecules. The single cell suspension is focused to a thin

stream of single cells with a laser light directed to it as the sample flows through a chamber. A number of detectors are used to detect any light scattered from cells as they flow through the beam. One detector is placed in front of the light beam (forward scatter (FSC)) and several at the side (side scatter (SSC)). Fluorescent detectors are used for detecting fluorochromes (Figure 2-5).

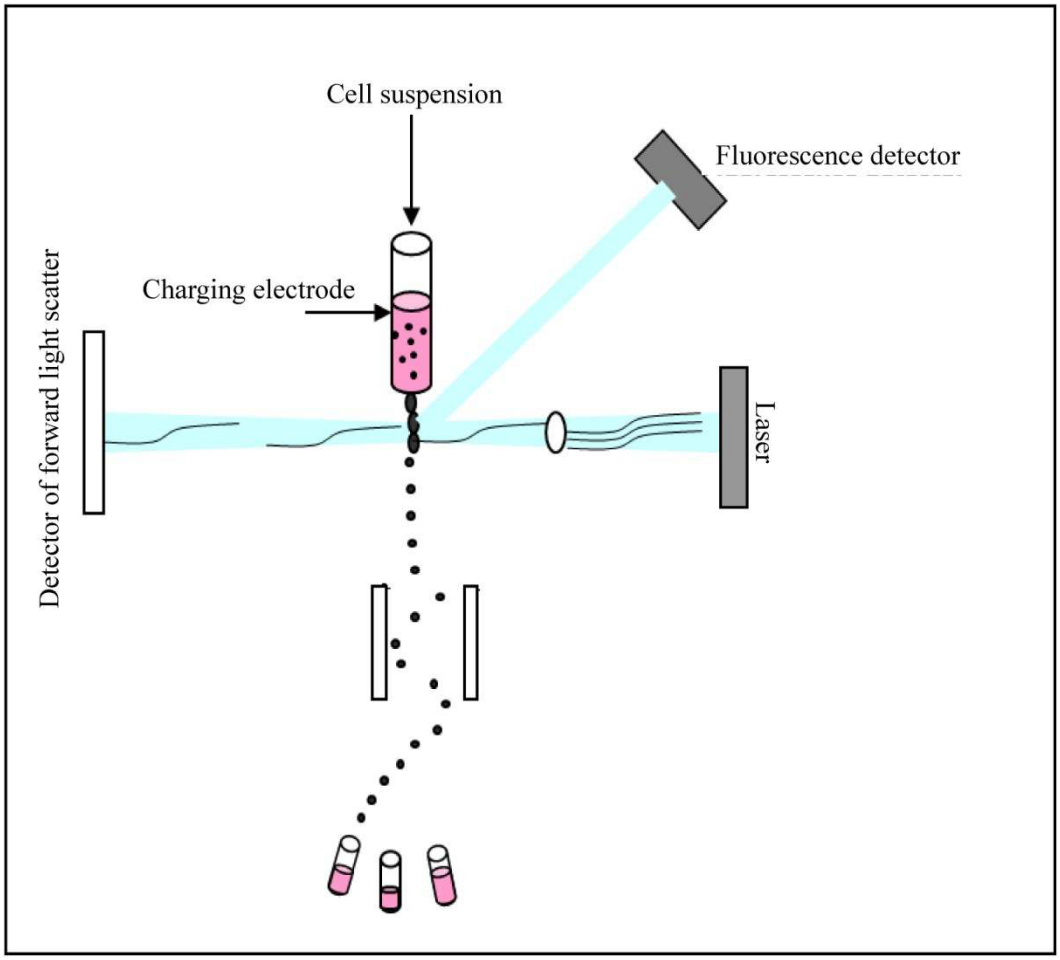

Figure 2-5: Basic principle of FACS.
Cells are sorted on the basis of light scatter (size and shape) and fluorescence by deflection of a thin stream of cell suspension.

FSC is correlated with cell size and shape while SSC depends on the density of the cell. The fluorochromes emit light when excited by a laser with the corresponding excitation wavelength. Fluorescence-activated cell sorting (FACS)

does not only quantify the signal but also separates the cells from a mixed population of cells based on the fluorescence profile. There are direct and indirect approaches to staining. Direct FACS staining involves the incubation with an antibody conjugated to a fluorochrome directly, while in indirect FACS staining, the primary antibody is detected by a specific secondary fluorochrome-labelled antibody.

2.3.1 Identification of side population (SP)

A 'side population', characterised by its ability to rapidly efflux the DNA-binding Hoechst 33342 dye through ABCG2 transporter, has been defined recently in a number of tissues (Terunuma, Jackson, Kapoor *et al.* 2003; Budak, Alpdogan, Zhou *et al.* 2005). This population is thought to be rich with primitive stem cells. Hoechst is excited at UV lengths 351-364 nm to emit a blue fluorescence at 465nm. Goodell *et. al.* in 1996 were first to introduce this FACS-based Hoechst efflux method to isolate the side population that can be detected on a dual wavelength profile (Hoechst red vs Hoechst blue) from murine bone marrow (Goodell, Brose, Paradis et al. 1996). An adaptation of this method was used to isolate and attempt to characterise the side population from undifferentiated and differentiated HBEC, and epithelial cells derived from lung biopsies. More details can be found in sections 5.4.2 and 5.4.3.

For these studies, cells were harvested (section 2.1.1.2) and re-suspended in fresh media (BEGM) at $1x10^6$ cells/ml. Incubation of the cells with 5 µg/ml Hoechst 33342 was carried out for exactly 90 min at 37°C, shaking continuously. As a negative control, duplicate samples were treated with 50 µM verapamil hydrochloride, a calcium ion influx inhibitor, for 5 min prior to incubation with

the Hoechst dye. After incubation, cells were cooled on ice, centrifuged (1200 rpm for 8 min at 4°C), and re-suspended at $0.5x10^6$ cells/ml in Hank's balanced salt solution (HBSS) containing: (HEPES), 1 mM Magnesium chloride (MgCl2), 2mM Calcium chloride (CaCl2), 2% foetal calf serum (FCS). In order to discriminate cells 2 µg/ml propidium iodide (PI), which binds to the DNA, was also included. Cells were kept on ice at all times after incubation to prevent further dye efflux. A Coulter Altra Flow Sorter (Beckman Coulter Altra) was used to analyze cells and to isolate the side population for further characterisation. A FSC vs SSC plot was generated to gate the live population depending on PI staining (live cells stain positive for PI). Then, a Hoechst Red vs Hoechst blue profile (emission detections were 670/30-nm band-pass and 450/65-nm band-pass filters) was generated. Statistical analysis was generated using winMDI 2.8 software. All side population experiments were carried out on cells from donor 1.

2.4 Molecular methods

To investigate the effect of injury on the relative expression of specific epithelial genes from HBEC using mRNA levels, reverse transcription; combined with quantitative real time polymerase chain reaction (qPCR) were utilised. Details of the target genes investigated are found in specific sections dealing with epithelial stem/progenitor characterisation in wound healing.

2.4.1 Total RNA preparation from animal cells

RNA was extracted from cells after experimental treatment using RNeasy mini kit and RNase-Free DNase Set purchased from Invitrogen. All steps were carried out

at room temperature according to the manufacturer's protocol on clean bench surfaces and equipment to minimize contamination by RNases and human RNA. All centrifugation steps were carried out at 13000 rpm.

Cells were lysed by adding 600 µl RLT buffer, containing ß-mercaptoethanol (100:1), directly to plates or flasks (40 ul per transwell was used for differentiated HBEC). Cells were then harvested using a cell scraper and stored in eppendorf tubes at -80ºC until RNA extraction. The lysates were next briefly spun, homogenised by passing through a QIAshredder column and centrifuged for 2min. 600µl of 70% ethanol was added to the samples, mixed well, and was applied to RNeasy mini column and centrifuged for 1 min.

DNA digestion was performed using the Qiagen RNase-free DNase set as follows: 350 µl Buffer RW1 was added to the RNeasy mini column and centrifuged for 1 min discarding the supernatant. Meanwhile, 10 ul of the DNase I stock was mixed gently with 70 µl buffer RDD, applied directly onto the RNeasy silica-gel membrane. After incubation at 30°C for 15 min, 350 µl buffer RW1 was added to the RNeasy mini column and centrifuged for 1 min discarding the supernatant. The RNeasy column was then transferred into a new 2 ml eppendorf tube and washed twice by adding 500 µl buffer RPE onto the column, centrifuging for 1 min, and discarding the supernatant. The RNeasy column was again placed into a new 2 ml tube and centrifuged for 2 min to remove residual RPE. Finally, to elute the RNA, the RNeasy column was transferred into a 1.5 ml eppendorf tube and 40 µl RNase-free water was added directly onto the RNeasy silica-gel membrane and centrifuged for 1 min. The supernatant was transferred to a new labelled eppendorf tube and stored at -80°C.

2.4.2 Complimentary DNA (cDNA) synthesis

2.4.2.1 Polymerase chain reaction (PCR)

Polymerase chain reaction involves three main steps, denaturation of the template complimentary DNA (cDNA) strands, annealing of the primer pairs added to the template DNA strands and finally the elongation of the primers by the RNA polymerase to create nascent copies of the template strands. These steps are usually repeated 20-30 times to give an exponential increase of the target sequence flanked by the opposing primer pairs.

2.4.2.2 Primer design

Primers were designed with the aid of Beacon designer 6.0 software (Premier Biosoft International). The following were used as a guide when primers were designed: An optimal size of 18-20 base pairs (bp) (longer primers would have high annealing temperatures), and similar annealing temperatures of forward and reverse primers, 50% G/C content (since a higher percentage might lead to non-specific annealing, the 3' end of the primers should not be rich with G/C), and finally the specificity of the primers to the desired genes were checked using the Basic Local Alignment Search Tool (BLAST) (Altschul, Madden, Schaffer *et al.* 1997) (http://blast.ncbi.nlm.nih.gov/Blast.cgi). Lists of the primers used can be found in the specific chapters.

2.4.2.3 Reverse Transcription

Complimentary DNA (cDNA) is synthesized from a single stranded mRNA template using reverse transcription (RT). RNA concentration was first measured

using a Nanodrop spectrophotometer (ND 1000 (Wilmington, USA)). 1 µl sample was added onto the Nanodrop for measurement after blanking the machine with DEPC-treated water. The purity of RNA was indicated by the A_{260nm}/A_{280nm} ratio which should be 1.8 and 2.0 since this ratio is used to assess the purity of RNA (or DNA). For all experiments, this ratio was 1.87-2.16.

cDNA was then prepared using the Superscript 1st Strand System (VX11904018) according to the manufacturer's protocol. Table 2-2 lists the reagents to prepare Mix 1 and Mix 2 respectively for 20 µl cDNA.

Table 2-2: Mix 1

10 µl RT reaction	
10 mM dNTP mix	1 µl
50 ng/ µl Random hexamers	2 µl
RNA	0.5 µg
DEPC-water	up to 10 µl

Non-template controls (NTC) were prepared in parallel by leaving out the RNA. Each sample was incubated at 65°C for 5min to denature the RNA secondary structure, chilled on ice for 1 min and centrifuged briefly. Mix 2 was then prepared (Table 2-3).

Table 2-3: Mix 2

10 µl RT reaction	
10X RT buffer	2 µl
25 mM $MgCl_2$	4 µl
0.1 M DTT	2 µl
RNAse OUT	1 µl

In order to anneal the random hexamers to RNA, 9 µl of the Mix 2 was added to each of the denatured samples, mixed gently by pipetting, and centrifuged briefly. The samples were incubated for 2 min at 25°C and 1 µl of SuperScript. II RT was added to each sample by gentle pipetting. A duplicate set of samples was also prepared as above leaving SuperScript II RT enzyme out as negative controls (RT-). Reverse transcription reactions were carried out (Table 2 3: RT-PCR cycling conditions) in a Techne Gradient PCR block (GMI, Minnesota).

Table 2-4: RT-PCR cycling conditions

25°C for 10min
42°C for 50min
70°C for 15min to inactivate
4°C to hold

After the reaction was complete, the samples were chilled on ice for 2 min and centrifuged briefly to ensure all contents were at the bottom of the tube. RNaseH (1 µl) was then added to each sample and incubated for 20 min at 37°C. The samples were again centrifuged briefly, and stored at 4°C for short term (2 weeks) or at -20°C for long term storage.

2.4.2.4 Verification of cDNA

Synthesized cDNA was then checked for the expression of the housekeeping gene glyceraldehyde-3-phosphate dehydrogenase (GAPDH). A polymerase chain reaction (PCR) was carried out to amplify GAPDH.
(5'TCTAGACGGCAGGTCAGGTCCACC forward in exon 4, and 3'CCACCCATGGCAAATTCCATGGCA reverse, in exon 8). and Table 2-6 list the reagents used to prepare the master mix and the cycling conditions at which

PCR was run, respectively. PCR products from cDNA samples were separated and analyzed by agarose gel electrophoresis. 1% agarose tris acetate-EDTA (TAE)-gels were used to run the samples with 0.5 µg/ml ethidium bromide added to the agarose gel mixture to permit visualisation of the cDNA with a UV transilluminator. TAE buffer was prepared by mixing 242 g of tris base with 57.1ml glacial acetic acid and 100 ml 0.5 M EDTA (pH:8); and deionized distilled water was then added to make up 1 L of solution. A Syngene gel doc with a GeneSnap acquisition, GeneTools analysis, and GeneDirectory database software (Cambridge, UK) was used to record images. Meanwhile, 10 µl of sample was added to 3 µl Orange G loading dye to monitor the progress of the gel electrophoresis. Gels were then run horizontally in TAE buffer for 30-40 min at 40-50 volts. A 1 kb DNA ladder was used for comparison to determine the concentration and molecular weights of cDNA fragments (suitable for DNA sized between 500 – 1 kb). Figure 2-6 below shows differentiated HBEC cDNA GAPDH expression, verifying the cDNA with good quality for investigation.

Table 2-5: GAPDH PCR master mix

PCR Reaction (1X)	**µl**
10x PCR buffer	5
50mM stock Mg_2^+	1.5
5µM stock dNTPs	2
100µM stock GAPDH forward	1
100µM stock GAPDH reverse	1
DEPC-water	37.5
taq	1
cDNA template	1

Table 2-6: GAPDH PCR cycling conditions

94°C	1.30 min
50°C	1.30 min
72°C	1.30 min
72°C	10 min
4°C	HOLD

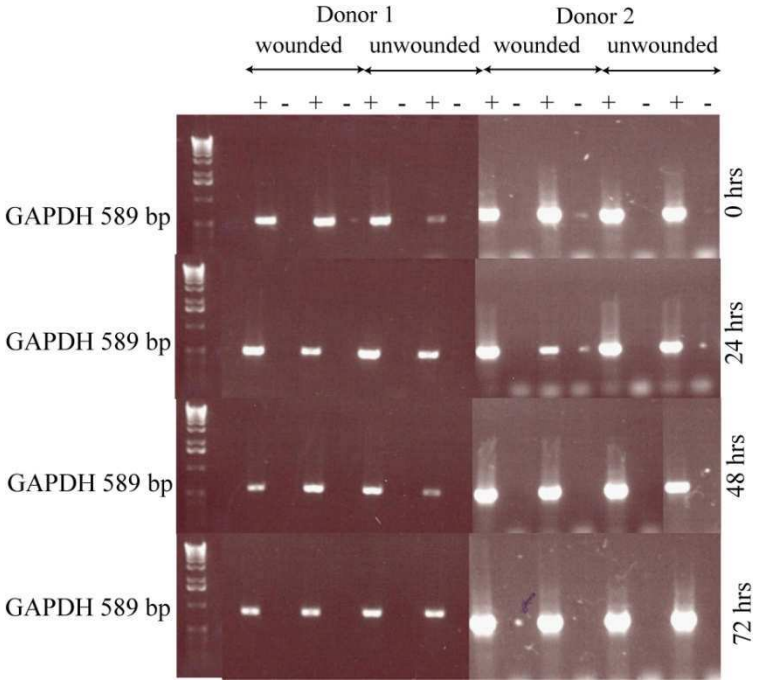

Figure 2-6: GAPDH expression in differentiated HBEC cDNA.
Wounded and unwounded samples in duplicates were used per donor. The image shows RT+ and RT- samples at different time points post-wounding.

2.4.3 Quantitative real time PCR (qPCR)

DNA amplification monitoring in real time is the basis of quantitative PCR (qPCR). Currently, there are four chemistries for qPCR: Taqman® (Applied Biosystems, Foster City, CA, USA), Molecular Beacon, Scorpions® and SYBR® Green (Molecular Probes), all of which detect the PCR product *via* a fluorescence signal. Taqman®, Molecular Beacon, and Scorpions® are dependant on fluorescence resonance energy transfer (FRET) to produce a signal. This is achieved *via* a fluorogenic coupled dye and a quencher moiety. However, SYBR® Green is a fluorogenic dye that fluoresces when in solution but emits

strong signal when bound to double-stranded DNA. Taqman® probes, used in real-time experiments in this project, have a fluorescent reporter dye (R) attached to the 5' end and a quencher coupled to the 3' end hybridized to an internal region of the PCR product (Figure 2-7). The probe depends on the 5' activity of the Taq polymerase used to hydrolyse an oligonucleotide hybridized to the target amplicon. In close proximity, in the unhybridized state, the quencher and reporter dyes do not produce a fluorescent signal. As the polymerase replicates on the template where the Taqman® is bound (5' to 3'), the probe is cleaved releasing the reporter and quencher dyes, generating a fluorescence signal. Thus, with each cycle, depending on the amount of cleaved probe, the fluorescence increases proportionally.

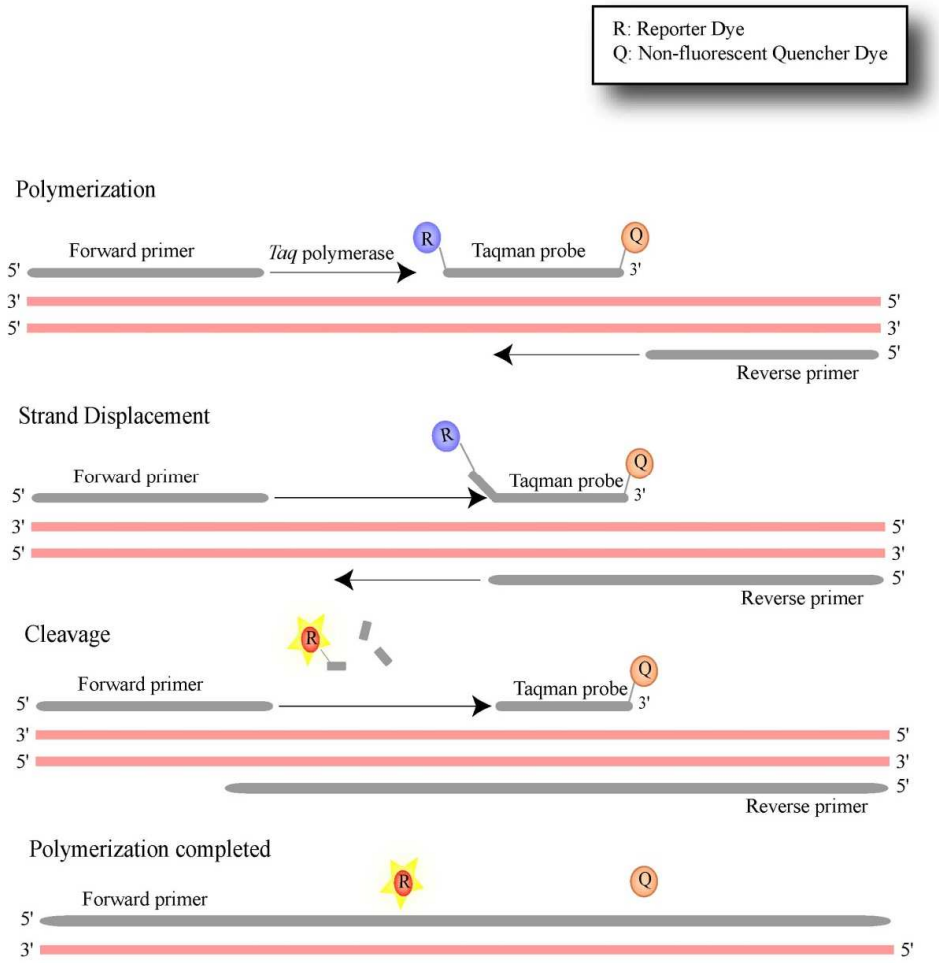

Figure 2-7: Taqman® probe design and function.

This fluorescence signal is detected using a laser light distributed on thin-walled reaction tubes with optical fibres. The fluorescence emission is directed to a spectrograph with charge-coupled device camera. Mx2005 QPCR system (Stratagene, Agilent Technologies UK Limited, Cheshire, UK) was used in this study and quantification was monitored using MxPro QPCR software. The number of threshold cycles (Ct) was measured and quantification was calculated using the Δ comparative method, as follows: ΔCt = Ct of target gene – Ct of housekeeping gene, obtaining a final value *via* $2^{-\Delta Ct}$. Hypoxanthine ribosyltransferase (HPRT) and 18S were used as endogenous housekeeping genes

for data normalization (de Kok, Roelofs, Giesendorf *et al.* 2004). Human HPRT1, FAM / MGB Probe, Non-Primer Limited, cat# 4333768T, Applied Biosystems. Total RNA, from differentiated HEBC grown at ALI and wounded, was collected at 0, 24, 48, and 72 hrs post-wounding, after which cDNA was synthesized as described above, then were run in triplicates in 96-well optical plates. A master mix (Table 2-7) was prepared (20 µl per well) and then run at the cycling conditions shown in Table 2-8.

Table 2-7: Quantitative PCR (qPCR) master mix

20 µl Real Time reaction	**µl**
2x Taqman Universal Master mix	10
900 nM Forward Primer	1.8
900 nM Reverse Primer	1.8
250 nM Probe	0.5
dH_2O	1.9
cDNA (diluted at 1:10 in DEPC water)	4

Table 2-8: qPCR cycling conditions

50 °C	2 min	1 cycle
95 °C	10 min	1 cycle
95 °C	15 sec	40 cycles
60 °C	1 min	

A standard curve was plotted to determine the efficiency of the reaction and to ensure similar efficiencies and conditions for all primers and probes used. This was carried out by setting up 2-fold dilutions in triplicates (1:2, 1:4, 1:8, 1:16, 1:32) of the samples for each of the primer sets and running the reaction as in Table 2-7 and Table 2-8. Ct values were normalized against either HPRT and 18S housekeeping genes, at each time, and Figure 2-8 compares the results for 18S

(A) and HPRT (B) mRNA expression by wounded and unwounded differentiated HBEC used in these studies. Analysis was done using the comparative quantification ΔCt method. Standard curves for all assays are shown in the relevant following sections. For molecular work, RNA was extracted from the same samples of which the supernatants were collected from for Luminex analysis. These included donor 1 and donor 2 differentiated HBEC, each done in 2 replicates. Real time PCR was carried out in triplicate.

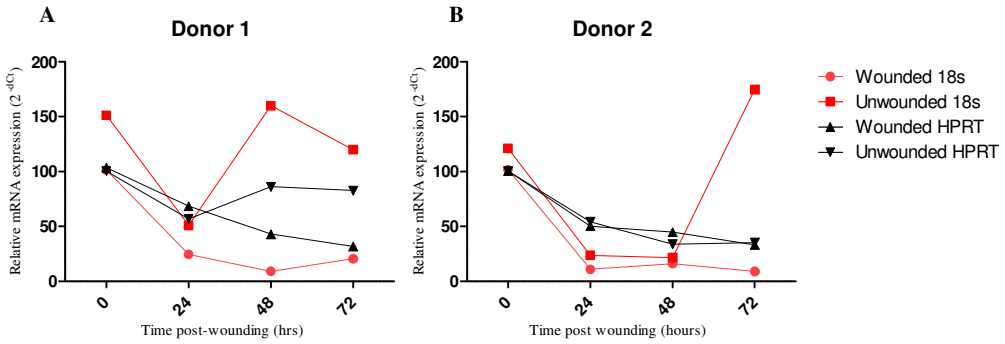

Figure 2-8: Housekeeping genes mRNA expression.
(A) is showing donor 1 while (B) is donor 2 18 s and HPRT mRNA expression. Both graphs are representative of the mean of two replicates per donor for each housekeeping genes for both wounded and unwounded cultures.

2.5 Statistical analysis

Statistical analysis was carried out on raw data using two-way ANOVA followed by a Bonferroni multiple comparison post-hoc test. For wound area measurements, a one-way ANOVA followed by Dunnett's multiple comparison post-test was used to calculate the date. GraphPad PRISM version 5.0 was used for all statistical analysis, with values representing the mean ± standard error of mean (SEM) of n separate experiments.

Chapter 3. Characterisation of a Differentiated Human Bronchial Epithelial Wound Repair Model *in vitro*

3.1 Introduction

As discussed in chapter 1, the airway epithelium has been proven to have an important role in both the normal and the diseased lung. The epithelium protects the lung from inhaled toxic particles such as smoke, bacteria, and viruses. It also serves anti-microbial, regulatory, and pro-inflammatory functions. Moreover, it possesses regenerative capabilities in order to maintain its integrity and fulfil these functions successfully. It is thought that resident stem or progenitor cells are present in specific niches along the respiratory tree and are responsible for the repair of the multi-layered epithelium's structure under normal wear and tear, as well as in diseased lungs.

As the airway epithelium is critical to the normal functioning of the lung, many attempts to study this tissue layer have been carried out since the late 1970s and early 1980s (Mathias, Yamashita and Lee 1996). A number of animal and human *in vivo* and *in vitro* models have been evaluated which mimic the airway epithelium in the adult body and which might contribute to an in-depth level of understanding of wound repair mechanism. Relevant models of the airway epithelium could also enable drug metabolism studies, the dissection of pathways important in control of permeability, and the study of a wide range of cellular processes at the molecular level.

3.1.1 Airway epithelial models

Historically, a number of models have been established to study the airway epithelium. These have been used to investigate the function, growth and self renewal of airway epithelium and to study differentiation, clonogenic potential, and characterisation of the resident stem or progenitor cell pools responsible for wound repair and their niches. These models include human and animal species both *in vitro* and *in vivo* and relevant examples are discussed below.

3.1.1.1 Animal and human *in vivo* models

Table 3-1: *In vivo* models of the airway epithelium

Animal tracheal generation	
· Scrape-wound of the Syrian Golden Hamster trachea	(McDowell *et al.* 1979), (Keenan *et al.* 1983)
Animal airway xenograft models	
· Rat tracheas	(Shimizu *et al.* 1992)
Human airway xenograft models	
· Primary HBEC seeded into denuded rat trachea then grafted into nude mice	(Engelhardt *et al.* 1992) (Engelhardt *et al.* 1995) (Zepeda *et al.* 1995)
· Foetal human epithelial cells seeded onto human foetal tracheas and implanted into SCID mice	(Delplanque *et al.* 2000)
· Human airway epithelial cells seeded onto rat tracheas and implanted into SCID mice	(Dupuit *et al.* 2000)

HBEC: human bronchial epithelial cells

SCID: severe combined immuno-deficient

McDowell *et. al.* were able to regenerate a female Syrian Golden Hamster tracheal epithelium after mechanical injury by scraping with a blunt probe (McDowell, Becci, Schurch *et al.* 1979), (Keenan, Combs and McDowell 1983). Studies in this model have shown a sequential repair mechanism starting with

dedifferentiation, followed by spreading and migration at wound edges, proliferation, and finally redifferentiation again.

Animal tracheal xenograft models have also been developed to study the repair mechanism and the role of airway epithelial resident stem and progenitor cells. One such example was carried out by Shimizu T. where rat tracheas were denuded by repeated thawing and freezing after which they were seeded with adult rat tracheal epithelial cells and implanted subcutaneously into syngeneic hosts (Shimizu, Nettesheim, Ramaekers *et al.* 1992). Briefly, cellular differentiation of tracheal epithelial regeneration was then investigated using a number of epithelial cell-specific markers to identify basal, ciliated, and secretory cells. They observed that at day 4 following implantation, epithelial cells were squamoid with around 1-3 cell layer thick, and contained one cell type, therefore were termed poorly differentiated cells expressing keratin 14 and GSI-B4. The epithelium looked pseudostratified by day 7 with secretory cell-specific marker expression on top of the columnar ciliated cells. Basal cells were also observed by this stage. Therefore, they concluded that all secretory and ciliated cells were derived from the poorly differentiated intermediates observed at day 4.

However, as useful as the above models have proved to be, the histological differences that exist between animals and human airways should be taken into account. The model of Shimizu T. has been adapted for human studies by Engelhardt J.F. (Engelhardt, Yankaskas and Wilson 1992) (Engelhardt, Schlossberg, Yankaskas *et al.* 1995), (Zepeda, Chinoy and Wilson 1995) to try and identify and characterise the human epithelial progenitors. Dissociated human airway epithelial cells were introduced into rat trachea depleted of its own epithelial layer which was then grafted into a recipient immunodeficient nude

mouse. This model was first established to evaluate the efficiency of gene transfer in human airways for cystic fibrosis. However, it was observed that these therapies were successful only when the recipient airway epithelium was undifferentiated and regenerating at high levels (Engelhardt, Yankaskas and Wilson 1992). On the other hand, Zepeda *et. al.* adapted the xenograft model to evaluate cellular proliferation and differentiation in human bronchial epithelium. The individual retrovirus-marked cells were monitored as transgene expressing cells and it was observed that one cell type within the bronchial epithelium was responsible for the regeneration *via* high self renewal capacity and pluripotent development, but this population remains to be characterised (Zepeda, Chinoy and Wilson 1995).

A very similar model has also been developed by Deplanque *et. al.* in humanized severe combined immunodeficient (SCID) mice to investigate potential airway progenitor cells (Delplanque, Coraux, Tirouvanziam *et al.* 2000). Briefly, human foetal tracheal grafts, from which the native epithelium was eliminated, were repopulated with total epithelial cells obtained enzymatically from foetal airways. New formed epithelia were confirmed in sex-mismatched combinations of host and donor tissues. In similar experiments, embryonic rudiments were used as the donor tissue which also replenished the denuded host grafts with all epithelial cells and glands. This open-air xenograft model in nude mice has a very important potential in elucidating the role of inflammation during epithelial regeneration from diseased patients. Finally, this humanized SCID (SCID-hu) mice model has been adapted by Dupuit F. *et. al.* to study the proliferation activity, the differentiation level, and the integrity of the barrier in the adult human epithelium. Similarly to the foetal study, human airway cells were dissociated by enzymatic

dissociation form fresh human airway tissue and were then inoculated to the humanized tracheal grafts eliminated from their epithelium by frequent freezing and thawing (Dupuit, Gaillard, Hinnrasky *et al.* 2000). They observed that the regeneration of a well-differentiated human airway epithelium with normal function in this model followed similar events to the ones seen after injury: cell migration and proliferation, then stratification, and finally differentiation.

3.1.1.2 Animal and human models *in vitro*

Table 3-2: *In vitro* models of airway epithelium

Submerged primary cultures	
· HBEC seeded on feeder cell layers in low serum growth medium	(Lechner *et al.* 1981)
· HBEC seeded on collagen gels in serum free medium supplemented with growth factors	(Lechner *et al.* 1982)
· HBEC seeded on surface coated tissue culture dishes in serum free medium with growth factors	(Masui *et al.* 1986)
· HBEC seeded on plastic tissue culture plates in serum free medium with growth factors	(Chopra D P. 1987)
Air liquid interface (ALI) cultures	
· Guinea pig tracheal epithelial cells seeded onto Whitcutt chamber (with semi permeable gelatin membrane) and fed basally	(Whitcutt MJ 1988)
· Mice tracheal epithelial cells seeded onto tissue culture semi-permeable support membranes in culture medium, fed basally	(Davidson *et al.* 2000)
· HBEC seeded on collagen gel as substratum at ALI for ciliogenesis	(de Jong *et al.* 1994)
· Human nasal epithelial grown at ALI in serum free media (BEGM:DME/F12 with supplements)	(Lee *et al.* 2005)
· HBEC (commercially bought) seeded on polyester Transwell inserts, and fed basally with BEGM:DME/F12 with supplements	(Lin *et al.* 2007)
· 3D tissue model of the human bronchial wall (epithelial cells on Transwell inserts in BEGM: DMEM) at ALI	(Choe *et al.* 2006)
Carcinoma cell lines	
· Immortalized human bronchial epithelial cell line (BEAS- 2B) using SV40 and adenovirus 12	(Reddel *et al.* 1988)
· Transformed bronchial epithelial cells with SV40 (16HBE140-)	(Cozens *et al.* 1994)
· Adenocarcinoma derived epithelial cell line (Calu-3)	(Shen *et al* . 1994)
· Retrovirally infected airway epithelial cells (NuLi-1)	(Hahn *et al.* 1999)

The use of epithelial cell culture techniques that maintain a polarised and well differentiated pseudostratified epithelium, containing mucus-producing cells and cilia on the surface mimicking the epithelium *in vivo*, has been developed over recent years. These epithelial cell culture models serve a number of advantages including: the ability to control the environment for the study of epithelium maintenance, differentiation, and inflammation in health and disease (e.g. asthma, COPD, cystic fibrosis) (Holgate, Davies, Puddicombe *et al.* 2003; Puchelle, Zahm, Tournier *et al.* 2006), elucidation of drug transport pathways since both apical and basolateral membrane surfaces are exposed (Giangreco, Groot and Janes 2007), prevention of non-epithelial cell contamination that may interfere with data analysis, extended epithelial cell viability compared to tissue isolation, and finally minimizing the use of animals (Mathias, Yamashita and Lee 1996). There are three major cell culture systems of airway epithelial cells: organ culture and tissue biopsies, primary cultures, and carcinoma cell lines. Organ cultures and tissue explants were the earliest *in vitro* systems developed for short-term studies (Lane, Miller and Drummond 1976). They were maintained confluent on the basement membrane or on an external substrate respectively. Primary cultures of airway epithelial cells have been developed using mouse, hamster, guinea pig, rat, rabbit, dog, pig, cow, horse, and human (see references in Table 3-2). Human bronchial epithelial cells were usually obtained from outgrowths of normal human bronchial tissue explants and grown in culture on surface-coated dishes using a serum-free medium supplemented with insulin (5 µg/ml), epidermal growth factor (EGF, 5 ng/ml), transferrin (10µ/ml), hydrocortisone (0.2 µM), gentamycin (50 µg/ml), bovine pituitary extract (BPE, 353 µg of protein per ml) on feeder cell layers and collagen gels (Lechner, Haugen, Autrup *et al.* 1981; Lechner, Haugen,

McClendon *et al.* 1982) and surface coated dishes (Masui, Wakefield, Lechner *et al.* 1986). Moreover, in 1987 human airway epithelial cells were cultured and passaged successfully maintained in serum-free medium on a plastic surface exhibiting typical *in vivo* epithelial characteristics (Chopra, Sullivan, Willie, *et.al.* 1987), these have been used for a number of studies. For example, Neugebauer *et. al.* suggested that ECM molecules present in submerged cultures are important for promoting attachment and confluence while the specific shape of the cells and the cell-cell contact are one of the most important signals for differentiation and ciliogenesis (Neugebauer, Endepols, Mickenhagen *et al.* 2003). For ciliogenesis to take place mimicking an adult human epithelium, cells should be floating in the medium forming spheroids (Jorissen, Van der Schueren, Tyberghein *et al.* 1989), attached to collagen gels (Chevillard, Hinnrasky, Pierrot *et al.* 1993) or grown at ALI culture (de Jong, van Sterkenburg, Hesseling *et al.* 1994). Serially passaged normal human bronchial epithelial cells (NHBEC) monolayers were developed in transwell inserts *via* ALI for the evaluation of drug absorption (Lin, Li, Cho *et al.* 2007). Moreover, in 2003, Lopez-Sonza *et. al.* were able and for the first time to successfully culture cells from nasal or bronchial brushings *in vitro* to create polarozed ciliated cell sheets of human bronchial epithelium, enabling the investigation of electrical and secretory properties of the airway epithelium with an added advantage of comparing the role of the epithelium in health and disease (Lopez-Souza, Avila and Widdicombe 2003). Brieflly, they grew the cells on inserts using specialized differentiation media at ALI.

HBEC lines: BEAS-2B (immortalised human epithelial cells using adenovirus 12 and simian virus 40), 16HBE14o- (bronchial epithelial cells obtained form a 1-year old male heart-lung transplant patient and transformed with SV40 large

antigen) and Calu-3 (human bronchial epithelial cell line derived from an adenocarcinoma of the lung) and a relatively new NuLi-1 (infected airway epithelial cells with retroviruses) exist to date with the latter closest to a primary human bronchial epithelium (Ehrhardt, Forbes and Kim 2008). BEAS-2B are grown using submerged culture rather than at an ALI (Ehrhardt, Kneuer, Fiegel *et al.* 2002). One advantage of these cell lines is to reduce the variability that might arise from donor to donor when culturing primary epithelial cells. However, since they are transformed cells, it has to be argued that there is a limit to their value as a model of the epithelium *in vivo*. These cell lines have been used previously to investigate physiological processes in the airway epithelium. 16 HBE14o- and Calu-3 cell lines have been identified as the better differentiated cell lines due to their ability to form polarized cell layers and the ability to express major intercellular junctions including desmosomes and functional tight junctions, and thus are considered suitable drug absorption models (Gruenert, Finkbeiner and Widdicombe 1995). On the other hand, although the BEAS 2B is the cell line most widely used, they have a limited potential in forming drug junctions, and might therefore be unsuitable for drug absorption studies (Forbes 2000)

Recently, primary HBEC were immortalized by retrovirus infection to express cell cycle protein cdk4 in order to stop the inhibition of cells growing on plastic in normal atmospheric conditions *via* inhibitory effects of p16 and over-expression of the catalytic component of human telomerase reverse transcriptase (hTERT) (Vaughan, Ramirez, Wright *et al.* 2006). The cells were then grown on top of a type I collagen gel containing fibroblasts. In these cultures, a pseudostratified columnar epithelium with cilia, goblet cells and basal cells was established. Further studies using organotypic constructs or xenograft models will help

determine the potential use of tissue engineering in vivo as a therapy for damage or diseased organs replacement.

Choe *et. al.* in 2006, described a protocol to establish a 3-D tissue model of the human bronchial wall which includes a well-differentiated epithelium, sub-epithelial fibroblasts and type I collagen, useful for physiological and pathophysiological studies (Choe, Tomei and Swartz 2006). They used commercial HBEC, grown on transwell culture plates using BEGM: DMEM (1:1 ratio) submerged for seven days, and which then were raised to air liquid interface for a further seven days. This system could easily be adapted for work with biopsy-derived cells or embryonic stem cells for tissue engineering work.

3.1.2 Regeneration of the airway epithelium after injury

3.1.2.1 Repair of the airway epithelium *via* migration and proliferation

The integrity of the airway epithelium is compromised frequently during adult life as a result of continuous exposure to various inhaled toxins and pathogens present in the atmosphere. It is well adapted to maintaining its function and structure *via* an established reparative mechanism involving epithelial cells and potential resident stem or progenitor cells present in their niches throughout the airway lining. Very little is known about the mechanisms underlying epithelial repair processes due to the complexity of the respiratory tree.

The structure and functions of the airway epithelium are discussed in the chapter 1. Briefly, there are eight morphologically distinct epithelial cell types that could be classified into three groups according to their functional and biochemical criteria: basal, columnar ciliated and secretory (mucous goblet and serous) cells (Knight and Holgate 2003). Of those in the basal layer may be the most important

in wound repair. They are attached to the basement membrane *via* hemidesmosomes (Wang, Evans, Cox *et al.* 1992) anchoring the columnar and secretory cells through desmosomes providing an anchoring junction of the columnar cells to the basement membrane through the basal cells (see Figure 1-2).

Several *in vivo* and *in vitro* assays and wound models have been developed historically to study human airway epithelial biology and wound repair. *In vitro*, confluent cell monolayers have been mechanically wounded by gently scraping the layer using a fine pipette tip (Leir, Baker, Holgate *et al.* 2000). Another wounding technique involves the deposition of a drop of 1 M sodium hydroxide (NaOH) on the primary cell layer followed by phosphate buffer saline (PBS) or normal media to neutralise it (Puchelle 2000) (Zahm, Kaplan, Herard *et al.* 1997) creating a standard wound every time. Another approach to investigate the role of the epithelium alone, without other outside interference, involved collected human bronchial tissues which were injured with a frozen 2 mm diameter metallic probe thus only the epithelium is eliminated leaving the ECM healthy (Legrand, Gilles, Zahm *et al.* 1999). *In vivo* injury models have also been used by Pilweski *et. al.* in 1997 to study the integrin expression of the damaged epithelium (Pilewski, Latoche, Arcasoy *et al.* 1997). Human bronchial sections were transplanted into SCID mice after which an injury was created using gauge needle on the walls of the xenograft (Pilewski JM 1994).

The airway epithelial repair mechanism has been extensively investigated previously either through following repair processes histologically over time or through cell culture models. The injury level can vary from the loss of surface epithelial permeability, loss of airway epithelial cells, to partial shedding or

complete denudation of the basement membrane. A series of cellular events take place following injury starting with dedifferentiation of cells, rapid spreading and migration of the cells at the edge of the wound, proliferation, and then differentiation again (McDowell, Becci, Schurch et al. 1979). These events have been observed in both *in vivo* and *in vitro* models (Figure 3-1) but still very little is known about the specific molecular mechanisms controlling these events.

Spreading and migration of cells

It has been established that migration of cells at the edge of the wound is the first step after desquamation of the epithelium in the repair process through the protrusion of lamellipodium extension (plasma membrane) due to cytoskeleton reorganization. This takes place after G actin and filamentous (F)-actin polymerization leading to an in increase in F actin in the lamellipodia of the basal cells forming adhesions with ECM (Puchelle 2000) suggesting a role for basal cells in wound repair. To study the migratory potential of epithelial cells, Zahm *et. al.* were able to track the spreading cells using the DNA binding Hoechst 33258 fluorescent dye after which fluorescence images were captured (Zahm, Kaplan, Herard et al. 1997). A trajectory-based method and video microscopy techniques were adapted to investigate the rate of spreading of the migratory cells. It was observed that the higher the migration speed, the closer the distance from the wound edge. In 1998, Kim S.J. *et. al.* demonstrated a role for EGF in wound healing through a concentration dependant stimulation of guinea pig tracheal epithelial cells (GPTEC) migration. A small mechanical wound was created on GPTEC monolayer followed by capturing video microscopy over a 24 hr period to calculate the wound area remaining. In addition, collagen/laminin-binding

integrins α2β1, and α6β4 altered distribution facilitated spreading and migration in epithelial cells (Pilewski, Latoche, Arcasoy et al. 1997).

New epithelial cell proliferation and re-differentiation

Following migration of cells to cover an injury in the lung, proliferation takes place to replace cells and maintain the structure of the epithelium. The airway epithelium is amongst the slowly renewing organs together with the pancreas, liver, and thymus. Rapid renewing organs, such as the intestinal epithelium, are believed to turn over with very high kinetics in the normal steady state being replaced every 5 days approximately (Stripp 2008). Another distinction between rapid and slow turnover tissues is their response to injury where in the slow turnover seen in lung epithelium, proliferation is stimulated after injury and is dramatically increased following the migration and spreading of cells to cover the particular wound depending on the level and position of damage (Puchelle 2000). Several reports, including data from our laboratory in Nottingham, have suggested the presence of resident stem cells proliferating in response to injury in the airway epithelium (Stripp and Reynolds 2008) (Neuringer and Randell 2004) (Wadsworth, Nijmeh and Hall 2006). Resident adult stem cells can be defined as a self-renewing population of cells undergoing division throughout the adult lifetime giving rise to more differentiated cell types within a specific organ where each system has been evolved to suit its own unique environment (Rawlins 2008). Transient amplifying (TA) cells are one level down the hierarchical stem cell organization defined as the immediate daughter of all adult stem cells which divide and gives rise to the differentiated cell types to maintain the tissue but with a more limited self-renewal capacity (Stripp 2008). However, since the lung epithelium is considered a slowly self-renewed organ, one type of cell population

suspected to be responsible for the repair mechanism are called 'facultative progenitor cells'. This population was observed to have roles in the normal and damaged airway as shown in unpublished data by Stripp and Reynolds, and were seen to have differentiated characteristics when quiescent (Stripp 2008).

Several growth factors have been noted to mediate bronchial epithelial repair *via* cell migration or proliferation stimulated by injury. EGF is able to accelerate wound repair in the airway epithelium independently of cell proliferation (Kim, McKinnis, Nawrocki et al. 1998). For example, BrdU incorporation into undifferentiated and differentiated human bronchial epithelial cells (HBEC) was seen to be reduced at 24 hrs post injury after EGF treatment and an increase in cellular BrdU labelling in wounded cultures treated with anti-EGFR antibody suggesting a repair effect of EGF at early time points *via* migration independent of cell proliferation (Wadsworth, Nijmeh and Hall 2006). The potent endothelial cell mitogen, VEGF, has been observed to increase cell proliferation and thus may assist in the wound repair process where BrdU-labeled epithelial cells increased in VEGF-treated lung tissues (Wadsworth, Nijmeh and Hall 2006) although the mechanism is not known yet.

Additional studies here evaluated the potential role of nitric oxide in repair processes. Physiological concentrations of nitric oxide (NO) can promote airway epithelial wound repair *via* migration *in vitro* which is associated with increased expression of MMP-9 (Bove, Wesley, Greul *et al.* 2007). On the other hand, it has been observed that increased synthesis of NO has been associated with altered wound healing, reduced epithelial wound repair and thus may contribute to the remodelling process seen in chronic inflammatory conditions (Guo, Comhair, Zheng *et al.* 2000). Elevated levels of NO inhibit epithelial cell migration and

wound repair *via* the mitogen-activated protein kinase (MAPK) phosphatase (MKP)-1 mechanism, inhibition of extracellular-regulated kinase 1 and 2 (ERK1/2) activation, as well as activation of the transcription factors hypoxia-inducible factor 1α (HIP-1α) and p53 (Bove, Hristova, Wesley *et al.* 2008).

As discussed earlier, a number of inflammatory cells such as neutrophils are recruited to the site of injury as a host-defence mechanism. One group of products that are released by neutrophils to kill microorganisms at the site of inflammation are called defensins, and recent data have suggested that they may also contribute to epithelial repair (Aarbiou, Ertmann, van Wetering *et al.* 2002). After scrape-wounding the NCI-H292 cell line, it was observed that defensins induce airway epithelial wound closure in a dose and time-dependant manner, *via* activation of the ERK1/2, p38, c-jun N-terminal kinase (JNK), and the EGFR. As wound be expected, wound closure involved cell migration and proliferation. Moreover, neutrophil defensins were observed to elevate mucin gene expression of airway epithelium (Aarbiou, Verhoosel, van Wetering *et al.* 2004).

Airway epithelial cells also continuously interact and detect microorganisms through Toll-like receptors (TLRs) leading to induction of pro-inflammatory mediators. It has been observed that activation of TLR2 and TLR 5 (after infecting human airway epithelial cells *in vitro* with Staphyococcus aureus) induce cell migration, wound repair, and proliferation (Shaykhiev, Behr and Bals 2008). Thus, epithelial cells are able to sustain their integrity in a non-inflammatory manner by sensing microbes *via* TLRs.

The expression of a family of zinc-dependant neutral endopeptidases that degrade the ECM, called matrix metalloproteinases (MMP), has been observed in injured airway epithelium. For example, MMP-7 and -9 are produced by epithelial cells

after mechanical wounding, and are required for cellular migration (Legrand, Gilles, Zahm et al. 1999). Another MMP present in pathological states is membrane type 1 MMP (MT1-MMP) and this is also produced in the abnormal airway epithelium. MT1-MMP is not present in normal airway epithelium but is upregulated in airways of subjects suffering from COPD and asthma (Ohuchi, Imai, Fujii *et al.* 1997). When MT1-MMP knockout (KO) mice were exposed to naphthalene, a decrease in airway epithelial cell proliferation was observed. In addition a novel role for MT1-MMP in airway epithelial repair has been established *via* a keratinocyte growth factor receptor (KGFR)-dependant role in clara cell proliferation (Atkinson, Toennies, Holmbeck *et al.* 2007).
Moreover, TGF-β and hepatocyte growth factor (HGF) are secreted and activated following injury to the airway epithelium. HGF is secreted by fibroblasts while the HGFR is expressed at the basolateral surface of human bronchial cells, thus HGF is essential for normal epithelial integrity in the airways (Myerburg, Latoche, McKenna *et al.* 2007). In addition, it has been observed that in response to mechanical wounding, a rapid induction of integrin-dependant activation of TGF-β occurs, leading to slower wound closure (Neurohr, Nishimura and Sheppard 2006).

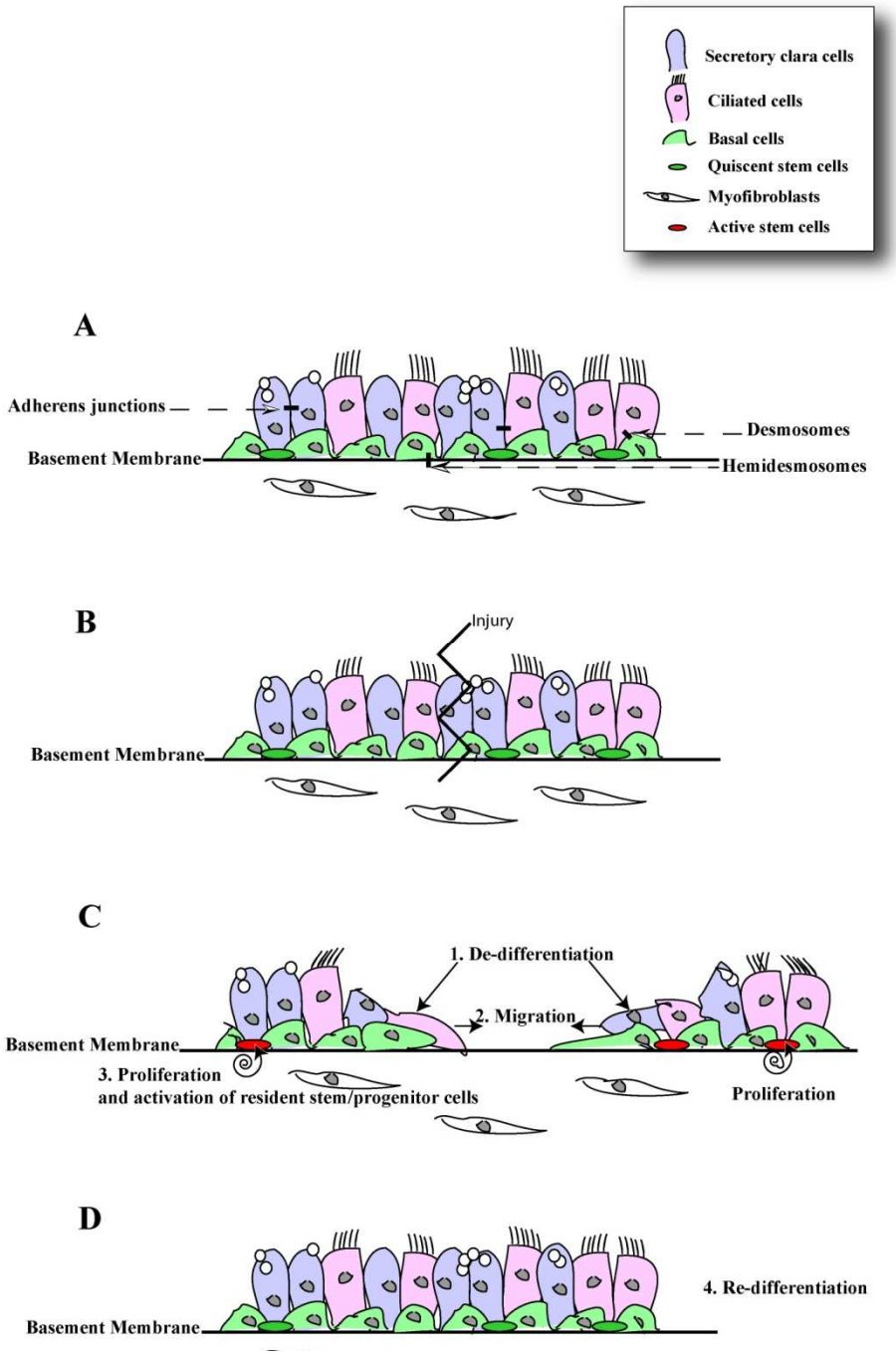

Figure 3-1: A schematic diagram of airway epithelial regeneration after injury
(A) is a representation of an airway epithelium consisting of basal, ciliated, and secretory cells attached to the basement membrane *via* hemidesmosomes. When the airway epithelium is injured (B), cells at the edge of the wound undergo de-differentiation (1), migration (2), activation and proliferation of quiescent resident stem cells away from the wound (3) (C). Re-differentiation of the epithelial cells takes place, with ciliated and secretory cells (D).

3.1.2.2 Epithelial cell-extracellular matrix (ECM) interactions in airway epithelial regeneration

As described above, the airway epithelial regeneration is clearly a complex process involving both resident stem/progenitor cells (discussed in the next section) and also factors able to control this process. Secretion of ECM proteins and their interactions with ECM is a part of the wound healing process together with the release of cytokines and chemokines and modulators of cell migration, proliferation and differentiation (Sacco, Silvestri, Sabatini *et al.* 2004). An up-regulation of cell adhesion receptors, not normally observed in the normal basement membrane, binding to the inflammation matrix proteins has been found post injury of the airway epithelium.

On the other hand, matrix metalloproteinases (MMP), secreted by repairing cells, have a direct role in wound healing in remodelling the provisional matrix. One example is MMP9 (or gelatinase B) involvement in the repair program through migration of basal cells (Buisson 1996). Others are MMP3, 11, and 7, all expressed by epithelial cells. MMP7 plays a role in the repair through migration as well as the shedding of E-cadherin which is required for the repair process (McGuire, Li and Parks 2003). MMP3 and 11 are also involved in epithelial cell migration and ECM remodelling, however, these MMPs are expressed by basal cells that also express the mesenchymal marker vimentin suggesting a mesenchymal phenotype is important for cell migration (Buisson AC 1996). In addition to the role of MMPs in migration, MMP2, and 9 are also involved in cell proliferation during wound healing (Sigurdson, Sen, Hall Iii *et al.* 2003).

Non-integrin mediated cell-ECM interactions have also been shown to have a potential importance in affecting bronchial epithelial repair. Hyaluronic acid (HA)

receptor CD44 is a cell surface receptor for the matrix proteoglycan hyaluronate as well as collagen I, IV, and fibronectin (Sacco, Silvestri, Sabatini et al. 2004) and is thought to be involved in cell-cell adhesions, cell-ECM interactions, homing and cell migration. CD44 expression has been observed to be altered after cell damage specifically its interaction with HA ; it was up-regulated in the epithelium of asthma subjects (Leir, Baker, Holgate et al. 2000). We have also shown CD44 up-regulation at the margins of scrape-wounded bronchial epithelial cells *in vitro* with a role in cell migration and other processes in the late phases of epithelial repair (Wadsworth, Nijmeh and Hall 2006). It has also been shown that cytokine expression during inflammation of the airway epithelium plays a role in the general modulator of epithelial wound healing- CD44-HA interactions, regardless of CD44 expression (Leir, Holgate and Lackie 2003). CD44 includes a family of glycoproteins, all encoded by the same gene, with 80-200kDa protein size. A role for CD44 in leukocyte activation and in tumour progression, as well as re-epithelisation of corneal epithelium has been suggested previously (Marhaba and Zöller 2004) (Yu, Guo and Zhang 1998).

3.1.2.3 Resident stem/progenitor cells of the airway epithelium

Basal cells and non-ciliated secretory epithelial cells have been shown to exhibit proliferative capacity and progenitor characteristics (Keenan, Combs and McDowell 1983; Boers, Ambergen and Thunnissen 1998; Borthwick, Shahbazian and Krantz 2001). Stem cells niches were investigated in transgenic mice by Borthwick *et. al.* (Borthwick, Shahbazian and Krantz 2001) by studying a subset of cells identified as the label retaining cells (LRC), characterized by their ability to retain a label of bromodeoxyuridine (BrdU) or [3H] thymidine (both are

proliferation markers that are incorporated into cell DNA). A short pulse of label can be used to identify rapidly proliferating TA cells, while a long-term pulse will mark progenitor/stem cells with slower turnover (Borthwick, Shahbazian and Krantz 2001). Borthwick *et. al.* used LRC to determine which murine tracheal epithelial cells were retaining a long-term BrdU labelling. An injury was required to stimulate proliferation in normal epithelium. BrdU positive cells were noted alongside the basal and luminal tracheal positions with LRC localized to gland ducts. Schoch et al were able afterwards to isolate basal cells using the Keratin 5 promoter driven enhanced green fluorescent protein (EGFP) expression as a marker and observed a 12-fold increase in the ability to generate large colonies *in vitro* compared to EGFP-negative basal cells (Schoch, Lori and Burns 2004). These studies were a step closer to isolating the airway epithelial stem/progenitor cells which were suspected to be basal cells. Another approach to investigating the airway epithelial stem/progenitor cells responsible for restoration following injury is by the use of cell-surface antigens. A study by Hajj *et. al.* demonstrated that basal cells are at least TA cells of the airway epithelium (Hajj, Baranek, Le Naour *et al.* 2007) by using CD151 and tissue factor (TF), both basal cell markers, for epithelial sorting after which the sorted basal cells were able to regenerate a pseudostratified epithelium capable of expressing MUC5AC (a mucin marker) and cystic fibrosis transmembrane receptor (CFTR, a chloride channel expressed on the surface of ciliatedcells) amongst other specific epithelial differentiation markers when grown on collagen IV-coated membranes. A study by Hong *et. al.* was carried out using dual immunofluorescence of mice airway epithelial tissues treated with naphthalene using the biotinylated Griffonia Simplicifolia isolectin B4 (GSI-B4, a specific epithelial basal marker), Clara cell

secretory protein (CCSP), keratin-14 (K14, another basal cell marker), with BrdU (Hong, Reynolds and Watkins 2004). They observed an increased proliferation of non-ciliated basal cells following injury (by depletion of CCSP-expressing cells (CE)) leading to a restoration of the epithelium.

However, the strong proliferative capacity of secretory cells following physical or chemical injury has also suggested their definition as progenitor candidates. In an attempt to select a subset of airway epithelial cells, Deplanque *et. al.* followed a flow cytometry approach using an array of cell surface markers including, lectin ligands, CD44 and CD166, adhesion molecules and the aquaporin-3 (AQP3) water channel (Avril-Delplanque, Casal, Castillon *et al.* 2005). They implanted human foetal tissues subcutaneously into SCID mice flanks after being sorted using a flow cytometry. They observed that $AQP3^{+}$ (a basal cell marker) cells grafted were not as efficient as $AQP3^{-}$ cells in their epithelium restoration concluding that secretory cells had progenitor cell activity. However, it was still suggested that progenitor cells are present on both basal and supra-basal subsets within the human airways, despite the fact that basal cells took five months to eventually differentiate into a healthy epithelium. Moreover, both Clara cells (most abundant in distal human lung and proximal and distal rodent and rabbit's lung) and pulmonary neuroendocrine cells (PNEC) have been proposed as progenitors of the airway epithelium. Using naphthalene treated mouse airway, a rare population of dual positive cells (co-expressing both Clara cell secretory protein (CCSP) and calcitonin gene-related peptide (CGRP)) were localized to neuroepithelial bodies (NEB) suggesting NEBs serve an environment for the variant Clara cells (vCE) progenitor population that are resistant to naphthalene injury (Reynolds, Giangreco and Power 2000). Following that observation, Hong

et. al. , in an attempt to prove that PNECs are a stem cell pool capable of re-epithelisation, tested the rate of cell proliferation within the NEB microenvironment and demonstrated that NEB contains slow-cycling populations (LRCs) but that PNECs failed to renew the epithelium after CE ablation (Hong, Reynolds and Giangreco 2001). Finally, another microenvironment besides NEB recently thought to provide a stem cell niche is the broncheoalveolar duct junction (BADJ) thought to contain broncheoalveolar stem cells (BASC) in mice co-expressing both surfactant protein C (spc), and CCSP (Kim 2007).

3.2 Objectives

The aim of the studies described in this chapter was to further characterise the differentiated human bronchial epithelial wound repair model *in vitro*, using primary epithelial cell cultures grown under air liquid interface (ALI) conditions. This model was then used to investigate repair mechanisms, proliferation and to attempt identification of the epithelial cell types responsible for healing the injured epithelium.

3.3 Methods

Primary human bronchial epithelial cells (HBEC, donor 1) were cultured as described in section 2.1.1.5 and differentiated as described in section 2.1.1.6. For wounding experiments, differentiated HBEC were wounded as described in section 2.1.1.7 in 12-well transwell plates while undifferentiated HBEC were in 24-well plates. Measurements of wound area were done using SPOTCam software at the times specified in the relevant following sections. An outline of the wound was created using the software tools and measurements of the wound area were given. This was done at different times post-wounding (0-28 hrs range).

3.3.1 Characterisation of *in vitro* differentiation HBEC model at ALI

To determine the differentiation level of HBEC grown at ALI, cells were fixed at week 1, week 2 and week 3 of ALI using 4% formaldehyde at 4ºC overnight. Immunofluorescence was carried out on the fixed cultures as described in section 2.2.1 then treated with the following primary mouse monoclonal antibodies: anti-MUC5AC (for mucin cells, at 1:1500 dilution), anti-β-tubulin IV (for ciliated cells, at 1:1500 dilution). Goat-raised anti-mouse secondary antibody conjugated to Alexafluor488 (1:250) was then added to detect the bound primary antibodies. To visualize filamentous (F) actin, cells were incubated with 1:40 dilution of AlexaFluor488-conjugated phalloidin (Molecular Probes) for 30 min at room temperature (Kikuchi, Shively, Foley *et al.* 2004). Nuclei were counterstained using 1 µg/ml DAPI. Undifferentiated cultures in 24-well plates were also treated with the above antibodies as control cultures and all sources of antibodies

purchased are listed in Appendix A. Laser scanning confocal microscopy was performed using a Zeiss Axio Observer D1, Hamamatsu electron multiplier CCD Camera C9100-13, with a Yokogawa spinning disk system. Volocity 4.2.1 analysis software (Improvision) was used to analyze the images.

3.3.2 Proliferation assay

To study the proliferation capacity of HBEC in undifferentiated or differentiated states, cells were grown in 24-well plates or 12-well transwell plates in BEGM (1 ml per well) or BEDM respectively (section 2.1.1.5). Cell layer(s) were wounded and then fixed at 0, 4, 8, 16, 24, and 48 hrs post-wounding using 4% formaldehyde at 4ºC overnight. Unwounded controls were also set up for each of the time points. Immunofluorescence (IF) was then carried out on all cultures according to section 2.2.1 using the nuclear proliferation marker Ki-67. Primary antibodies used were: mouse monoclonal anti-Ki-67 (1:100 dilution, MIB-1, Abcam) for undifferentiated cultures, and rabbit polyclonal anti-Ki-67 (1:50, ab833, Abcam) for differentiated cultures that were dual stained with epithelial markers and thus the need for both monoclonal and polyclonal mouse and rabbit proliferation antibodies. The relative specificity of both antibodies was first investigated by dual staining HBEC cultures with both the monoclonal and polyclonal primary anit-Ki67 antibodies. Bound primary antibodies were detected using goat-raised anti-mouse and anti-rabbit secondary antibodies conjugated to Alexafluor488 and RhodamineRedX, respectively (Molecular Probes, 1:250). Eight random fields per well were digitally captured with a 20x objective lens. Ki-67 labelling index was expressed as the mean number of labelled cells per field ± SEM at each time point.

3.3.3 Dual staining of HBEC with ki-67 and specific epithelial cell markers

To investigate the cell types involved in wound repair of the airway epithelium *in vitro*, differentiated HBEC were wounded and fixed at different times post-wounding, and were studied using a panel of airway epithelial specific markers shown in Table 3-3 together with the proliferation marker Ki-67 in Table 3-4. Dual staining was performed by treating the samples first with rabbit polyclonal antibodies detected with RhodamineRedX secondary antibody, and then by treating with the mouse monoclonal primary antibodies where detection was done by AlexaFluor488.

As previously described, laser scanning confocal microscopy was performed using a Zeiss Axio Observer D1, Hamamatsu electron multiplier CCD Camera C9100-13, with a Yokogawa spinning disk system. Images were captured in slices which were around 0.1 µm thick. Volocity 4.2.1 analysis software, Improvision, was used to analyze the images.

Table 3-3: Specific epithelial cell markers

Antibody name	Concentration	Source	Characteristic
Mouse monoclonal anti-CD44	1:100	Development Studies Hybridoma Bank (DSHB), Clone H4C4	Specific for the human hyaluronate receptor CD44
Mouse monoclonal anti-CK14	1:200	Chemicon, Hampshire, UK	Cytokeratin 14, epithelial basal cell markers
Rabbit polyclonal anti-CC26	1:500	Chemicon, Hampshire, UK	Clara cell specific marker
Rabbit polyclonal anti-CCSP	1:100	Abcam	Clara cell secretory protein
Rabbit polyclonal anti-AQP3	1:500	Abcam	Aquaporin-3, foetal basal cell marker

Table 3-4: Proliferation markers

Antibody name	Concentration	Source	Characteristic
Mouse monoclonal anti-Ki-67	1:100	DAKO, clone MIB-1	Nuclear proliferation marker
Rabbit polyclonal anti-Ki-67	1:50	Abcam, clone ab8333	Nuclear proliferation marker

3.3.4 Relative CD44 mRNA expression in HBEC

RNA was extract from differentiated wounded HBEC grown at ALI, at 0, 24, 48, and 72 hrs post-injury as described in section 2.4. Reverse transcriptase (RT) polymerase chain reaction (PCR) was then carried out as described in section 2.4.2.3 to synthesise cDNA which was then tested using the housekeeping gene GAPDH as described in section 2.4.2.1. The relative mRNA expression was then quantified using real-time quantitative PCR (section 2.4.3). Primers/Probe set was designed using Beacon Designer 5.0 Software and probes were obtained as FAM-labeled Taqman probes. Table 3-5 lists the sequence of primers and probe. Figure 3-2 shows the standard curved that was used to validate the assay.

Data was analyzed using the comparative ΔCt method as described in section 2.4.3. All values were normalised against the endogenous housekeeping genes, 18s or HPRT (see Figure 2-8 in section 2.4.3 for HPRT and 18s mRNA expression by differentiated HBEC). Final values represent the mean fold difference, as a percentage compared to 0hrs, of relative mRNA expression ± SEM of four separate experiments. Two donors were used for these experiments, each including two replicates.

Table 3-5: Primers and probe used

# of bases	Primer Name	Primer sequence 5'-3'	Position	Product length
24	CD44-F1	GCTGCTACTTCTTAAAACCTCTGC	exon 1 position 162	106
24	CD44-R1	GGTTGAAAACAGTGACCTAAGACG	exon 1 position 267	

# of bases	Probe Name	Primer sequence 5'-3'	Position
24	CD44-P	AGCGAGCGAAGGACACACCCAAGC	exon 1 position 234

Probes were 3' TAMRA, 5' 6-FAM purchased from Eurgentec S.A

CD44 accession number: NM_001001392

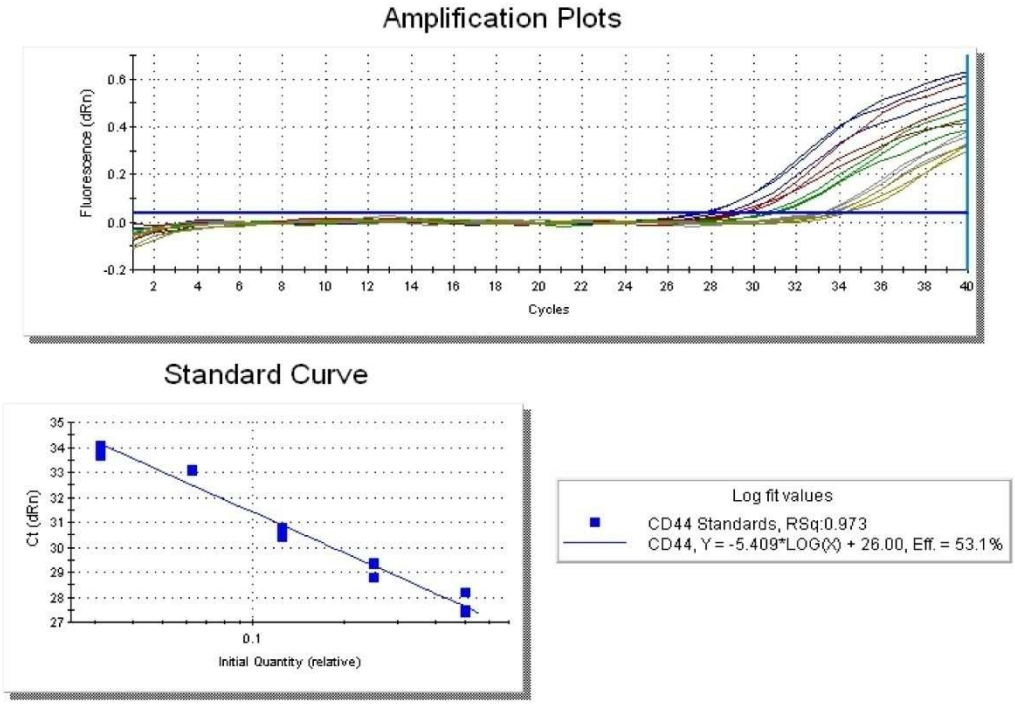

Figure 3-2:Real time PCR standard curve for CD44.
Amplification plot, and a standard curve for CD44 mRNA expression by differentiated HBEC is shown to assess the efficiency of the real time taqman assay using the CD44 primer/probe set designed using Beacon Designer 5.0 software. Efficiency of 53.1% (100% is the optimum value) can be observed with little variability between triplicate repeats.

3.4 Results

3.4.1 Primary human bronchial epithelial cells (HBEC) are capable of generating a pseudostratified mucociliated epithelium *in vitro*

A *in vitro* model of primary human bronchial epithelial cells (HBEC) was adapted from Danahay *et. al.* (Danahay, Atherton, Jones et al. 2002). Undifferentiated HBEC, purchased commercially from Lonza ,were grown in submerged culture on polyester microporous membranes in transwell inserts for seven days followed by air liquid interface (ALI) for a further 21 days for differentiation (as described in section 2.1.1.6). A pseudostratified epithelium was observed at day 28 with well developed ciliated cells present on the surface, as seen in the scanning electron micrographs taken by Dr. Samuel Wadsworth in our laboratory (Figure 3-3 below) (Wadsworth, Nijmeh and Hall 2006). Accumulation of mucus on the surface of the transwell membranes was observed during the time course of differentiation.

Differentiated HBEC were characterised by studying their expression of the differentiation markers MUC5AC (for mucin cells), β-tubulin IV (for ciliated cells), and filamentous (F) actin (for organization and inter-connectedness), demonstrated by laser confocal microscopy images in Figure 3-4, Figure 3-5, and Figure 3-6. Undifferentiated HBEC, grown on plastic in submerged conditions, demonstrated a different phenotype to differentiated cells grown on polyester microporous inserts at ALI for one, two, or three weeks (designated as ALI 1, 2, or 3 respectively). An increase in cell density in ALI conditions was observed, marked by nuclear counter-staining using DAPI (blue, Figure 3-4). Stronger inter-connectedness in ALI 3 cultures was observed compared to undifferentiated and

ALI 1 and 2 cells, indicated through F-actin phalloidin staining (Figure 3-4 A, B, C, and D).

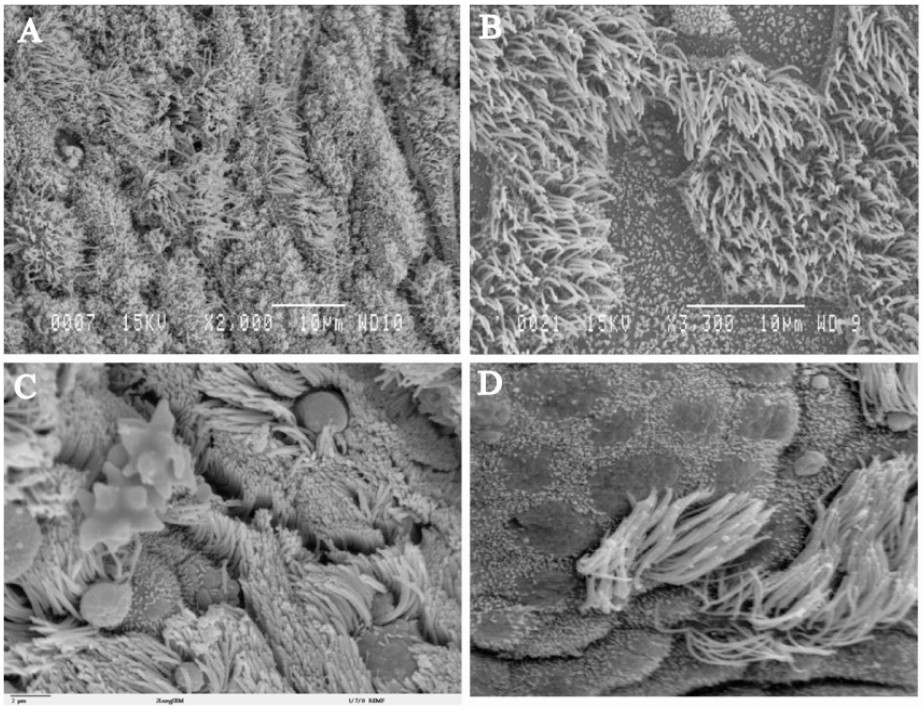

Figure 3-3:Ciliated nature of HBEC *in vitro*.
Scanning electron micrographs of differentiated HBEC at ALI demonstrate the ciliated nature of the apical cells (A). Higher magnification shows well developed cilia in this *in vitro* model (B). C and D were taken from http://remf.dartmouth.edu/images/mammalianLungSEM/, A and B were taken from (Wadsworth, Nijmeh and Hall 2006).

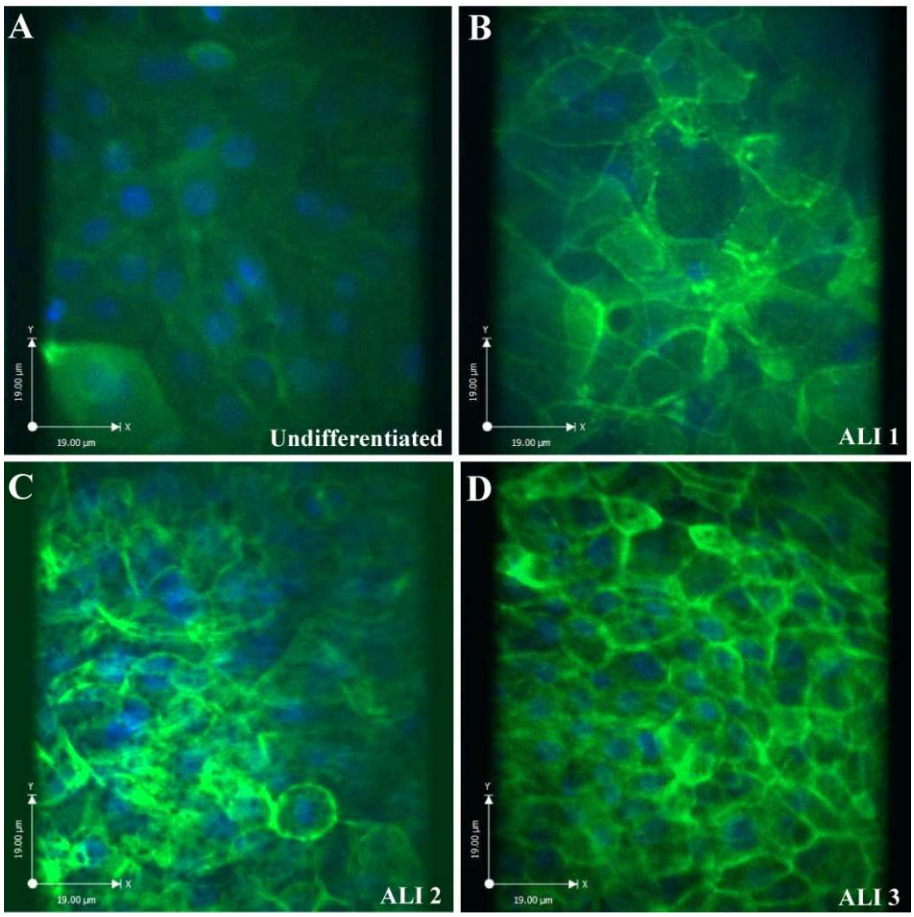

Figure 3-4: Representative F-actin fluorescence images of HBEC.
Confocal images show F-actin phalloidin staining (green 2°) of HBEC in undifferentiated cells (A), and differentiated cultures at ALI 1, ALI 2, and ALI 3 (B-D). Cells were counterstained with DAPI (blue). Images are representative of two individual experiments each done in duplicates and random images were chosen. (x40 magnification).

Moreover, expression of the ciliated marker β-tubulin IV was not detected in undifferentiated or ALI weeks 1 and 2 cultures, as observed in the images of side projections of the cultures (Figure 3-5 B, C, and D). β-tubulin IV positive cells (Figure 3-5 A), however, were seen on the apical surface of ALI 3 cultures (Figure 3-5 E). Similarly, side projections of images of undifferentiated ALI 1 and 2 cells did not show expression of MUC5AC (Figure 3-6 B, C, and D), while positive expression of MUC 5AC was seen at the apical layer of ALI 3 cells only (Figure 3-6 A and E). Side projections demonstrated that HBEC grown in submerged conditions on plastic formed a monolayer of cells compared to late

ALI conditions whereby a multi-cellular layer was apparent (Figure 3-5 B-E, Figure 3-6 B-E).

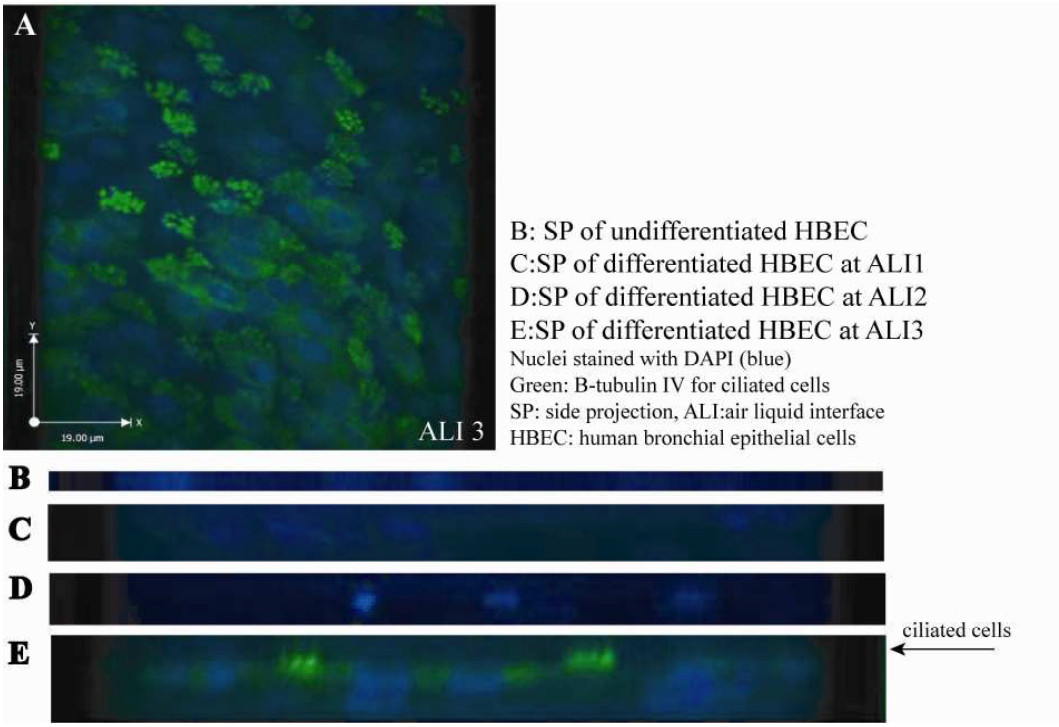

Figure 3-5: Representative β-tubulin IV fluorescence images of HBEC.
β-tubulin IV positive expression (green) was seen only in differentiated cultures at ALI 3 (A + E). B-E are side projections of the cultures showing expression of β-tubulin IV only at ALI week 3 (E, green) on the apical surface (arrow in E). Side projections also show a multi-cellular epithelium when differentiated (C-E), compared to a monolayer of cells in undifferetiated HBEC (B). Cells were counterstained with DAPI (blue). Images are representative of two individual experiments each done in duplicate and random fields were chosen (x40 magnification).

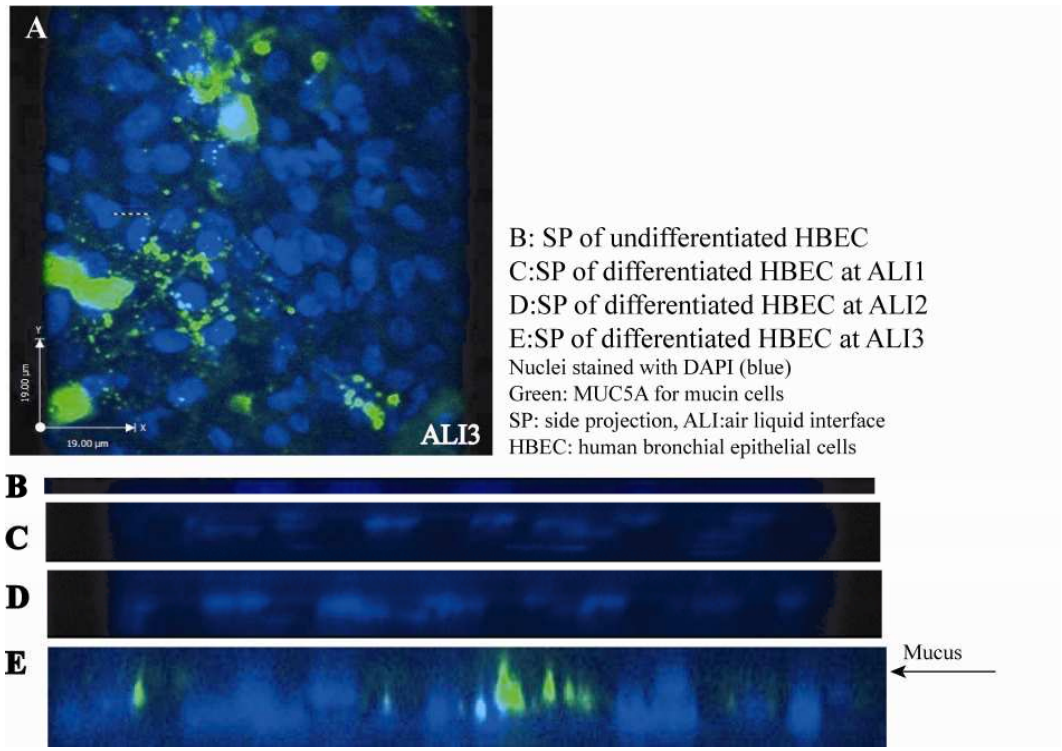

Figure 3-6: Representative MUC 5AC fluorescence images of HBEC.
MUC 5AC positive expression (green) was seen only in differentiated cultures at ALI 3 (A + E). B-E are side projections of the cultures showing expression of MUC 5AC only at ALI week 3 (E, green) on the apical surface (arrow in E). Side projections also show a multi-cellular epithelium when differentiated (C-E), compared to a monolayer of cells in undifferentiated HBEC (B). Cells were counterstained with DAPI (blue). Images are representative of two individual experiments each done in duplicate and random fields were chosen(x40 magnification).

3.4.2 Bronchial epithelium wound repair model

In order to reach a better understanding of wound repair, either in a healthy or a diseased epithelium, appropriate models were established to study the mechanism *in vitro* (as discussed in section 3.1.1.2). The *in vitro* model established in our laboratory was discussed in section 3.4.1. HBEC were allowed to reach complete mucociliary differentiation at ALI and were then scrape-wounded using a sterile p200 pipette tip. Scanning electron microscopy (SEM) images (Figure 3-7, obtained by Dr. Samuel Wadsworth) of differentiated HBEC grown at ALI show the scrape-wound (0.5 mm thickness) where the cell layers have been scratched down to the porous polyester membrane (red arrow, Figure 3-7 A). It can also be

observed that repair takes place by 24 hrs post-wounding leaving a 'scar' on the original wound area (Figure 3-7 B)(Wadsworth, Nijmeh and Hall 2006).

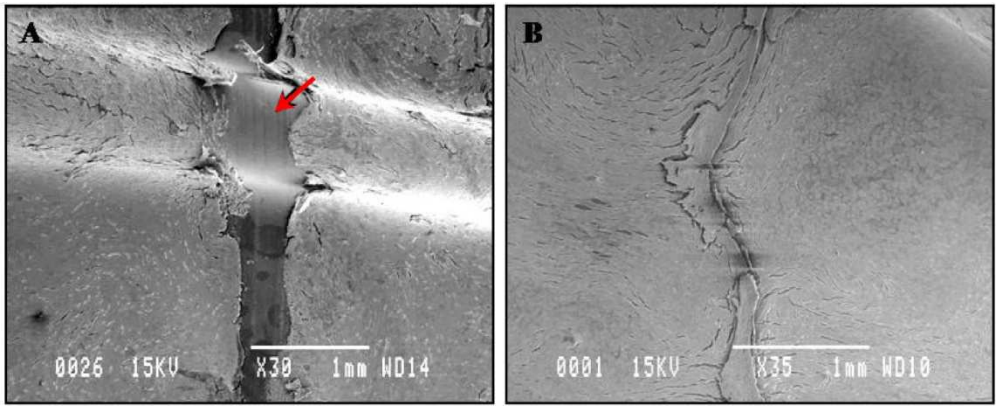

Figure 3-7: Wounding model of HBEC.
Scanning electron micrographs showing differentiated HBEC ALI cultures with a scrape-wound removing all cells down to the porous membrane (red arrow) of the transwell inserts with an approximately 0.5mm wound thickness (A). Rapid repair takes place with complete wound healing by 24 hrs (B) leaving a 'scar' on the original wound area. (Wadsworth, Nijmeh and Hall 2006)

The time course of wound repair was then studied using undifferentiated HBEC grown in 24-well plates and differentiated HBEC on 12-well transwell inserts. These were scrape wounded as described in section 2.1.1.7 and digital images were captured using a x2.5 objective lens at 0-48 hrs post-wounding (Figure 3-8 A-F and Figure 3-9 A-F). The area of the wound was measured using SPOTCam Advanced software and graphs were plotted with time point post-wounding versus the wound area in microns^2. Statistical analysis was done with one-way ANOVA and Dunnett's multiple comparison post-test using GraphPad Prism 5.0 software. Analysis was carried out on four different experiments each containing two wounds for undifferentiated cultures (a total of 8 wounds); and six individual experiments with two wounds each (a total of 12 wounds) for differentiated cells.

The graphs in Figure 3-8 and Figure 3-9) are representative of mean ± SEM of n wounds.

Complete wound closure occurred more rapidly in differentiated cultures than in undifferentiated cells (compare Figure 3-8 and Figure 3-9). For example, at 20 hrs post-wounding, all differentiated cultures showed 100% healing (n=12) whereas undifferentiated cultures (n=8) showed an average of 87 ± 96% of the wound area covered only by a later time point (48 hrs). In undifferentiated HBEC, healing starts at 4 hrs post-wounding followed by a significant decrease in wound surface area at 8, 16, 24, and finally 48 hrs (all $p < 0.05$ of baseline). In differentiated HBEC, the wound area was seen to significantly decrease ($p < 0.0001$) by 8hrs followed by 100% wound closure by 20 hrs post-wounding.

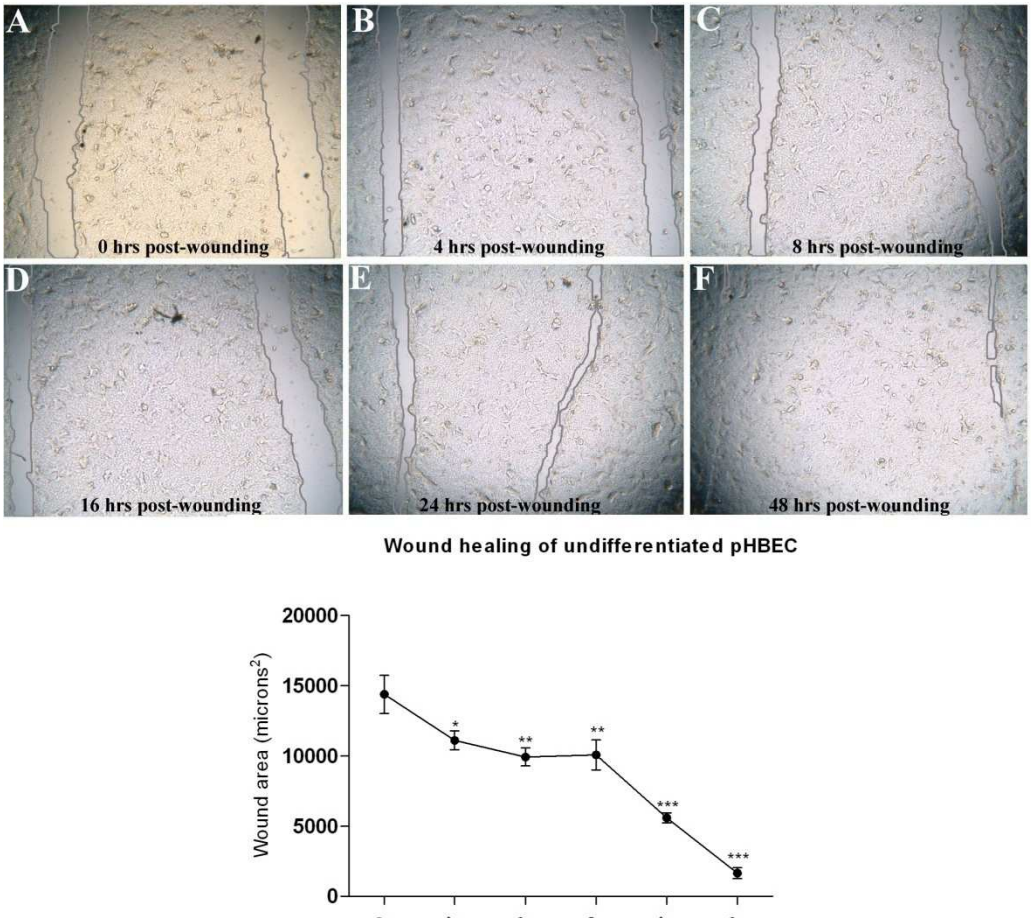

Figure 3-8: Wound healing of undifferentiated HBEC.
Brightfield images show the two parallel scrape wounds on undifferentiated HBEC at 0 hrs (A), 4 hrs (B), 8 hrs (C), 16 hrs (D), 24 hrs (E), and 48 hrs (F) post-wounding. The graph shows the mean wound area at each time point ± SEM of 8 separate wounds (in 4 different experiments). Statistics were calculated with a one-way ANOVA analysis and Dunnett's multiple comparisons post-test representing repair vs. 0hr baseline . *, **, and *** all represent $p < 0.05$.

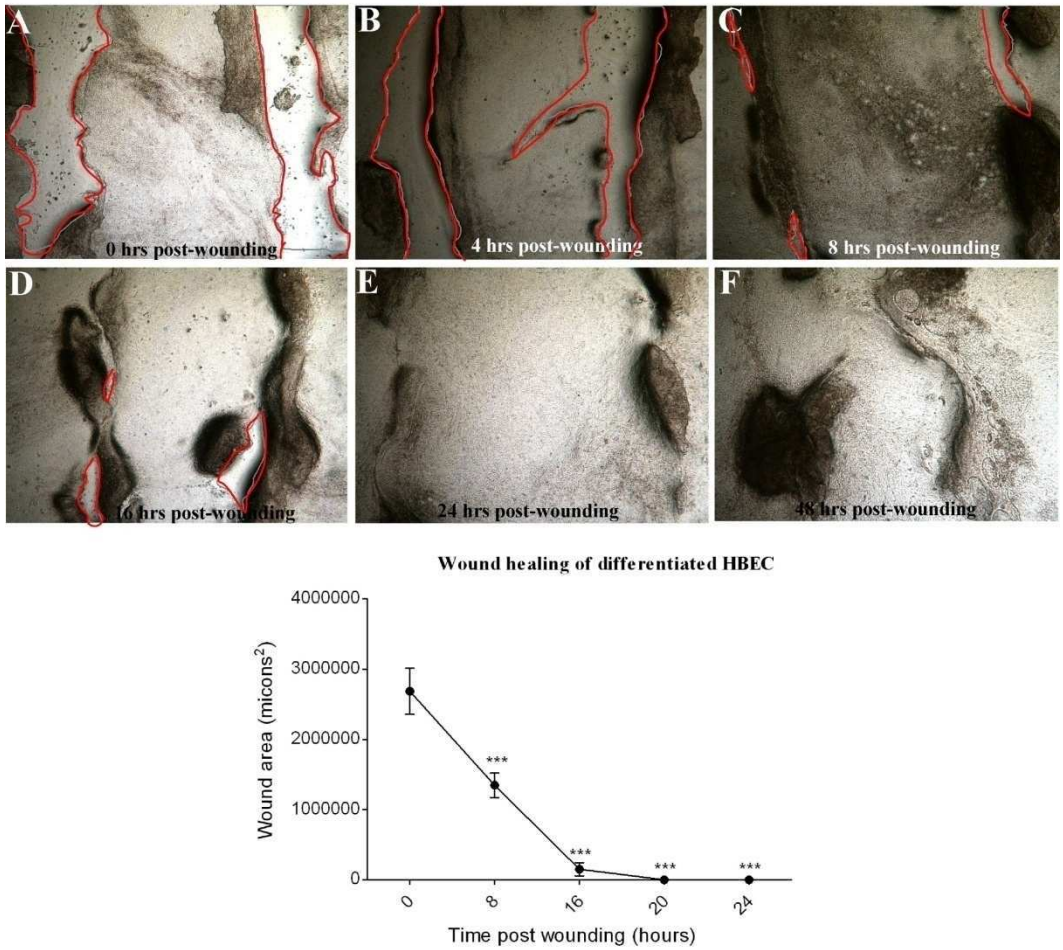

Figure 3-9: Wound healing of differentiated HBEC.
Brightfield images show the two parallel scrape wounds on differentiated HBEC at 0 hrs (A), 4 hrs (B), 8 hrs (C), 16 hrs (D), 24 hrs (E), and 48 hrs (F) post-wounding. The graph shows the mean wound area at each time point ± SEM of 12 separate wounds (of 6 experiments). Statistics were calculated with a one-way ANOVA analysis and Dunnett's multiple comparisons post-test representing repair vs. 0hr baseline. *** represents $p < 0.05$.

3.4.3 New cell proliferation post HBEC wounding

Having demonstrated that complete wound healing in differentiated HBEC cultures occurs by 20 hrs post-injury and at a faster rate than undifferentiated cultures, the cellular events involved in repair mechanism were then investigated, beginning with proliferation. Following migration of cells at the edge of a wound as a first step in the repair mechanism, proliferation of new cells away from the wound might be expected to maintain a constant supply of epithelial cells capable of regenerating a healthy epithelium. Proliferation assays were carried out on both undifferentiated and differentiated HBEC (section 3.3.2) using the proliferation marker Ki-67. Ki-67 is a protein present in the nuclei of human cells in all phases of the cell cycle except the resting stage G_0 and thus is a widely accepted proliferation marker (Gerdes 1990). Figure 3-10 A and B are representative immunofluorescence images of undifferentiated and differentiated HBEC, respectively, stained for nuclear Ki-67 (green). An increase in proliferation was seen in differentiated HBEC post-wounding which was significant ($p < 0.001$, $n=6$) by the 24 hrs time-point compared to its unwounded control culture (Figure 3-10). Interestingly, an immediate significant increase in proliferation was observed in wounded differentiated HBEC compared to unwounded cells (Figure 3-10 C, $p=0.024$, paired t-test) but this remains to be further investigated. These experiments were then repeated in undifferentiated HBEC, and in contrast to the differentiated model, no significant increase ($p > 0.05$) in proliferation was seen following wounding, although an increase in proliferation compared with basal was seen in both wounded and unwounded cultures at 48 hrs (Figure 3-10 D) as would be expected for normal growth of these cells in culture.

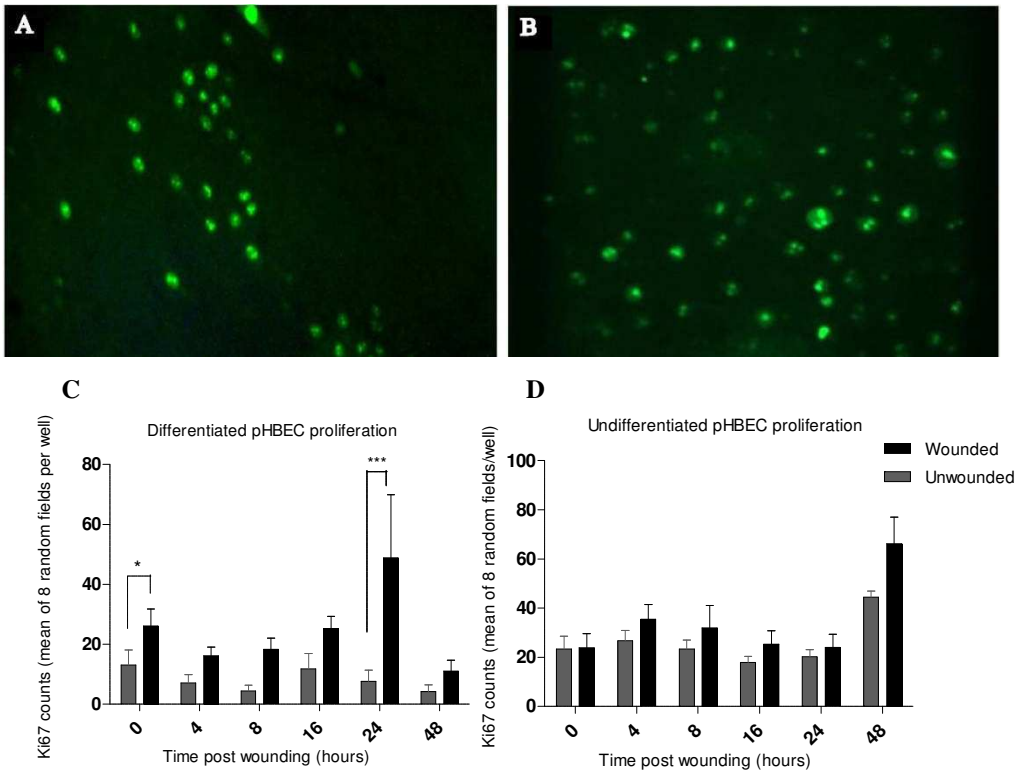

Figure 3-10: Proliferation of HBEC post-wounding.
A and B are representative immunofluorescence images of fields of cells distant from the wound margin showing nuclear Ki-67 staining (green, x20 magnification) of differentiated and undifferentiated HBEC respectively. Graphs show mean Ki-67 counts ± SEM of 6 separate experiments in differentiated (C) and undifferentiated (D) HBEC. Statistical analysis was done by a two-way ANOVA and a Bonferroni post-test for both graphs and a paired t-test at 0hrs in C. *** represents $p<0.001$, * represents $p=0.024$.

3.4.4 Characterisation of human bronchial epithelial cells (HBEC) involved in wound repair *in vitro*

The previous figures show an increase in proliferation taking place at around 24 hrs post-wounding for differentiated HBEC which is after complete wound closure, which occurred by 20 hrs post-injury. The next step was to determine which types of cells were proliferating or migrating in the wounded cultures. To this end, differentiated and undifferentiated HBEC were immunofluorescently stained with antibodies against epithelial cell-specific markers (Table 3-3), as well as the proliferation marker Ki-67. Two antibodies against Ki-67 were used, a

mouse monoclonal (detected with an AlexaFluor 488 secondary antibody, green) and a rabbit polyclonal (detected with a RhodamineRed X secondary antibody, red). This was important since dual staining experiments required both secondary antibodies depending on which primary antibodies were used against the different epithelial cell-specific markers. Thus, it was important to first validate the two Ki-67 antibodies, by dual staining HBEC with both. It was confirmed that both the antibodies were recognizing the same set of cells (Figure 3 11).

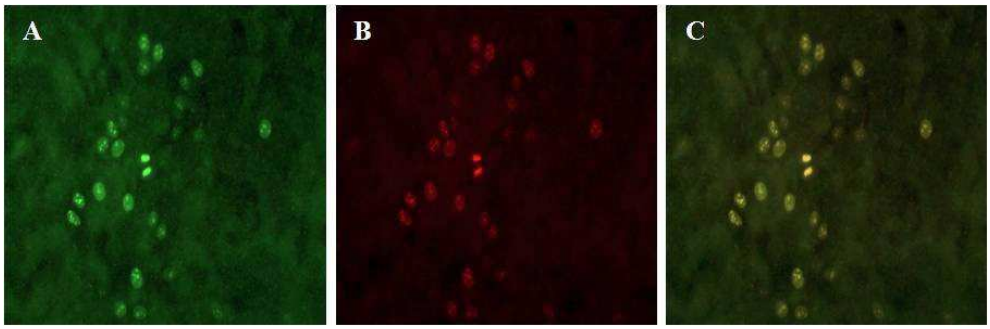

Figure 3-11: Dual Staining with Ki-67 monclonal and polyclonal antibodies.
Mouse monoclonal MIB1 (A, green secondary), rabbit polyclonal ab833 (B, red secondary), and merged (C, yellow). (x40 magnification)

It was observed that both cell populations were stained positive for basal cell markers CD44 and CK14 (Figure 3-12 A-D) but not the basal marker, AQP3. Moreover, to detect non-ciliated Clara cells, Clara cell-26 (CC26), and Clara cell secretory protein (CCSP) expression were investigated. Positive expression of CC26 was observed in both undifferentiated and differentiated cultures (Figure 3-12 E and F), although CCSP expression was not detected (possibly due to the quality of the antibody used in immunofluorescence technique).

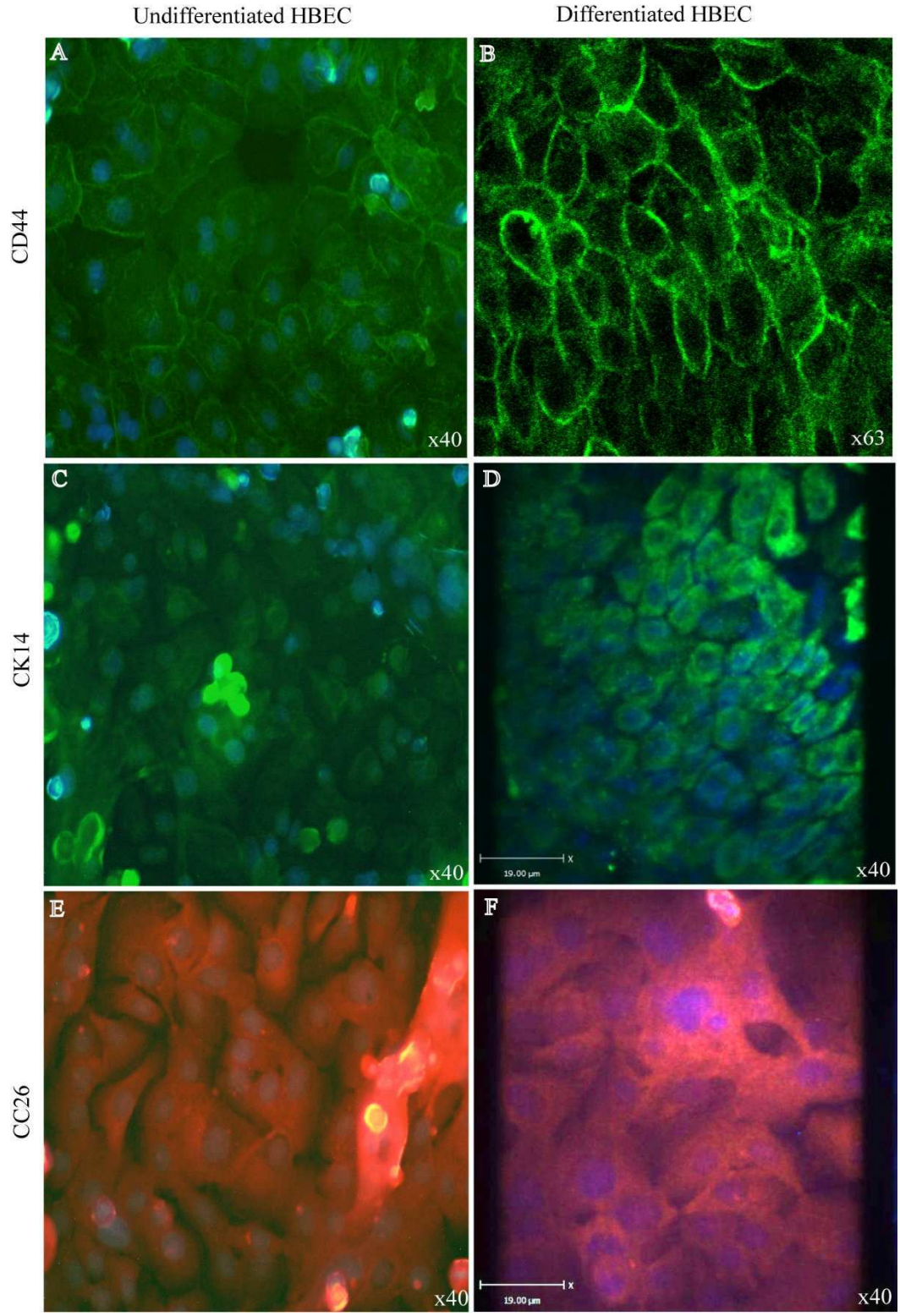

Figure 3-12: Staining for epithelial cell specific markers.
Immunofluorescence images of undifferentiated (A, C, E) and differentiated (B, D, F) HBEC using basal and non-ciliated cell markers. Both cell cultures were positive for basal cell markers CD44 (green, A and B), CK14 (green, C and D), and the non-ciliated Clara cell marker CC26 (red, E and F). Nuclei were counterstained with DAPI (blue). The images are representative of two separate experiments both carried out in duplicates and random fields were digitally captured. Staining for the basal marker AQP3 and the non-ciliated cell marker CCSP was not detected.

Side projection images of differentiated HBEC cultures captured with confocal microscopy showed CD44 and CK14 expression at the basal layer in contact with the substratum, and CC26 expression at the apical layer (Figure 3-13 A, B, and C). It was observed that proliferating Ki-67 positive cells were present at the basal layer of the cultures, co-expressing Ki-67 and CD44 or CK14 (Figure 3-13 A-B respectively). This implies the role of basal cells as potential progenitor cells responsible for wound repair.

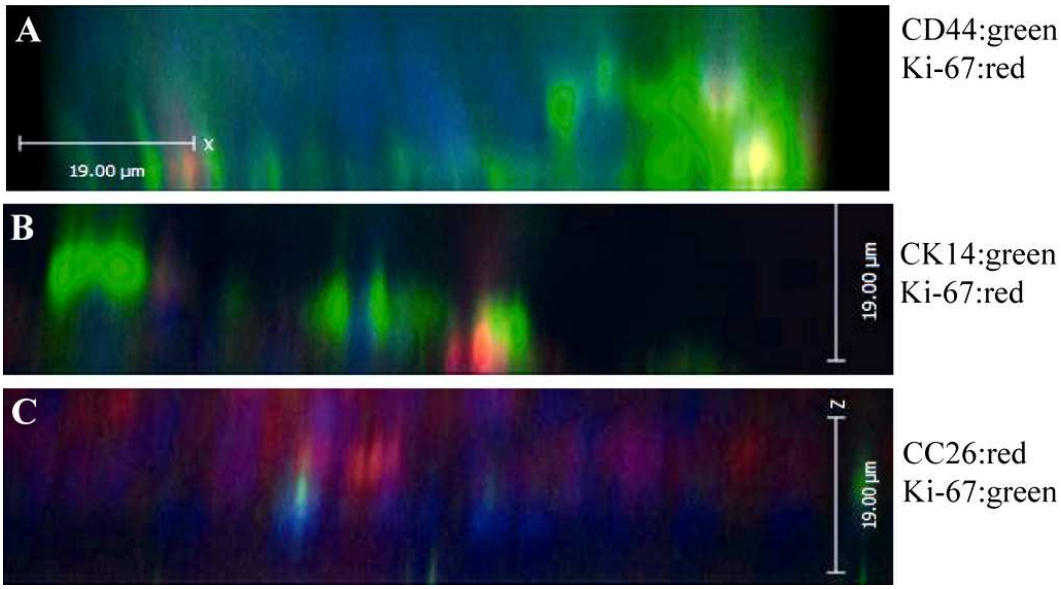

Figure 3-13: Side projections of proliferating cells post-wounding differentiated HBEC. Dual staining of differentiated HBEC cultures show positive staining of CD44 (green, A), CK14 (green, B), CC-26 (red, C). Ki-67 positive staining (red, A-B, and green, C) was observed at the basal layer of the cultures in side projection images. Nuclei were counterstained with DAPI (blue) (40X objective, n=2).

In Figure 3-14 below, basal cells appear to be involved in wound closure; shown by increased staining of CD44 and CK14 at wound edges (marked by white arrows), compared to areas away from the wound, as early as 0-4 hrs till at least 18 hrs following wounding. Very few proliferating cells were seen on the wound edges, suggesting that increased staining CD44 and CK14 were not due to the

presence of new cells. We have previously observed that basal cells migrate towards the denuded area by 8 hrs post-wounding, with lamellopodia following visible filopodia and extending out from the migratory cells towards the wound.(Wadsworth, Nijmeh and Hall 2006).

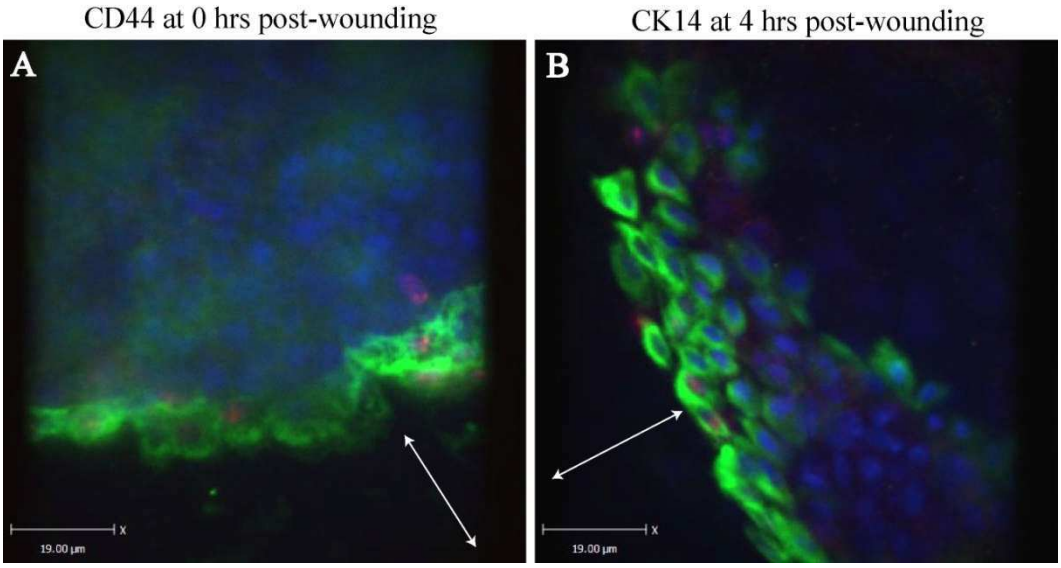

Figure 3-14: CD 44 and CK14 expression at wound edge.
CD44 (green, A) and CK 14 (green, B) increased staining at wound edges of differentiated HBEC at 0 and4 hrs post-wounding respectively. Wound is marked by white arrows. Few basal cells were seen proliferating at the wound edge: CD44/Ki-67 double positive (green/red) and CK14/Ki-67 double positive (green/red) cells. Nuclei were counterstained with DAPI (blue). (40X magnification, n=2).

3.4.5 CD44 mRNA expression post-wounding HBEC

CD44 was seen to be up-regulated at wound margins post-wounding, and was seen to be present in both migration and proliferation during wound repair. Determination of relative CD44 mRNA labels by differentiated HBEC at a range of time points post-wounding was carried out. Total RNA was extracted from wounded differentiated HBEC, at 0, 24, 48, and 72 hrs post-wounding as described in 2.4.1. This was followed by reverse transcriptase to synthesize cDNA, then real time PCR was carried out on the samples. Validation for the

assay was performed by assessing the efficiency of the CD44 assay and determining the optimum sample dilution, *via* a standard curve created with cDNA from differentiated HBEC (Figure 3-2). Relative mRNA values were calculated using the comparative ΔCt method. Initial experiments were performed to assess the use of 18S and HPRT as housekeeping genes (Figure 2-8). HPRT was chosen for two reasons: first, the Ct values obtained were closer to those for CD44, and second, because there was less variation observed between sample measurements in values. Thus; Figure 3-15 shows normalization against HPRT. Statistical analysis was calculated using a two-way ANOVA with a Bonferroni multiple comparison post-test, using GraphPad Prism 5.0 software.

No significant increase ($p=0.173$) in CD44 mRNA expression was seen post-wounding compared to unwounded cultures (Figure 3-15), suggesting that the increase in CD44 protein determined by immunofluorescence seen in the previous section may not be related to increased gene expression. However, the increase in CD44 above was seen in the time range of 0-24 hrs post-wounding, and CD44 mRNA expression was not investigated at those early time points.

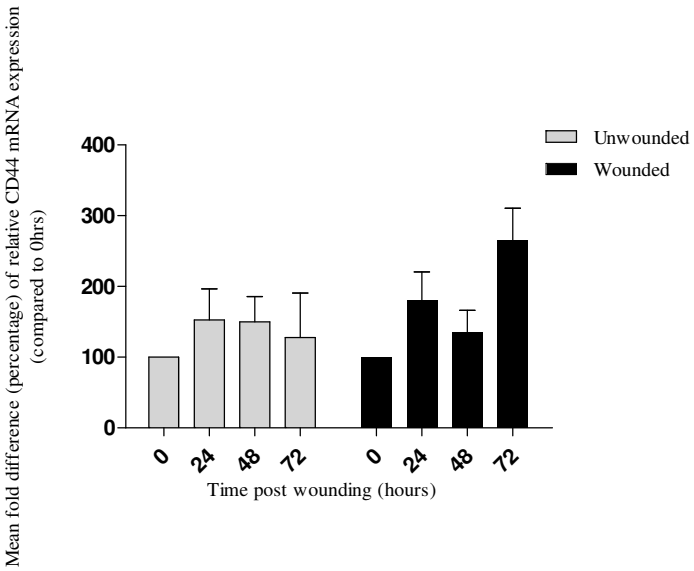

Figure 3-15: Relative CD44 mRNA expression by differentiated HBEC post-wounding. No significant difference in CD44 mRNA expression in injured cultures (p=0.173). Statistical analysis was carried out using a two-way ANOVA with a Bonferroni multiple comparisons post-test. Graph shows mean fold difference (percentage) ± SEM of four separate experiments carried out in triplicates and data was normalized to HPRT.

3.5 Discussion

3.5.1 A primary human bronchial epithelial cell (HBEC) wound repair model

A primary differentiated human bronchial epithelial cell (HBEC) model, adapted from previously published methods (Danahay, Atherton, Jones et al. 2002), was established and characterised to assess differentiation and reliability of the model for epithelial function studies. This model employs the air liquid interface (ALI) condition, seeding epithelial cells on transwell inserts, using specialized bronchial growth medium. Compared to other *in vitro* and *in vivo* models (described in Table 3-1 and Table 3-2), this model serves several advantages, including: easy access to cells with the ability to control environmental conditions, less use of animals with the added advantage that findings in human primary cell systems are likely to be more physiologically relevant, and finally ease of individual cell measurements. When characterising this model, a pseudostratified multilayered epithelium, similar to that *in vivo*, can be observed, containing ciliated cells (β-tubulin-IV at the apical layer), secretory cells (MUC5Ac at the apical layer), and basal cells (CD44 and CK14 on the basal layer). Filamentous actin also proves the interconnectedness of the cells in culture. In asthma and COPD, it has been shown that the airway epithelial damage contributes to airway remodelling possibly due to altered regulation of the repair process (Holgate 2008) (Jeffery 2001). In order to study the effects of injury, a scrape wound was created on the surface of cells and the healing process was monitored. This was used as it was felt to be a closer representative of the epithelial desquamation seen in asthma than the damage that is caused for example by toxic insults. It was observed the wound was completely healed by 20 hrs post-wounding in differentiated cultures leaving a ‘scar’ where

the original wound was created. However, the scrape wound was not healed even at a later time (48 hrs post-wounding) in undifferentiated HBEC.

3.5.2 Proliferation as one mechanism of scrape-wound repair *in vitro*

Repair involves two potential processes; cell migration and cell proliferation. In the differentiated cultures, epithelial cells were seen to start migrating at 0-4 hrs post-wounding up until 20 hrs, where complete wound closure was apparent in all wounded cultures. This was followed by a five-fold increase in proliferation at around 24 hrs post-wounding compared to normal controls (monitored by labelling with anti-Ki-67 antibody), to potentially maintain a constant number of cells during the healing process. It was interesting to see that there was a significant increase in proliferation in wounded cultures immediately after wounding (0hrs) compared to unwounded controls. This could be explained by an immediate response to loss of epithelial cell-cell contact resulting in intracellular signalling throughout the cultures as a result of injury. In undifferentiated HBEC, no change in proliferation was detected between wounded and unwounded cultures, although there was an overall increase in proliferation at late time points (by 48 hrs). This agrees with the hypothesis that the epithelium has a slow turnover of cells in the steady state. The increase in proliferation observed with time in undifferentiated cultures might be due in part to culture conditions since the wound was still not completely healed at 48 hrs post-wounding; proliferation was increased at that time point in both uninjured and injured cultures.

Previous studies have also shown that the first step of repair is migration of cells at the wound margins by lamellipodia (Zahm, Kaplan, Herard et al. 1997). This work used an *in vitro* model of human respiratory epithelium wound repair, where

epithelial cells were dissociated from human nasal polyps and cultured on collagen I matrix and chemically wounded. Migration was followed by proliferation of cells away from the wound (Puchelle 2000).

The wound model described can also potentially be used to reflect diseases characterised by repeated injury such as asthma and COPD (Wadsworth, Nijmeh and Hall 2006). It was possible to repeatedly wound these differentiated cells *in vitro* every 48-72 hrs (ensuring at least 75% of the wound was healed by that time) 8-12 times, creating a chronic injury model to study potential therapeutic agents which might influence repair, as well as defining the key pathways involved in epithelial repair. It was observed that the healing process following chronic wounding is similar to the process seen with acute wounding as described in this thesis, at least for the first 8-12 wound cycles, after which the cultures reached a repair 'crisis', where they were incapable of further repair. It was also observed that cultures treated with dexamethasone (an anti-inflammatory glucocorticosteroid) were able to repair over increased cycles of injury before reaching 'crisis'.

3.5.3 Basal cells are responsible for repairing the wound by migration followed by new cell proliferation *in vitro*

The findings described above were followed by investigating the phenotype of cells seen to repair the acute wound. In the HBEC model, dramatic CD44 and CK14 up-regulation at wound edges was observed as early as 0-4 hrs post-wounding, suggesting a role for migratory basal cells, at the early stages of wound repair. CD44 and CK14 expression was also detected at the basal layer of the cultures, and Ki-67 positive cells were co-expressing CD44 or CK14, suggesting that basal cells are also involved in proliferation. There were more proliferating

cells away from the wound, with very few Ki-67 positive cells at the wound edges. These findings suggest the migration and proliferation are two separate events taking place independently, since both events were taking place at different times and areas. This suggests a role of basal cells, or at least a subpopulation of basal cells, as a progenitor (stem) cell population responsible for wound repair in the bronchial epithelium.

In order to reach a better understanding of the involvement of CD44 in wound repair, which was seen to be increased at wound edges, as well as being involved in proliferation, relative CD44 mRNA expression was investigated in wounded differentiated HBEC. There was no significant difference between uninjured and injured cultures, which may suggest that the increase seen in CD44 protein expression was not due to increased gene expression. It has to be noted that since CD44 protein increase was observed at 24 hrs post-wounding and because CD44 mRNA expression was not investigated for time points earlier than 24 hrs, an early transient increase in CD44 mRNA cannot be excluded. Some technical difficulties emerged when carrying out Real Time PCR experiments. It was difficult to extract RNA from the differentiated HBEC grown on microporous membranes: this might have an effect on the integrity of the RNA although 240:280 ratios were generally high despite low yields. Moreover, as discussed before, the 12-well transwell inserts do not contain a large amount of cells compared to tissue culture flasks, and thus the procedure proved to be time consuming. CD44 involvement in wound repair has been previously reported (Leir, Baker, Holgate et al. 2000). It is a major receptor for hyaloronan, fibronectin, collagen, and some cytokines; and connects the extracellular environment to the inside of the cell and actin cytoskeleton, thus it may play a

role in repairing the damaged epithelium (Holgate 2000). Expression of CD44 isoforms was observed to be elevated in the epithelium of subjects with asthma and a bronchial epithelial repair model (Lackie PM 1997) (Leir, Baker, Holgate et al. 2000), suggesting a role in the pathology of the disease. However, *in vivo* studies show that although CD44 expression is increased, it does not occur in cell-matrix interaction areas, so the molecule must be participating in cell-cell communication (Lackie PM 1997). Since in asthma and some other respiratory diseases, it has been well established that the repair process is altered, the model described in this chapter could serve as good basis for understanding the mechanisms involved, investigating different wound responses of the disease, and possibly test potential therapeutic agents.

In summary, the data presented in this chapter provide characterisation of the processes involved in and *in vitro* model for the study of human airway epithelium wound repair. In the next chapter, the profile of inflammatory molecules secreted by these cultures following injury has been investigated.

Chapter 4. Secretory Profile of Bronchial Epithelium during Wound Healing

4.1 Introduction

In the previous chapter, I described a series of experiments designed to characterise the properties of a differentiated human bronchial epithelial model and mechanisms underlying wound repair. The work described in this chapter examines mediator production in this model.

4.1.1 Inflammatory function of the epithelium

The airway epithelium and its functions have been described in section 1.1.2. As the first contact with the environment, the epithelium has a number of key regulatory functions. A range of cytokines are produced by the respiratory tract epithelium in response to insults and these may either participate in the maintenance of inflammation in the airway epithelium in airway diseases or facilitate repair mechanisms. There are extensive data examining the potential role of both anti and pro-inflammatory cytokines in airway disease such as asthma and COPD: in both these candidates alteration in epithelial cytokine production may occur (discussed in detail later in this chapter). This chapter describes the profile of mediator production by the human airway model system in the presence or absence of wounding.

4.1.1.1 Cytokines and chemokines

Cytokines are soluble polypeptides and glycopeptides, usually of < 80 kDa in mass. They are involved in cell-cell interactions and primarily located in the local milieu. Cytokines are rarely individually produced, but rather simultaneously with other cytokines in certain patterns, resulting in amplification loops. These networks may also be negative in effect, where the production of one cytokine can inhibit the secretion of another. They generally function by binding to specific cell-surface receptors. Cytokines can also be classified functionally, as pro-inflammatory (e.g. lymphokines), chemoattractant (e.g. chemokines), anti-inflammatory cytokines, and growth factors (Borish and Steinke 2003). Lymphokines, produced by lymphocytes include: IL-2, IFN, TNF, and these are secreted by Th1 cells to trigger cell-mediated immunity responses (Viallard, Pellegrin, Ranchin *et al.* 1999). IL-4, IL-5, IL-6, IL-10, and IL-13, are secreted by Th2 cells and are responsible for mast cell and eosinophil recruitment and activation (Chung, Barnes 1999) (Chung 2001). Amongst the chemokines involved in airway disease, IL-8, growth related oncogene (GRO)-α, and ENA-78, are responsible for neutrophil activation and recruitment to the site of inflammation (Lukacs, Hogaboam, Kunkel *et al.* 1998). Chemokines function through cognate G protein coupled receptors. For example, RANTES is thought to be a chemoattractant for eosinophils and monocytes, and has been observed to be secreted by the human bronchial epithelial cell line BEAS 2B when stimulated by TNF- α (Stellato, Beck, Gorgone *et al.* 1995). Finally, MIP-1α, MCP-1, MCP-3, MCP-4 have also been seen to be involved in eosinophil recruitment to the airways which might result in airway epithelial damage (Lukacs, Standiford, Chensue *et al.* 1996) (Paine, Rolfe, Standiford *et al.* 1993)

This chapter describes the secretory profile of the human bronchial epithelial cell (HBEC) wound repair model *in vitro*, emphasizing the airway epithelium as not just a target for inflammation, but as a potential active source of the cytokines contributing to the inflammatory processes seen in airway disease.

4.1.1.2 Epithelium dysfunction and cytokine secretions in asthma

In asthma, the bronchial epithelium is structurally disturbed, resulting in incomplete repair, chronic inflammation, and an altered profile of the secretion of growth factors and inflammatory mediators. These processes may contribute to airway remodelling (**Naylor** 1962) either directly or indirectly. Figure 4-1 below summarizes some of the important cytokines secreted by the epithelium in asthma. IL-5, RANTES, and eotaxin have been shown to be secreted by the airway epithelium, stimulating Th2-like inflammation (Holgate 2007). In addition to RANTES, IL-16 has also been shown to be produced by epithelial cells; both can act as chemoattractants for eosinophils. Cultured human bronchial epithelial cells produce granulocyte CSF (G-CSF), and GM-CSF, promoting the survival of neutrophils *in vitro* (Cox G 1992) and eosinophils. The chemokine MCP-1 has been shown to be secreted on the apical surface of rat alveolar type II cells when grown *in vitro* on inserts, potentially activating macrophages in the alveolar space (Paine, Rolfe, Standiford et al. 1993), and possibly stimulating Th2 polarization. TNF-α, IL-1β, and IL-6 are produced by both epithelial cells and macrophages, in an autocrine loop. Other growth factors have also been observed to be secreted by the epithelium in asthma, such as platelet derived growth factor (PDGF), and fibroblast growth factor (FGF), both of which may be responsible for fibroblast and airway smooth muscle proliferation. The Th1 chemokine, interferon (IFN)-

inducible protein 10 (IP-10), has been shown to be elevated in a murine asthma model after exposure to allergen (Medoff, Sauty, Tager *et al.* 2002). The study showed that mice over-expressing IP-10 significantly exhibited increased airway hyperreactivity, eosinophillia, and $CD8^+$ lymphocyte recruitment compared with wild-type controls.

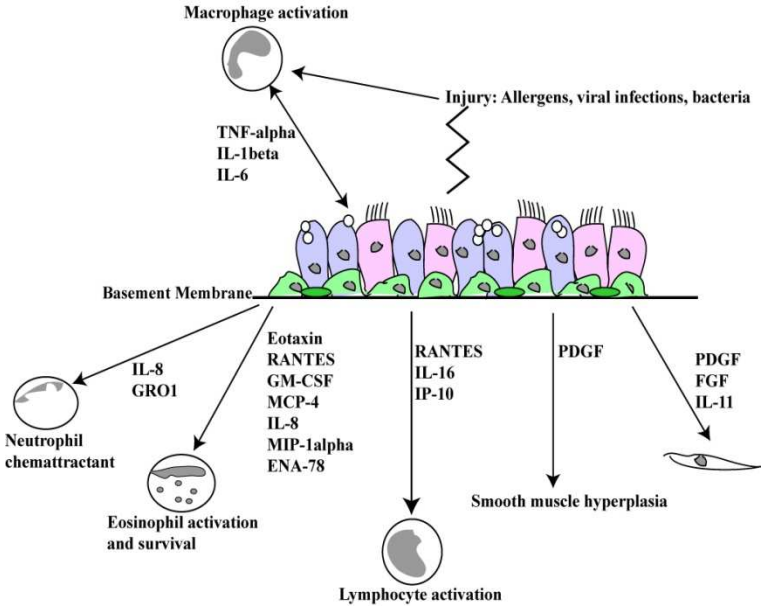

Figure 4-1: Overview of epithelial cell-derived cytokine secretion in asthma.
TNF: tumour necrosis factor. IL: interleukin. RANTES: Regulated on activation, normal T-cell expressed and secreted. MCP: Monocyte chemoattractant protein. MIP: macrophage inflammatory protein. ENA-78: epithelial-derived neutrophil activator. GRO: growth related protein. IP: Interferon-inducible protein. GM-CSF: granulocyte-macrophage colony-stimulating factor. PDGF: platelet-derived growth factor. FGF: fibroblast growth factor, promoting (myo)fibroblasts.

4.1.1.3 Epithelium dysfunction and cytokine secretion in COPD

Tissue damage, airway remodelling and inflammation also appear to have roles in COPD. Similarly to asthma and other inflammatory diseases, cytokines participate in the initiation of inflammation in COPD, the main sources being epithelial cells, macrophages, eosinophils, and neutrophils. Figure 4-2

summarizes some of the important cytokines released by epithelial cells obtained from COPD patients.

Cigarette smoke has been observed to induce G-CSF, MCP-1, IL-8, and leukotrienes (LT) - B4 secretion by the human pulmonary type II epithelial cell line A549 (Masubuchi, Koyama, Sato *et al.* 1998); these all participate in recruitment and activation of neutrophils which in turn can secrete a number of other mediators, including the neutrophil chemoattractant IL-8; these can lead to further tissue damage, remodelling, and mucus hypersecretion. RANTES mRNA expression has been seen to be elevated in the surface epithelium of patients with chronic bronchitis compared to healthy subjects (Zhu, Qiu, Majumdar *et al.* 2001), and may be responsible for recruiting eosinophils, thus explaining the eosinophilia observed in at least a subset of patients with COPD . Moreover, TNF-α has been shown to be produced by a range of cells in COPD, including epithelial cells. It induces the transcription of the IL-8 gene, and up-regulates IL-8 expression in the airway epithelium (Kicic, Sutanto, Stevens *et al.* 2006). It also stimulates epithelial cells to produce tenascin (an extracellular matrix protein) (Khair, Devalia, Abdelaziz *et al.* 1994). Airway bacterial load in COPD patients has been correlated with levels of IL-8 (Chung 2001), and up to 43% of chemotactic activity found in sputum from COPD patients can be attributed to IL-8 (Woolhouse, Bayley and Stockley 2002).

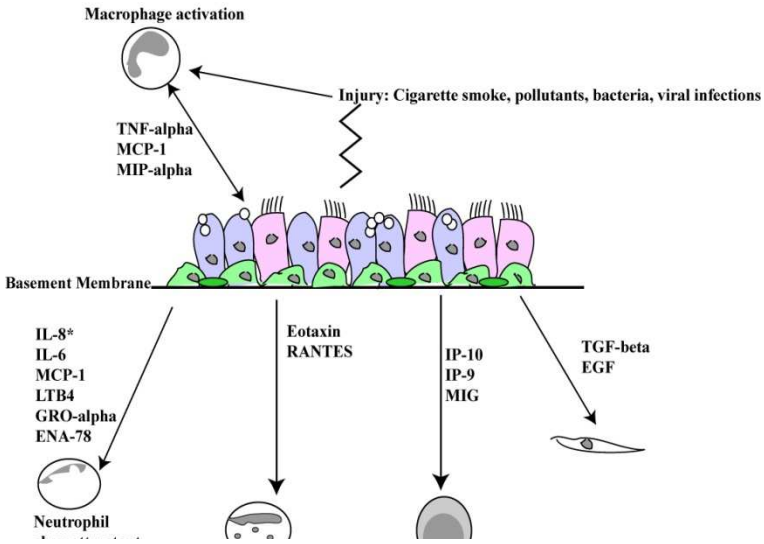

Figure 4-2: Overview of epithelial cell-derived cytokines in COPD.
TNF: tumour necrosis factor. IL: interleukin. RANTES: Regulated on activation, normal T-cell expressed and secreted. MCP: Monocyte chemoattractant protein. MIP: macrophage inflammatory protein. ENA-78: epithelial-derived neutrophil activator. LT: leukotriene GRO: growth related protein. IP: Interferon-inducible protein. MIG: Monokine Induced by Interferon-gamma. EGF: epidermal growth factor. *IL-8 seems to be more extensively secreted by epithelial cells in COPD than asthma.

Although the precise contribution of each individual cytokine to disease pathogenesis remains unclear, there seems to be differences in the profiles of cytokines produced in asthma and COPD (see Table 4-18). Further studies are needed in order to define these differences more quantitatively. On the other hand, the identification of some common cytokine pathways involved in both conditions suggests there may be common pathways controlling both inflammation and repair as well which contribute to the pathophysiology of both diseases.

4.2 Objectives

Since there is great evidence of epithelial derived cytokines and other mediators in the evolution of airway inflammation and in the injury-repair process in the human airway, the major aims of the studies described in this chapter were to define the secretory profile of the human bronchial epithelial cell (HBEC) wound repair model (described initially in chapter 3). A panel of 28 cytokines, chemokines, and growth factors, was investigated, including a wide range generally thought to be important in airway inflammation.

4.3 Methods

In all, three methods have been used in this study to investigate the secretory profile of wounded human bronchial epithelial cells (HEBC). Briefly, the Luminex system was employed to investigate the secretion of a panel of factors by wounded and unwounded HBEC, and is discussed in more detail in section 2.2.2. The luminex system employs flow cytometry, microspheres, lasers, and digital signal processing to permit the simultaneous measurement of multiple cytokines. In addition, an enzyme-linked immuno-sorbent assay (ELISA) was used to investigate specific individual cytokines, and is described below. Real time PCR was then performed following protein analysis to study mRNA expression levels. As mentioned earlier, two donors were used for the Luminex assay and molecular work (donor 1 and 2), each including two replicates.

4.3.1 Luminex assay

First, 1 ml per well of supernatant was collected from wounded differentiated HBEC, grown at ALI, at 0, 24, 48, and 72 hrs post-wounding as described in section 2.1.1.7. Unwounded controls were included for each time point. The Luminex assay was carried out as described in section 2.2.2.1, using a pre-mix human Procarta® Cytokine Assay kit (28-plex), to measure the concentration of a panel of cytokines, chemokines, and growth factors secreted by the scrape wounded differentiated bronchial epithelium model used in this study (a list of the analytes measured is given in Table 4-1). The detection limits for this assay were

0-20 000 pg/ml for each analyte. More details about the technique, standard curves, and controls are provided in section 2.2.2.

Table 4-1: List of analytes investigated using a commercially available Luminex kit

Analyte Symbol	Name and other Nomenclature
IL-8	Interleukin 8: CXCL8, neutrophil activating peptide (NAP)1
IL-6	Interleukin 6: interferon, beta 2
IL-1β	Interleukin 1 beta: lymphocyte activating factor (LAF)
ENA-78	Epithelial-neutrophil activating peptide 78: CXCL5
G-CSF	Granulocyte colony-stimulating factor
RANTES	Regulated upon activation, normal T-cell expressed, and secreted: CCL5
IP-10	Interferon-inducible protein 10: CXCL10
VEGF	Vascular Endothelial growth factor
MCP-1	Monocyte chemotactic protein 1: monocyte chemotactic and activating factor (MCAF), small inducible cytokine A2 (SCYA2)
IL-2	Interleukin 2: T-cell growth factor (TCGF), lymphokine
IL-4	Interleukin 4; B-cell growth factor (BCGF)
IL-5	T-cell replacing factor (TRF), eosinophil differentiation factor (EDF)
IL-7	Interleukin 7
IL-10	Interleukin 10: cytokine synthesis inhibitory factor (CSIF)
IL-12P40	Interleukin 12p40: IL-12b
IL-12P70	Interleukin 12p70
IL-13	Interleukin 13: allergic rhinitis (ALRH): bronchial hyperresponsiveness 1 (BHR-1)
IL-17	Interleukin 17: cytotoxic T-lymphocyte-associated antigen 8 (CTLA8)
FGF-basic	Basic fibroblast growth factor; FGF2
NGF	Nerve growth factor
Leptin	Acts through leptin receptor (LEPR)
Eotaxin	CCL-11
MIP-1β	Macrophage inflammatory protein 1 beta: CCL-4
MIP-1α	Macrophage inflammatory protein 1 alpha: CCL-3

TNF-β	Tumour necrosis factor beta
GM-CSF	Granulocyte monocyte colony-stimulating factor
IFN-γ	Interferon gamma: type II interferon, macrophage activation protein (MAF)

4.3.2 Enzyme-Linked Immuno-Sorbent Assay (ELISA)

For the quantitative determination of human IL-8 concentrations in cell culture supernatants from differentiated scrape wounded HBEC, a commercially available ELISA kit was used to further investigate IL-8 since the values obtained from the luminex experiment for that particular mediator were above the detection limit range of the assay. Briefly, this assay involves an analyte-specific monoclonal antibody pre-coated onto a microplate. After the sample had been added, the relevant protein present binds to the antibody. An enzyme-linked analyte-specific detection antibody is added and a substrate solution develops colour (through its digestion by the enzyme) in proportion to the amount of protein present in the sample. The intensity of the signal is subsequently measured (Figure 4 3).

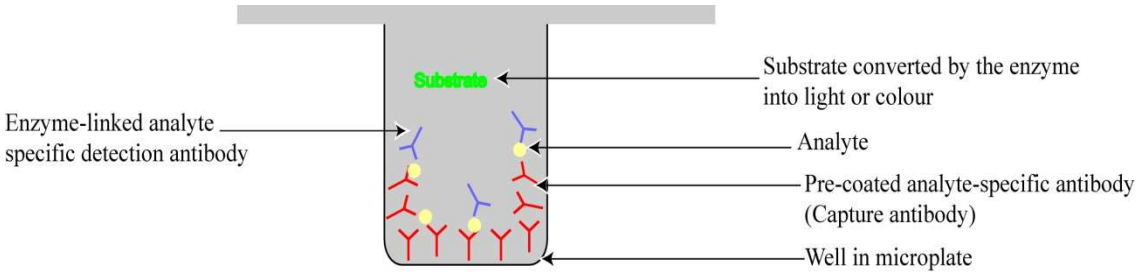

Figure 4-3: Basic principle of ELISA.

The Quantikine Human CXCL-8/IL-8 Immunoassay (Cat# D8000C was used following the manufacturer's protocol in a 96-well microplate. All reagents and equipment were provided with the kit and prepared according to the manufacturer's protocol.

Briefly, after reagents, samples, and standards were prepared, 100 µl Assay Diluent (buffered protein base with preservatives) was added to each well. Standard controls (lyophilized recombinant analyte in a buffered protein base with preservatives) or samples were then added, and incubated at room temperature for 2-3 hrs according to the specific assay carried out. The wells were washed four times with Wash Buffer (400 µl, 25x concentrated solution of buffered surfactant with preservatives), and desired conjugate was added for 1 hr at room temperature. The wells were washed again, and Substrate Solution was added and incubated for 20-30 min at room temperature protecting it from the light. Finally, Stop Solution (2 N sulphuric acid) was added to each well and the absorbance was read on a plate reader (Multiskan EX, Thermo Scientific, with Ascent software) at 450 nm within 30 min. γ correction was done at 540 nm or 570 nm in order to avoid optical imperfections which might occur if the readings were made at only 450. Data analysis was carried out using the ELISA plate reader software Ascent. Values for data analysis were done by first creating a standard curve (presented in Figure 4-4) from the standards that were included, using 4 parametric logistic fitting and this was used to determine the concentration of IL-8 in the samples.

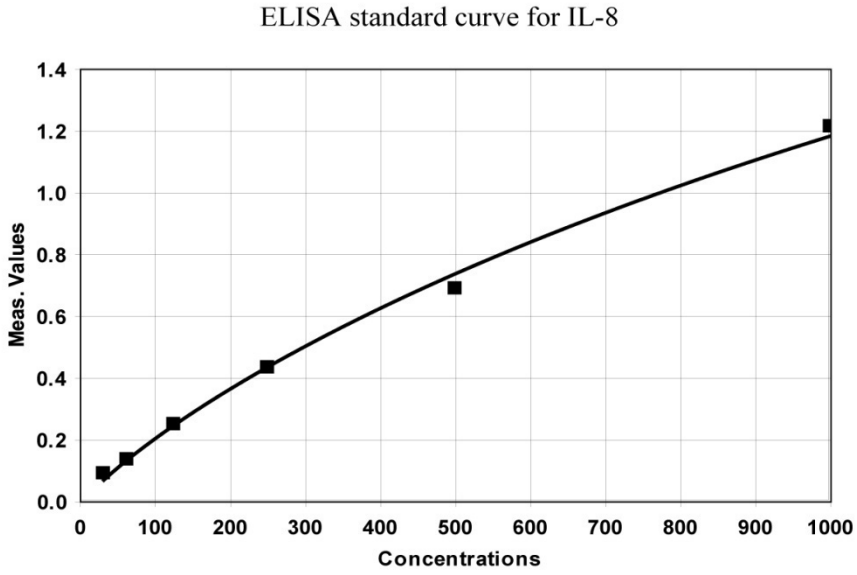

Figure 4-4: ELISA standard curve for IL-8.
A standard curve was generated from the standards included in the experiment, using Ascent software, using a four parametric logistic fitting. IL-8 concentration in the HBEC supernatants was determined using this standard curve. Concentrations are in pg/ml.

4.3.3 Quantitative Real Time PCR

To quantify mRNA expression of the cytokines that showed protein increase in wounded differentiated HBEC, Real Time PCR (Biosystems) was carried out on cDNA synthesized from RNA collected from differentiated HBEC following the protocols described in section 2.4. Primers and probes used are listed in Table 4-2 and Table 4-3 below. cDNA quality was validated by running a conventional PCR using GAPDH as discussed in section 2.4.2.4.

Table 4-2: Primer information

# of bases	Primer Name	Primer sequence 5'-3'	Position	Product length
27	IL-6 F	AGAAAGGAGACATGTAACAAGAGTAAC	Exon 2 position 266	63
23	IL-6 R	CAACCTGAACCTTCCAAAGATGG	Exon 3 position 328	
22	ENA-78 F	GCCCCTTTCACAGAGTAGAACC	Exon 4 position 1676	86
20	ENA-78 R	AAACCCGACAGGCATCTTCC	Exon 4 position 1761	
20	G-CSF F	GCTTCCTGGAGGTGTCGTAC	Exon 1 position 615	140
20	G-CSF R	CCGTTCTGCTCTTCCCTGTC	Exon 4 position 754	

Taqman® Gene expression assay for IL-8 was purchased from Applied Biosystems: cat.# HS99999034_m1

Table 4-3: Probe information

# of bases	Probe Name	Primer sequence 5'-3'	Position
27	IL-6	TCTGCCAGTGCCTCTTTGCTGCTTTCA	Exon position 298
22	ENA-78	CCCGCTGCCGCTCGTCTTCTGC	Exon 4 position1733
24	G-CSF	TTCTACGCCACCTTGCCCAGCCCT	Exon 4 position 630

Probes were 3' TAMRA, 5' 6-FAM purchased from Eurgentec S.A

Standard curves were generated as explained in section 2.4.3 for the following targets: IL-6, IL-8, ENA-78, and G-CSF, to validate the use of the chosen primers and probes and the appropriate working concentrations. IL-8 primer/probe set sequences are not presented in the table above since they were purchased and the sequences were not available. Optimum amplification efficiencies should be 100% (±10%), however, for the assays used in this study, they were between 75-90%, which are still considered acceptable. The slope of the standard curve (optimum is -3.322 for 100% PCR efficiency), showed a range from -3.626 till -4.074), validating the primers and probes as appropriate to use for experiments.

Figure 4-5: Amplification and dilution plots.
IL-6 (A), IL-8 (B), ENA-78 (C), and G-CSF (D). One outlier value was observed for G-CSF (panel D): this was however included in the fitting of the dilution plot.

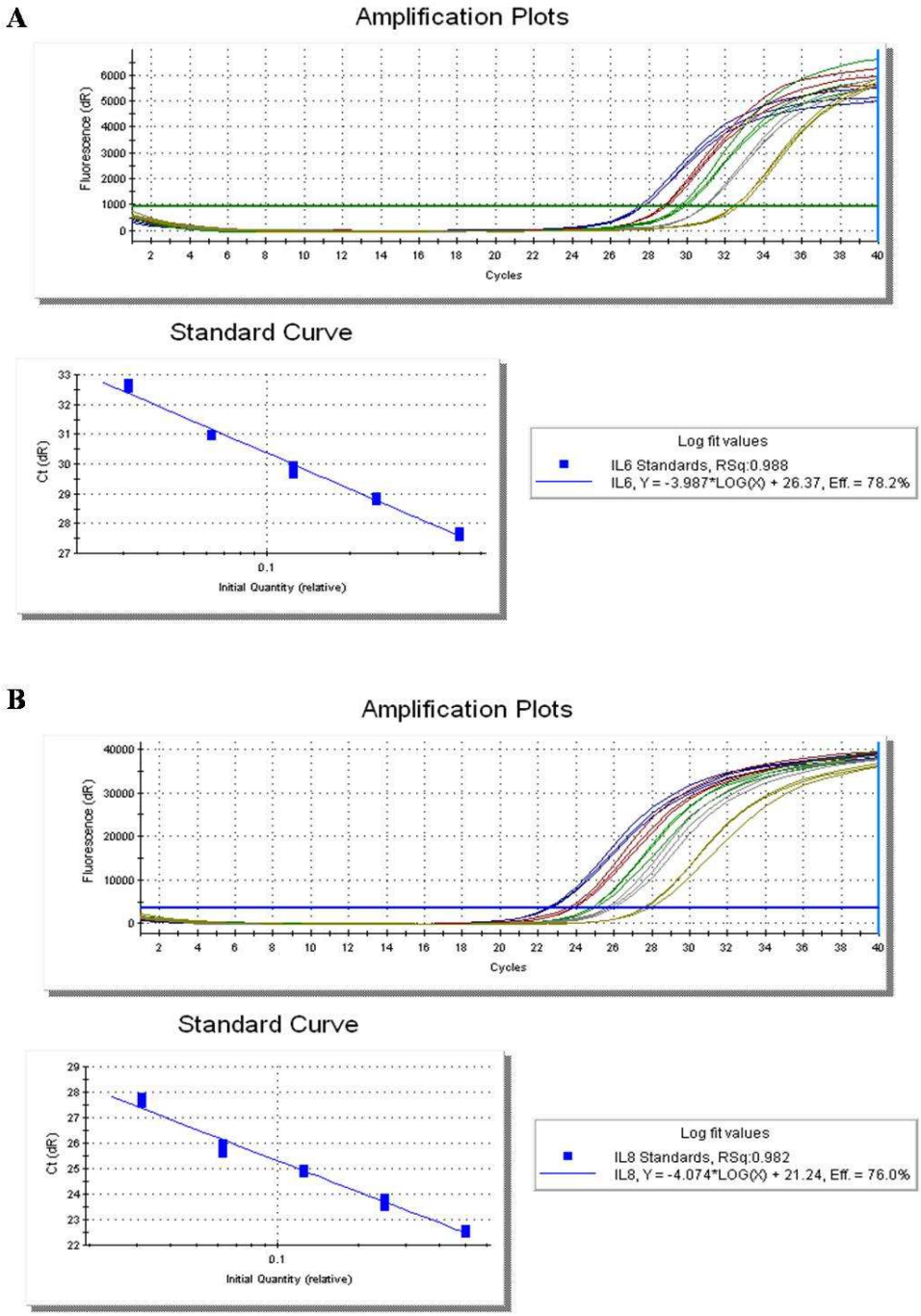

C

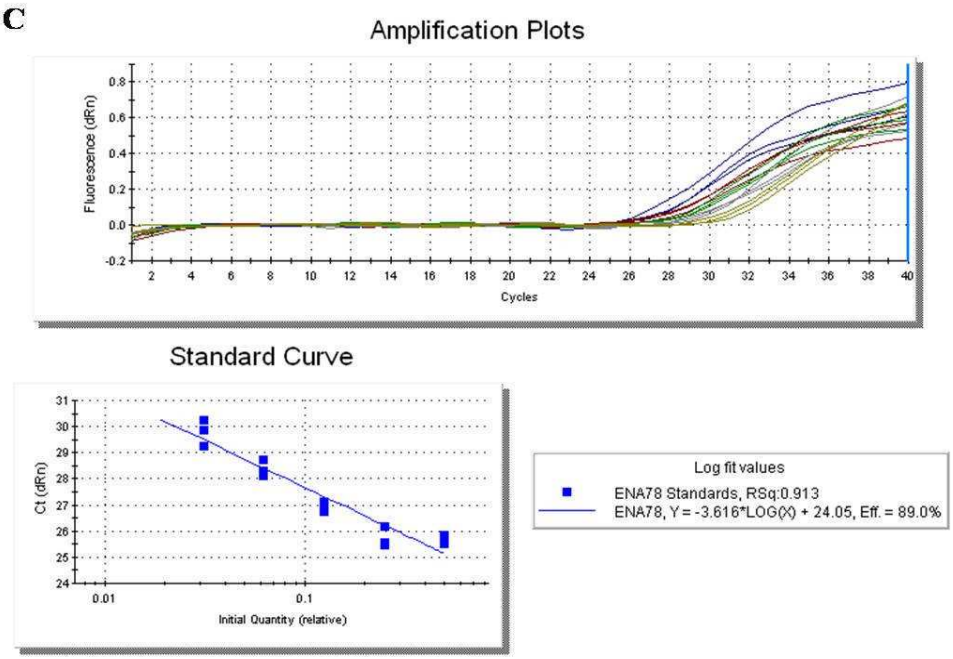
Amplification Plots
Fluorescence (dRn)
Cycles
Standard Curve
Ct (dRn)
Initial Quantity (relative)
Log fit values
ENA78 Standards, RSq:0.913
ENA78, Y = -3.616*LOG(X) + 24.05, Eff. = 89.0%

D

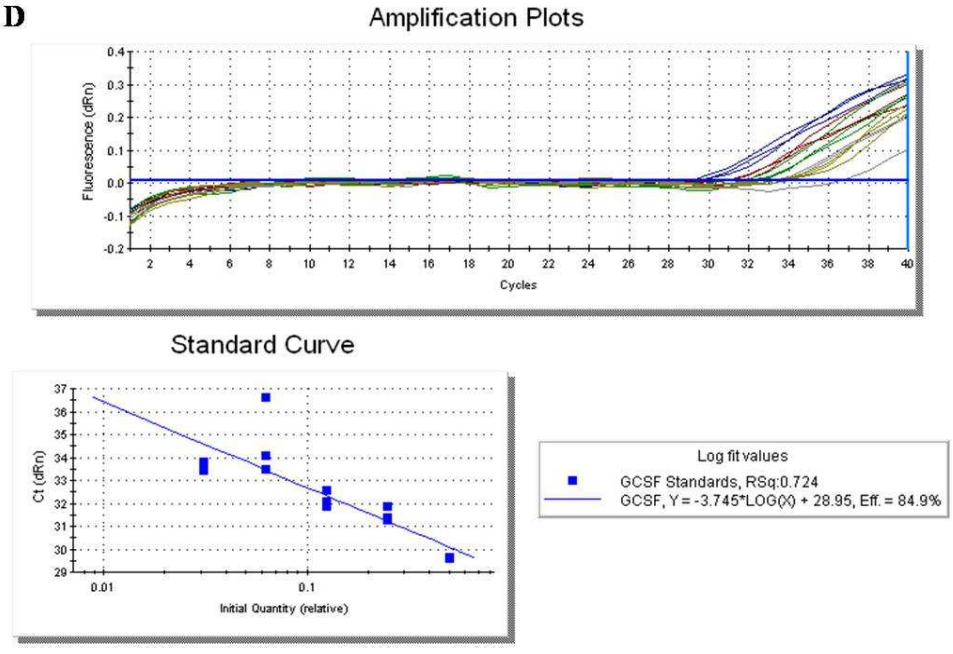
Amplification Plots
Fluorescence (dRn)
Cycles
Standard Curve
Ct (dRn)
Initial Quantity (relative)
Log fit values
GCSF Standards, RSq:0.724
GCSF, Y = -3.745*LOG(X) + 28.95, Eff. = 84.9%

4.4 Results

4.4.1 Cytokine secretion of wounded differentiated HBEC cultures

Quantitative determination of 28 factors (Table 4-1) in supernatants collected from differentiated HBEC cultures, grown at ALI and scrape-wounded, was carried out using the luminex assay and ELISA. Detection of 9 factors was observed including: IL-6, IL-8, ENA-78, G-CSF, IP-10, RANTES, IL-1β, VEGF, and MIP-1β. The results are discussed in the following sections. Raw data for all the analytes is presented in Appendix B. Two donors were used for these experiments each carried out in two replicates and the Luminex assay was done in duplicate. There were not sufficient values to carry out statistical analysis. Data are presented in tables as mean concentration (pg/ml) of the two replicates for each donor and the range is presented in brackets for each average.

4.4.1.1 Interleukin 6 (IL-6) secretion

IL-6 secretion was observed to be increased in wounded HBEC supernatants compared to unwounded cells at 72 hrs post-wounding in both donors although the variation between the two donors used was high (1.8 and 9 fold increase in wounded compared to unwounded cultures at 72 hrs post-wounding respectively). It was also observed that at each point the concentration level of IL-6 was higher in wounded cells compared to unwounded counterparts, in both donors. Table 4-4 below shows mean concentration of two replicates per donor as well as the range of the values. Values that were below the limit of detection was substituted by zero. The negative control contained an IL-6 concentration of 0.27 pg/ml

Table 4-4: IL-6 secretion by wounded and unwounded HBEC.
Table shows mean concentration (pg/ml)of two replicates per donor for two donors for wounded and unwounded cells at different time points. Ranges are presented in brackets showing the minimum and maximum concentration. Values below the limit of detection were substituted by 0.

	Donor 1 Mean of two replicates as pg/ml (range)		**Donor 2 Mean of two replicated as pg/ml(Range)**	
Time post-injury (hours)	**Wounded**	**Unwounded**	**Wounded**	**Unwounded**
0	0	0	0.55 (0.51-0.59)	0.37 (0.25-0.49)
24	12.64 (0-25.28)	0	17.52 (12.86-21.94)	5.94 (2.26-9.61)
48	49.87 (47.68-52.06)	0	53.24 (40.62-65.86)	12.60 (9.93-15.83)
72	154.5 (121.3-187.7)	88.28 (62.72-113.84)	135.58 (124.45-146.71)	14.33 (9.14-19.51)

4.4.1.2 Interleukin 8 (IL-8) secretion

There was a trend in higher IL-8 concentrations in wounded HBEC compared to unwounded cells in both donors. In donor 2 however, the concentration of IL-8 was above the limit of detection after the 0 hr time point (Table 4-5). An ELISA was thus carried out in order to dilute the samples. Generally, it was observed that IL-8 concentration was higher after wounding HBEC. For example, at 72 hrs post-wounding in both donors, there was an approximated 1.7 fold increase in IL-8 concentration in wounded compared to unwounded cells (Table 4-6).

Table 4-5: IL-8 secretion by wounded and unwounded HBEC measured using the luminex assay.
Table shows mean concentration (pg/ml) of two replicates per donor for two donors for wounded and unwounded cells at different time points. Ranges are presented in brackets showing the minimum and maximum concentration. For donor 1, only one of the values were present and thus a mean could not be calculated. OOR> represents the values that were above the limit of detection for the Luminex assay

	Donor 1 Mean of two replicates in pg/ml (range)		**Donor 2 Mean of two replicated in pg/ml (Range)**	
Time post-injury (hours)	**Wounded**	**Unwounded**	**Wounded**	**Unwounded**
0	95.21 (94.46-95.96)	143.94 (132.85-155.03)	5.10 (2.47-7.72)	12.43 (8.05-16.81)
24	2805.25 (2664-2946.5)	1272.86 (926.91-1618.8)	OOR>	OOR>
48	4289.7 (4180.9-4398.5)	1672 (1648-1696)	OOR>	OOR>
72	18663 (18663-OOR>)	6372 (5887.3-6856.7	OOR>	OOR>

Table 4-6: IL-8 secretion by wounded and unwounded HBEC measured using ELISA.
Table shows mean concentration (pg/ml) of two replicates per donor for two donors for wounded and unwounded cells at different time points. Ranges are presented in brackets showing the minimum and maximum concentration. Values below the limit of detection were substituted by 0. For donor 1, only one of the values were present and thus a mean could not be calculated. OOR> represents the values that were above the limit of detection for the Luminex assay

	Donor 1 Mean of two replicates in pg/ml (range)		**Donor 2 Mean of two replicated in pg/ml (Range)**	
Time post-injury (hours)	**Wounded**	**Unwounded**	**Wounded**	**Unwounded**
0	0	0	110.5 (98-123)	217.5 (153-282)
24	3544.5 (2371-4718)	1750 (1931-3138)	7196.5 (6538-7855)	2095.5 (0-4191)
48	22380 (17104-27656)	14292 (11513-17071)	8194.5 (7110-9279)	4715.5 (4667-4764)
72	19435 (16392-22478)	10920 (8513-13327)	15227 (11648-18806)	8701.5 (8018-9385)

4.4.1.3 Epithelial neutrophil-activating peptide 78 (ENA-78) secretion

An increase was seen in ENA78 secretion in wounded HBEC cultures in both donors by 24hrs post-wounding. For example, at 72 hrs post-wounding, an approximated 16 fold increase was observed in donor 1 in wounded vs unwounded cultures, and an 8 fold increase in donor two. Table 4-7 shows the mean concentration of two replicated per donor in pg/ml in both wounded and unwounded HBEC. Range of the values are also presented in brackets. Values that were below the limit detection of the assay were substituted by 0.

Table 4-7: ENA-78 secretion by wounded and unwounded HBEC.
Table shows mean concentration (pg/ml) of two replicates per donor for two donors for wounded and unwounded cells at different time points. Ranges are presented in brackets showing the minimum and maximum concentration. Values below the limit of detection were substituted by 0.

	Donor 1 Mean of two replicates in pg/ml (range)		**Donor 2 Mean of two replicated in pg/ml (Range)**	
Time post-injury (hours)	**Wounded**	**Unwounded**	**Wounded**	**Unwounded**
0	0	0	0	0
24	34.06 (0-68.12)	0	184.68 (166.8-202.55)	24.87 (0-49.74)
48	192.32 (151.34-233.3)	0	1168.8 (1088.7-1248.9)	106.58 (101.08-112.08)
72	1207.57 (515.93-1899.2)	73.77 (31.76-115.77)	937.69 (614.97-1260.4)	120.96 (66.67-175.24)

4.4.1.4 Granulocyte colony stimulating factor (G-CSF) secretion

G-CSF secretion was observed to be higher in wounded HBEC compared to unwounded cells in both HBEC donors by 24 hrs post-wounding. For example, at 72 hrs post-wounding, there was 2.2 fold increase in wounded cultures from donor 1 compared to unwounded cells, and a 62.8 fold increase in wounded cells

vs. unwounded cells from donor 2. A high variability can be seen between donors as well as within donors at some points.

Table 4-8 shows mean concentration of G-CSF in pg/ml, in wounded and unwounded cultures, of two replication in each donor. A range of the values at each time point is also presented. Values that were below the limit of detection were substituted by 0.

Table 4-8: G-CSF secretion by wounded and unwounded HBEC.
Table shows mean concentration (pg/ml) of two replicates per donor for two donors for wounded and unwounded cells at different time points. Ranges are presented in brackets showing the minimum and maximum concentration. Values below the limit of detection were substituted by 0.

	Donor 1 Mean of two replicates in pg/ml (range)		**Donor 2 Mean of two replicated in pg/ml (Range)**	
Time post-injury (hours)	**Wounded**	**Unwounded**	**Wounded**	**Unwounded**
0	0	0	0	0
24	32.70 (17.74-47.65)	0	1.22 (0-2.44)	0
48	31.38 (27.09-35.66)	0	202.15 (171.81-232.48)	0.23 (0-0.45)
72	292.60 (182.48-402.71)	130.57 (90.31-170.83)	165.2 (83.68-246.72)	2.63 (0-5.26)

4.4.1.5 Interferon-inducible protein 10 (IP-10) secretion

Wounded and unwounded HBEC both secreted IP-10 at different time points post-wounding. There was a hint of increase in wounded cells of donor 2 at 72hrs post-wounding compared to its unwounded counterpart. However, in general, it seems that wounding HBEC does not affect IP-10 secretion dramatically. Table 4-9 shows IP-10 mean concentration (pg/ml) of two replicates per donor for two donors in wounded and unwounded HBEC. Range is also presented in brackets to show the variability between donors and amongst them.

Table 4-9: IP-10 secretion by wounded and unwounded HBEC.
Table shows mean concentration (pg/ml) of two replicates per donor for two donors for wounded and unwounded cells at different time points. Ranges are presented in brackets showing the minimum and maximum concentration.

	Donor 1 Mean of two replicates in pg/ml (range)		**Donor 2 Mean of two replicated in pg/ml (Range)**	
Time post-injury (hours)	**Wounded**	**Unwounded**	**Wounded**	**Unwounded**
0	0	0.01 (0-0.01)	1.08 (1-1.15)	1.47 (0.98-1.96)
24	0.44 (0.29-0.58)	0.14 (0.09-0.19)	61.43 (60.99-61.87)	69.11 (53.24-84.97)
48	3.40 (3.21-3.58	0.21 (0.19-0.23)	335.92 (323.04-348.79)	297.11 (270.06-324.16)
72	30.46 (13.81-47.11)	53.10 (2.47-101.25)	667.94 (643.89-691.98)	480.43 (475.85-485.01)

4.4.1.6 Vascular endothelial growth factor (VEGF) secretion

There was a high variability in VEGF concentration between samples in these experiments and a high level of VEGF was seen to be secreted by HBEC both wounded and unwounded. However, there seems to be a hint of increase in VEGF secretion after wounding especially in donor 2 at 48 and 72 hrs post-wounding. Table 4-10 shows mean concentration in pg/ml of two replicates per donor in both donors. Range is also presented in brackets to assess the variability between samples.

Table 4-10: VEGF secretion by wounded and unwounded HBEC.
Table shows mean concentration (pg/ml) of two replicates per donor for two donors for wounded and unwounded cells at different time points. Ranges are presented in brackets showing the minimum and maximum concentration. OOR> : out of range above.

	Donor 1 Mean of two replicates in pg/ml (range)		**Donor 2 Mean of two replicated in pg/ml (Range)**	
Time post-injury (hours)	**Wounded**	**Unwounded**	**Wounded**	**Unwounded**
0	25.4 (22.49-28.31)	43.07 (41.69-44.44)	5.1 (2.3-5.6)	6.87 (1.95-11.78)
24	277.79 (272.8-282.78)	291.70 (289.07-294.32)	224.2 (97.9-350.5)	296.95 (272.2-321.7)
48	434.82 (429.16-440.48)	354.57 (332.69-376.45)	10792- OOR>	2351 (2089-2613)
72	977.53 (796.95-1158.1)	773.77 (664.53-883.01)	OOR>	OOR>

4.4.1.7 Regulated upon activation, normal T cell expressed and secreted (RANTES) secretion

RANTES secretion was observed to be low in HBEC in wounded and unwounded cultures especially in donor 1, however, it seems to increase in response to wounding especially at a later time points (such 72 hrs). For example, at 72 hrs post wounded cultures from donor 2, there was an approximated 4 fold increase in the wounded cultures compared to unwounded cells. Table 4-11 shows mean concentration (pg/ml) of two replicates per donor. Two separate donors were used in this study. Ranges are also included in the table below in brackets. The variability between samples in RANTES secretion was not high.

Table 4-11: RANTES secretion by wounded and unwounded HBEC.
Table shows mean concentration (pg/ml) of two replicates per donor for two donors for wounded and unwounded cells at different time points. Ranges are presented in brackets showing the minimum and maximum concentration. Values below the detection limit were substituted for by zero.

	Donor 1 Mean of two replicates in pg/ml (range)		**Donor 2 Mean of two replicated in pg/ml (Range)**	
Time post-injury (hours)	**Wounded**	**Unwounded**	**Wounded**	**Unwounded**
0	0	0	0.03	0.03 (0.02-0.04)
24	0	0	0.69 (0.34-1.04)	0.71 (0.62-0.79)
48	6.11 (0-12.22)	0	5.63 (5.41-5.85)	2.66 (2.09-3.22)
72	31.38 (24.27-38.48)	0	10.78 (9.7-11.86)	3.44 (2.3-4.57)

4.4.1.8 Interleukin 1β (IL-1) secretion

Although IL-1β secretion by differentiated HBEC was observed to be low, there was a slight increase in wounded cultures compared to unwounded ones especially in donor 2. In addition, there seems to be a higher increase with time in the wounded HBEC compared to unwounded cells. Table 4-12 shows mean concentration (pg/ml) of two replicates per donor for two donors. Ranges are also provided in brackets. Variability between samples in IL-1β secretions seems to be low. All values that were below the detection limit of the assay were substituted by zero. Table 4-12 shows mean concentration (pg/ml) of two replicates per donor. Two separate donors were used in this study. Ranges are also included in the table below in brackets

Table 4-12: IL-1β secretion by wounded and unwounded HBEC.
Table shows mean concentration (pg/ml) of two replicates per donor for two donors for wounded and unwounded cells at different time points. Ranges are presented in brackets showing the minimum and maximum concentration. Zero represents the values that were below the detection limit of the assay.

	Donor 1 Mean of two replicates in pg/ml (range)		**Donor 2 Mean of two replicated in pg/ml (Range)**	
Time post-injury (hours)	**Wounded**	**Unwounded**	**Wounded**	**Unwounded**
0	0	0	0.14	0.06 (0.03-0.08)
24	0	0	0.2 (0.08-0.36)	0.18 (0.14-0.21)
48	0	0	0.57 (0.52-0.61)	0.36 (0.28-0.44)
72	0.33 (0.19-0.46)	0	0.96 (0.91-1.01)	0.4 (0.36-0.44)

4.4.1.9 Macrophage inflammatory protein 1β (MIP-1β) secretion

MIP-1β secretion was observed to be very low in differentiated HBEC. Although there were none detected in donor 1, donor 2 showed some increase in wounded cultures compared to unwounded cells at 24, 48, and 72 hrs post-wounding. Table 4-13) shows mean concentration (pg/ml) of two replicates per donor. Two separate donors were used in this study. Ranges are also included in the table below in brackets

Table 4-13: MIP-1β secretion by wounded and unwounded HBEC.
Table shows mean concentration (pg/ml) of two replicates per donor for two donors for wounded and unwounded cells at different time points. Ranges are presented in brackets showing the minimum and maximum concentration. Zero represents the values that were below the detection limit of the assay.

	Donor 1 Mean of two replicates in pg/ml (range)		**Donor 2 Mean of two replicated in pg/ml (Range)**	
Time post-injury (hours)	**Wounded**	**Unwounded**	**Wounded**	**Unwounded**
0	0	0	0.16 (0.15-0.16)	0.17 (0.16-0.18)
24	0	0	1.09 (0.94-1.23)	0.35 (0.3-0.4)
48	0	0	3.56 (3.08-4.02)	1.15 (1.11-1.19)
72	0	0	5.19 (3.75-6.63)	2.33 (1.52-3.13)

4.4.1.10 Cytokines that were not detected in our HBEC cultures

Out of the 28 mediators investigated, only the above cytokines were detected in HBEC culture supernatants. The rest were below the detected limit range of the assay. Those cytokines included: IL-2, IL-5, IL-7, IL-10, IL-12 p70, IL-13, IL-17, MIP-1α, TNF-β, GM- CSF, MCP3, IFN-γ. There were a few cytokines that were detected only in donor 2 but the values were very close to the concentration of the negative control and thus were not investigated further. These included: IL-4, IL-12 p40, NGF, leptin, eotaxin. Finally, FGF-basic was detected in donor 2 but there was a decrease in its concentration observed in both wounded and unwounded HBEC.

4.4.2 Cytokine mRNA expression by wounded and unwounded differentiated HBEC

The trend towards an increase in cytokines secretions described in the previous section could be explained due to a number of processes. It could be due to an increase in transcription, an increase in the release of preformed cytokines, or a decrease in the breakdown of these cytokines by the cells. Hence, the increase seen in cytokines at the protein level was further studied by the investigation of IL-6, IL-8, ENA-78, and G-CSF relative mRNA expression using Real Time PCR; in order to see whether this increase in protein was due to an increase in transcription. These cytokines were chosen because of the data suggesting these were most likely to be differentially regulated following wounding. RNA was extracted from wounded differentiated HBEC, at 0, 24, 48, and 72 hrs, with unwounded controls provided as described in section 2.4.3. Real time PCR was carried out using the primers and probes listed in Table 4-2 and Table 4-3. Data was analyzed using the approaches described in section 2.4.3. HPRT was again used to normalize the values generated from Real Time PCR experiments for the reasons explained in section 2.4.3. For each cytokine, values were captured at relevant time points from the samples obtained from wounded and unwounded cultures. The tables below show mean fold increase (as a percentage) of $2^{-\Delta Ct}$ normalised to 0hrs and the range of the two replicates in brackets. Two different donors were used each in two replicates, and the real time PCR was carried out in triplicate. It has to be noted that no conclusive results could be retrieved from the real time data since it was technically very difficult to extract RNA from the transwell inserts and from the tables below, the 24 hrs time point in donor 2 does not seem reliable in all four cytokines.

4.4.2.1 IL-6 mRNA expression by wounded and unwounded HBEC

There was a hint of increase in IL-6 mRNA expression in wounded cultures compared to unwounded cells especially in donor 2. For example, at 24 hrs post-wounding, a 6 fold increase was observed in the mRNA expression in wounded cells compared to unwounded controls in donor 2 and a 1.4 fold increase in donor 2 (Table 4-14).

Table 4-14: IL-6 relative mRNA expression by wounded and unwounded HBEC.
The table shows mean fold increase of two replicates per donor of two donors (2^{-dCt}) normalized to 0hrs.

	Donor 1 Mean fold increase of two replicates in 2^{-dCt} as a percentage normalized to 0hr (range)		**Donor 2 Mean fold increase of two replicates in $2^{-dCt(}$ as apercentage normalized to 0hr (range)**	
Time post-injury (hours)	**Wounded**	**Unwounded**	**Wounded**	**Unwounded**
0	100	100	100	100
24	13.3 (13.2-13.4)	9.7 (1.9-17.5)	955.5 (341-1570.6)	159.1 (66.8-252.2)
48	33.25 (16.6-49.9)	83 (72.4-93.6)	215.7 (184.0-247.4)	57.1 (92.3-201.6)
72	35.7 (26-45.4)	8.25 (5.1-11.4)	933.8 (642.0-1225.5)	277.8 (56.6-498.9)

4.4.2.2 IL-8 mRNA expression in wounded and unwounded cultures

IL-8 relative mRNA expression was seen to be higher in wounded HBEC compared to unwounded controls especially at 24 hrs post-wounding in donor2. Although the expression was quite different in two donors, the increase in expression seen in wounded cells correlates with the increase at the protein level (Table 4-15).

Table 4-15: IL-8 relative mRNA expression by wounded and unwounded HBEC.
The table shows mean fold increase of two replicates per donor of two donors (2^{-dCt}) normalized to 0hrs.

	Donor 1 Mean fold increase of two replicates in 2^{-dCt} as a percentage normalized to 0hr (range)		**Donor 2 Mean fold increase of two replicates in 2^{-dCt}(as apercentage normalized to 0hr (range)**	
Time post-injury (hours)	**Wounded**	**Unwounded**	**Wounded**	**Unwounded**
0	100	100	100	100
24	111.75 (72.3-151.2)	69.2 (16.9-121.5)	367.1 (568.3-675.8)	136 (119.4-152.4)
48	41.6 (27.7-79.3)	125.6 (101.2-150)	341.3 (230.5-453.0)	190.1 (185-195)
72	84.6 (80.5-88.7)	25.5 (24.9-26)	486. (281-691)	386.6 (108.1-278.5)

4.4.2.3 ENA-78 mRNA expression in wounded and unwounded HBEC.

ENA-78 mRNA expression was observed to be higher in wounded HBEC compared to unwounded ones in both donors by 24hrs post-wounding (Table 4-16). At 48 hrs post-wounding in donor 1, there could have been a technical error in the real time method since in all three cytokines thus far, the unwounded was higher than the wounded which contrasts all the other time points and the other donor.

Table 4-16: ENA-78 relative mRNA expression by wounded and unwounded HBEC.
The table shows mean fold increase of two replicates per donor of two donors (2^{-dCt}) normalized to 0hrs.

	Donor 1 Mean fold increase of two replicates in 2^{-dCt} as a percentage normalized to 0hr (range)		**Donor 2 Mean fold increase of two replicates in 2^{-dCt}(as apercentage normalized to 0hr (range)**	
Time post-injury (hours)	**Wounded**	**Unwounded**	**Wounded**	**Unwounded**
0	100	100	100	100
24	838.4 (516.6-1160)	317.4 (16.3-618.4)	931.4 (592-1270.8)	165.2 (71.5-258.9)
48	91.9 (9.8-174.4)	226.4 (210.8-241.9)	531.2 (337.8-724.5)	238.7 (198.2-279.1)
72	792.2 (228.3-1356)	121.5 (80.9-162)	1041.8 (1524.7)	167.9 (0.1-334.9)

4.4.2.4 G-CSF mRNA expression in wounded and unwounded HBEC

An increase was seen in G-CSF mRNA expression in response to wounding in both donors by 24 hrs post-wounding (Table 4-17). The problem with the 48 hr time point in donor 1 remains clear in G-CSF data as well.

Table 4-17: G-CSF relative mRNA expression by wounded and unwounded HBEC.
The table shows mean fold increase of two replicates per donor of two donors (2^{-dCt}) normalized to 0hrs.

	Donor 1 Mean fold increase of two replicates in 2^{-dCt} as a percentage normalized to 0hr (range)		**Donor 2 Mean fold increase of two replicates in $2^{-dCt(}$ as apercentage normalized to 0hr (range)**	
Time post-injury (hours)	**Wounded**	**Unwounded**	**Wounded**	**Unwounded**
0	100	100	100	100
24	40.4 (35.1-45.7)	10.1 (4.7-15.4)	3803.9 (3000-4607.8)	231.6 (222.6-240.5)
48	19.7 (6.3-33.1)	41.6 (37.5-45.6)	1392 (1156.9-1627)	412.1 (374.2-450)
72	21.7 (19.8-23.9)	6.9 (6.7-7)	2436.4 (1164.7-3708.1)	733.1 (250-1216.)

4.5 Discussion

The aim of the studies described in this chapter was to investigate the expression of a panel of cytokines and chemokines (Table 4-1), potentially involved in airway inflammation, in the wounded HBEC model. The major findings are listed in Table 4-18 with a comparison of the results from the data presented in this chapter using the HBEC scrape-wounded model and previous studies of epithelial cell-derived cytokines in asthma and COPD using tissue samples. In summary, a trend of increase was seen in IL-6, IL-8, ENA-78, G-CSF, VEGF, RANTES, IL-1β, and MIP-1β protein expression in wounded cultures. There was not a clear increase in IP-10 protein. Interestingly, some of the above mediators have previously been shown to be up-regulated in the epithelium of patients with COPD or asthma patients.

There were not sufficient data points to carry out statistical analysis. This is due to the fact that these commercially available HBEC are technically challenging to differentiate and the procedure is both expensive and time consuming. Thus during the course of this study, there was insufficient time to work with more than two donors. Currently, epithelial cells from biopsies are being investigated which could be used in the future instead of the commercially available cells, allowing the investigation of patient and normal samples. Moreover, due to the variation in both donors, the data was presented in tables to identify potential trend increases in both donors in spite of the differences amongst them. Another limitation for this work was the limit of detection for all the cytokines (e.g some of the cytokines were above that limit of detection). This could be potentially solved by

using more than one dilution of the sample during the experiment. Finally, it proved very difficult to extract RNA from the polyester membranes and thus the amount and quality of the RNA was poor and thus the data at this point is not conclusive for the mRNA expression. Another RNA extraction protocol could be carried out to see if the results are clearer in the future.

Table 4-18: Epithelial cell-derive cytokines in our scrape-wounded model, compared to previous findings involving the epithelium in patients with asthma and COPD

Analyte	Scrape wound		Asthma	COPD	Major functions
	Wounded	Unwounded			
IL-8	√√	√	√√	√√	Neutrophil chemoattraction
lL-6	√√	√	√√	√√	Macrophage and epithelial cell activation
IL-1β	√√	√	√√	√√	Macrophage and epithelial cell activation
ENA78	√√	√	√√	√√	Eosinophil activation in asthma Neutrophil chemoattraction in COPD
G-CSF	√	√	√	√	Blood neutrophil chemoattractantion
RANTES	√√	√	√√	√√	Lymphocyte activation in asthma Eosinophil activation in COPD
IP-10	√	√	√√	√√	Lymphocyte activation
VEGF	√	√	√√	√√?	Th2 an Th1 activation Leukcyte accumulation
MCP-1	—	—	√	√√	Neutrophil chemoattraction
IL-2	—	—	—	—	Growth and differentiation of T cells Eosinophilia
IL-4	—	—	—	—	Increase in Th1 cells and IgE levels Eosinophil growth
IL-5	—	—	—	—	Increase in Th2 cells Eosinophil maturation
IL-7	—	—	—	—	T cell homeostasis
IL-10	—	—	—	—	Inhibitory cytokine
IL-12 P40	—	—	√√	√?	Th1-dependant immunity
IL-12 IL70	—	—	√?	√?	Produced by antigen presenting cells Th1-dependant immunity
IL-13	—	—	—	—	Induction of proliferation of airway epithelial cells
IL-17	—	—	—	—	Produced exclusively by activated T-lymphocytes to activate epithelial cells, endothelial cells, and fibroblasts Increases T-cell proliferation
FGF-basic	—	—	√√	√√	Stimulation of proliferation and differentiation of fibroblasts and endothelial
NGF	—	—	√√	√?	Stimulation of proliferation and differentiation of nerves
Leptin	—	—	↓	?	Re-epithelisation processes in skin wounds
Eotaxin	—	—	√√	√√	Eosinophil chemoattraction
MIP-1β	√√	√	?	?	Promotion of accumulation of lymphocytes , macrophages, monocytes, and natural killer
MIP-1α	—	—	√√	√√	Eosinophil chemoattraction Macrophage activation
TNFβ	—	—	√?	√?	Induction of GM-CSF, G-CSF, IL-1, collagenase, and prostagladin E2 synthesis by fibroblasts
TNFα	—	—	√√	√√	Eosinophil activation and survival
GM-CSF	—	—	√√	√?	Eosinophil activation and proliferation Maturation of heomatopoeitic cells Endothelial migration
IFN-gamma	—	—	?	?	Decrease in eosinphil and Th2 cell numbers Activation of epithelial and endothelial cells Lower IgE levels

√: Expressed. √√: Increased expression. ?: Not definite. ↓: Decreased expression.

The data presented in the table were collected from a number of previsous studies, and the references are provided in the text.

Nine mediators were identified to be secreted in our wounded HBEC model *in vitro*, with some being elevated after injury, as shown in Table 4-18. These will now be discussed below in turn.

4.5.1 Interleukin 6 (IL-6)

The pro-inflammatory and anti-inflammatory cytokine, IL-6, has been observed to be 30-fold higher in supernatants collected from asthmatic children epithelial cell cultures compared to non asthmatic subjects (Kicic, Sutanto, Stevens et al. 2006), suggesting that despite the lack of inflammatory stimuli, epithelial cells of asthmatic patients appear to be producing higher levels of this anti-inflammatory mediator. It has also been previously shown that IL-6 release was higher in TNF-α-exposed primary human bronchial epithelial cells extracted from COPD patients, at 6, 24, and 48 hrs post-treatment (Patel, Roberts, Lloyd-Owen *et al.* 2003). In the studies described in this thesis, scrape-wounded HBEC cells produced potentially higher levels of IL-6 compared to uninjured cultures especially at 72 hrs post-wounding (Table 4-4). A hint of increase was also seen in IL-6 mRNA expression in wounded cultures correlating positively with the protein level. On the other hand, IL-6 could have been preformed and the increase in protein may not have been due to increased transcription of the IL-6 gene, or there might have been altered breakdown of IL-6 by the cells following wounding.

IL-6 is involved in T cell and B cell growth, as well as induction of IgE production (DiCosmo, Picarella and Flavell 1994), all of which are features of airway inflammation. This could in theory be manipulated by blocking IL-6

pathways, which could potentially reduce the inflammatory response seen in asthma and COPD.

4.5.2 Interleukin 8 (IL-8)

A number of cell types present in the asthmatic airways including epithelial cells, are thought to produce the chemokine IL-8. IL-8 has been reported to be elevated in the airway epithelium from asthmatic patients compared to normal bronchial epithelium (Marshall, Perks, Ferkol *et al.* 2001) (Marini, Vittori, Hollemborg *et al.* 1992). However, in one study by Kicic *et. al.,* IL-8 levels were determined in supernatants collected from epithelial cell culture supernatants from asthma (n=7) and non-asthma (n=12) patients. There was no difference between IL-8 levels compared to normal subjects (Kicic, Sutanto, Stevens et al. 2006). In epithelial cells extracted from COPD patients, cultured, and stimulated with TNF-α, IL-8 secretion was observed to be higher at 6 and 24 hrs post-treatment compared to unstimulated cultures, and higher IL-8 production was seen in epithelial cells obtained from COPD patients compared to normal subject(Patel, Roberts, Lloyd-Owen et al. 2003). IL-8 gene expression and release by bronchial epithelium was also higher in human bronchial epithelial cells exposed to cigarette smoke (a risk factor of COPD) in a concentration and time-dependant pattern (Mio, Romberger, Thompson *et al.* 1997). IL-8 plays an important role in inflammation by attracting neutrophils to the site of infection or inflammation, as seen in asthma and COPD (Nocker, Schoonbrood, van de Graaf *et al.* 1996). In addition, IL-8 is thought to have growth factor properties and might have a potential involvement in airway epithelial wound repair. In an attempt to study the cellular and molecular mechanisms during events of airway epithelial reconstitution, there was an

increase in IL-8 expression during cell migration and proliferation steps and a progressive decrease during airway epithelial differentiation (Coraux, Hajj, Lesimple *et al.* 2005).

Interestingly, following scrape-wounding human bronchial epithelial cells grown at ALI, IL-8 levels in supernatants appear to be higher at 72 hrs post-wounding in wounded cultures in both donors used. As for the IL-8 mRNA expression, again the variability was high between the samples during the course of the experiment, but there was a trend towards increased mRNA expression by 24 hrs post-wounding in wounded cultures. In conclusion, therefore, there is a suggestion that IL-8 may be elevated post-wounding. But it's involvement in wound repair of the HBEC model remains to be investigated.

4.5.3 Epithelial-neutrophil activating peptide 78 (ENA-78)

In addition, ENA-78 secretion was observed to be increased in our wounded HBEC model compared to unwounded cultures, especially at 72 hrs post-wounding. ENA-78 mRNA levels were also seen to be elevated in the wounded cultures at 24 hrs compared to normal cultures. The protein and gene expression of the neutrophil chemokine ENA-78 has been observed to be 3-fold increased in bronchial epithelium treated with Rhinovirus, and therefore it is thought to play a role in virus induced inflammation in the airways (Donninger, Glashoff, Haitchi *et al.* 2003). Epithelial ENA-78 expression by asthmatic subjects was observed to be higher than non asthma subject controls when exposed to ozone (Bosson J. 2003). This increase could explain in part the neutrophilia that is seen in some patients with asthma. Moreover, ENA-78 is a monocyte chemoattractant, and may be important in sustaining airway inflammation through monocyte recruitment,

further implicating its role in the pathology of airway disease (Kawaguchi, Kokubu, Matsukura *et al.* 2003). ENA-78 has also been thought to be an pro-angiogenic factor possibly contribute to the high angiogenic activity seen in idiopathic pulmonary fibrosis (IPF) patients (Thannickal, Toews, White *et al.* 2004).

4.5.4 Regulated upon activation, normal T-cell expressed, and secreted (RANTES)

RANTES is a chemokine for eosinophils, T cells, and monocytes/macrophages. Production of RANTES was observed to be higher in differentiated HBEC cultures when wounded compared to unwounded cells. When RANTES mRNA levels were previously examined in patients with mild asthma, no difference was seen compared to normal patients, although RANTES was seen to be constitutively expressed in airways by epithelial cells, smooth muscle cells, and sub-epithelial cells (Berkman, Krishnan, Gilbey *et al.* 1996). However, RANTES mRNA expression was 5-fold elevated in patients with chronic bronchitis compared to healthy non-smoking subjects, with strong expression in the epithelium and sub-epithelium compartments (Zhu, Qiu, Majumdar et al. 2001).

4.5.5 Interleukin 1β (IL-1β)

IL-1β is a pro-inflammatory cytokine involved in the activation of macrophages and epithelial cells, and may play an important protective role against inflammation. Its expression was seen to be elevated in bronchial epithelium of asthma patients correlating with the number of IL-1β producing macrophages (Sousa, Lane, Nakhosteen *et al.* 1996). However, when the amount of IL-1β was measured from supernatants from asthmatic children human bronchial epithelial

cell cultures, similar amounts were observed compared to normal epithelial cultures (Kicic, Sutanto, Stevens et al. 2006). IL-1β secretion was also seen to be elevated by the epithelium, 24 hrs after exposure to cigarette smoke in COPD patients compared to healthy never smoker subjects (250.0% mean increase and 383.3%, respectively) (Rusznak, Mills, Devalia *et al.* 2000). IL-1β levels, when measured in our HBEC wounded cultures, showed a an increase compared to uninjured cultures, although the concentration levels were relatively low in all conditions.

4.5.6 Macrophage inflammatory protein 1β (MIP-1β)

The macrophage and T lymphocyte chemoatractant, MIP-1β, is said to be produced by a number of cell types including the bronchial epithelium. In one study, MIP-1β levels in the broncheoalveolar lavage fluid (BALF) of 12 smokers affected by chronic bronchitis and 14 smoking, 15 non-smoking and six ex-smoking healthy subjects, were investigated. Significantly higher levels were seen in patients with chronic bronchitis compared to smokers, non-smokers, or ex-smoker subjects (Capelli, Di Stefano, Gnemmi *et al.* 1999). The studies on MIP-1β to date are limited since this chemokine has rarely been associated with disease, and thus its role in inflammatory disease remains to be clarified. In our differentiated HBEC cultures, MIP-1β was only detected in donor 2 in our studies. A possible increase could be observed in the scrape-wounded cultures compared to unwounded cells at 72 hrs post-wounding in these samples where it could be detected, but the significance remains unclear.

4.5.7 Granulocyte colony stimulating factor (G-CSF)

The colony stimulating factor hormone G-CSF that stimulates the bone marrow to produce granulocytes and stem cells (Petit, Szyper-Kravitz, Nagler *et al.* 2002), did show higher levels in supernatant collected from scrape-wounded differentiated HBEC compared to unwounded cells especially at 72 hrs post-wounding. Significant increase, however, was observed at the mRNA level. G-CSF expression by epithelial cells exposed to bacterial infection has been thought to prolong polymorphonuclear leukocytes (PMN) survival by delaying apoptosis. This is thought to be particularly important in the inflammation observed in cystic fibrosis (Saba, Soong, Greenberg et al. 2002). GM-CSF is thought to be more involved in airway inflammatory diseases rather than G-CSF, and especially in asthma, where it plays a role in eosinophil activation and growth; however it was not detected in our scrape-wounded HBEC cultures. Higher levels of GM CSF in supernatants collected from asthmatic epithelial cells was observed to be elevated when compared to normal samples (0.88 ± 0.09 vs. 0.21 ± 0.105 (SD) ng/5 x 10^5 cells). An increase in GM CSF mRNA from asthmatic epithelial was also observed in the same study compared to normal samples (Soloperto, Mattoso, Fasoli *et al.* 1991), suggesting a possible role in eosinophil infiltration and activation in asthmatic airways. Another study confirmed these results when epithelial cells from asthma patients were obtained by brushings and investigated through their expression of GM-CSF. A higher percentage of cells compared to normal epithelial cells (39% vs. 0% respectively) (Vachier, Chiappara, Vignola *et al.* 1998) were observed to be expressing GM-CSF. However, in the experiments described in this thesis, we were unable to detect GM-CSF production by airway epithelium. The reasons for this remains unclear but could be partly explained

either as technical errors during the course of the assay or GM-CSF expression requires a more complex inflammatory environment than our HBEC scrape-wound model can provide.

4.5.8 Interferon-inducible protein 10 (IP-10)

Although chemokine IP-10 was seen to be expressed by HBEC grown at ALI, no clear difference was observed between scrape-wounded cultures compared to normal unwounded cells in our current study. IP-10 is known to be produced by a number of cell types, particularly epithelial cells (Sauty, Dziejman, Taha *et al.* 1999). It acts as a chemoattractant for Th1 and natural killer cells. Increased levels of IP-10 have been observed in both COPD (Saetta, Mariani, Panina-Bordignon *et al.* 2002) and asthma (Miotto, Christodoulopoulos, Olivenstein *et al.* 2001). In an attempt to take this finding forward, Spurrell *et. al.* infected primary human epithelial cells with human rhinovirus type 16 (HRV-16), and observed an increase in IP-10 levels in collected supernatants (Spurrell, Wiehler, Zaheer *et al.* 2005). Rhinovirus type 16 (HRV-16) infections trigger exacerbations of both asthma and COPD (Spurrell, Wiehler, Zaheer et al. 2005).

4.5.9 Vascular endothelial growth factor (VEGF)

A slight increase was seen in the expression of VEGF in our wounded and unwounded HBEC *in vitro* at 48 hrs post-wounding. But there was a very high concentration being produced by HBEC in general and thus the values were above the limit of detection. However, VEGF is thought to be overproduced by the epithelium in asthmatic subjects activated with Th2 driven inflammation, leading to leukocyte accumulation, causing angiogenesis and leakage, goblet cell metaplasia, and myocyte hyperplasia, causing tissue remodelling (Rothenberg

2004). VEGF has also been shown to be up-regulated in Th1-associated states (such as COPD), albeit at lower levels. However, in another study, serum VEGF levels were the same in samples from COPD and normal patients (Cheng, Wang, Yu *et al.* 2008).

4.5.10 Other undetected cytokines

On the other hand, some of the cytokines, previously thought to be epithelial derived and overproduced in asthma and COPD, were below the detection range in our cultures or were very close to the concentration seen in the negative control sample. This could be explained in several ways. First, epithelial cells do not produce these mediators at all in differentiated cell cultures. Secondly, physical wounding did not prove to be a relevant stimulus, and these mediators need another stimulus to be produced such as interaction with inhaled irritants. Finally, it is possible that there is a need for inflammatory cells to be present in order to stimulate the epithelial cells to produce these mediators. The model used portrays the involvement and response of only the epithelial cells in isolation. Examples of such cytokines are MCP-1, eotaxin an TNF-α.

MCP-1 has been shown previously to be present in asthmatic epithelium (Folkard, Westwick and Millar 1997), whereas 1.5-fold higher levels of MCP-1 were seen in epithelial cells from COPD patients, recruiting mast cells and macrophages into the epithelium (Capelli, Di Stefano, Gnemmi et al. 1999). Another important factor with a role in asthma and COPD is TNF-α, thought to be mostly produced by macrophages and epithelial cells (Devalia, Campbell, Sapsford *et al.* 1993), whereas TNF-β is mainly produced by activated lymphocytes. Higher levels of TNF-α from epithelial cells in asthma have been previously reported in human

lung (Ohkawara Y 1992). Eotaxin was another cytokine not detected in our differentiate HBEC cultures, contrary to previous findings in asthma and COPD. Eotaxin protein and mRNA expression was seen in the airways of asthmatics, mainly in the epithelium (Mattoli, Stacey, Sun *et al.* 1997) suggesting its role in eosinophil recruitment in asthma, but also in T lymphocytes, macrophages and eosinophils.

To conclude, the epithelium has been previously suggested to be a target and source of release of a number of inflammatory cell mediators and cytokines. This suggests a role for the airway epithelium in the inflammatory changes seen in a number of airway diseases including asthma and COPD. Investigation of the secretory profile of human bronchial epithelial cell (HBEC) wound repair model provided a clear profile for mediators produced in this *in vitro* model, and allowed assessment of the effect of wounding on the epithelial derived cytokine profile. Although this physical wound might be different than the damage occurring in asthma and COPD, further research to determine if modifying the epithelial response to this mechanical wound, or carrying out functional repair studies by targeting some of the cytokines involved above, or possibly using co-culture models, would be of value in evaluating inflammatory airway responses.

Chapter 5. Identification of Potential Airway Epithelial Cell Progenitors

5.1 Introduction

In the last two chapters, I described some of the key mechanisms underlying the control of repair of wounded epithelial cells in the human airway. These processes potentially involve a population of resident stem cells in the airway, as discussed in Chapter 1 and Chapter 3, and as in other adult organs(Weiss, Berberich, Borok *et al.* 2006). Stem cells can be defined as multipotent undifferentiated cells able to reconstitute the various tissues of an organ, depending on where they reside. Stem cells give rise to transient amplifying (TA) cells with self renewal and regenerative characteristics (Figure 1-5). In the lung, both basal cells and variant Clara cells present in neuroepithelial bodies, are thought to function as the stem cell population (Engelhardt 2001), (Hong, Reynolds and Giangreco 2001). More recently, 'side population' cells, characterised by their ability to efflux Hoechst dye, have been identified in the lung. This population of cells is thought to contain a primitive stem cell population (Summer, Kotton, Sun et al. 2003) with mesenchymal and epithelial phenotypes. However, to date, no single lung stem cell has been fully characterised with the ability to give rise to the full range of epithelial lineages. It is also thought that local regional niches regulate the phenotype and expansion of stem cells. Distinct sub populations of the epithelium, thought to acquire 'stemness', are discussed in the following sections.

5.1.1 Clonogenic potential of the airway epithelial cells

The lung contains a diverse number of cell types, and as discussed earlier, a number of *in vivo* and *in vitro* models have been developed to facilitate the investigation and identification of stem cells. One method of studying the putative airway epithelial stem cell populations is the *in vitro* colony forming efficiency (CFE) assay, developed by Randell *et. al.* (Randell 1992). This method was adapted from a tracheal xenograft model with recombinant retroviral markers used to assess the clonal expansion of airway epithelial cells (Zepeda, Chinoy and Wilson 1995) (Engelhardt, Schlossberg, Yankaskas et al. 1995). One disadvantage of the CFE *in vitro* model is less efficient differentiation, than that which is seen *in vivo*, but it was used primarily to asses the proliferative potential of stem or progenitor cell populations and not the progenitor-progeny relationship in the airway epithelium. The CFU assay index was used by Schoch and colleagues to evaluate the clonal growth potential of murine tracheal epithelial cells (Schoch, Lori and Burns 2004). Briefly, a single cell suspension of mouse tracheal epithelial cells was derived from β-galactosidase-expressing ROSA26 mice into non-ROSA26 tracheal epithelial cells and then grown at air liquid interface (ALI) for 3 weeks. X-Gal staining revealed ROSA26 LacZ-positive colonies within the airway epithelium, indicating a population of cells with progenitor capabilities resides in the basal layer. 1.7% of the epithelial cells formed colonies of different sizes, demonstrating high proliferative capacity and suggesting this subset may be good candidates for a stem or TA cell population. Many attempts have been carried out to try and identify the progeny-progenitor relationship, and to study the different epithelial cell types in the mouse trachea responsible for reconstituting a pseudostratified epithelium following damage.

One such method is to isolate and purify various rat tracheal epithelial cell types, inoculating them into denuded rat tracheas which are then subcutaneously grafted onto the backs of immunodeficient mice (Hook, Brody, Cameron *et al.* 1987). It was observed that purified Clara cells could reconstitute an epithelium similar to the bronchiolar epithelium in native rat tracheas, while a mixed population of tracheal cell types could generate a mucociliary epithelium resembling the pseudostratified tracheal lining seen in normal conditions *in vivo*.

5.1.2 A distinct 'side population' resides in the lung

In 1996, Goodell *et. al.* used the vital DNA binding dye, bisBenzimide H trihydrochloride (Hoechst) 33342 (Arndt-Jovin and Jovin 1977), to identify and isolate replicating and quiescent cell populations from murine bone marrow in order to study hematopoietic stem cells (HSC) (Goodell, Brose, Paradis et al. 1996). While experimenting with staining the murine bone marrow cells using the vital dye, Hoechst 33342, a complex fluorescence pattern of Hoechst staining was observed in the whole bone marrow, where Hoechst fluorescence was detected by simultaneous monitoring at two emission wavelengths (Hoechst blue versus Hoechst red). A small subset of cells (named the side population (SP)), with low fluorescent intensity according to the above dual wavelength, was isolated, containing murine HSC surface markers (stem cell antigen (Sca)-1). Their HSC activity was 1000 fold increased compared to other cells present (as determined in repopulation experiments), and by measures of enrichment (CFU index). It was concluded that this distinct pattern of staining was due to high and rapid Hoechst efflux mediated by ABCG2, which is blocked by the voltage dependant calcium channel inhibitor verapamil (Figure 5-1). This was the first use of a single dye to

define a stem cell population. Subsequently, similar studies in human adult bone marrow, umbilical cord blood and porcine bone marrow using Hoechst 33342 produced very similar results to those observed with murine bone marrow.

Side population identification has proven important in studies in stem cell biology of renewing tissues, including the lung, since there is a lack of surface stem cell markers to date which accurately define this cell population. SP have been identified in a number of other tissues including human and murine mammary epithelial cells (Alvi, Clayton, Joshi *et al.* 2003), rabbit limbal epithelial cells (Umemoto, Yamato, Nishida *et al.* 2006), human epidermal keratinocytes (Terunuma, Jackson, Kapoor et al. 2003), mice lungs (Summer, Kotton, Sun *et al.* 2004), mice airway epithelium (Giangreco, Shen and Reynolds 2004), and human tracheobronchial epithelium (Hackett, Shaheen, Johnson *et al.* 2008).

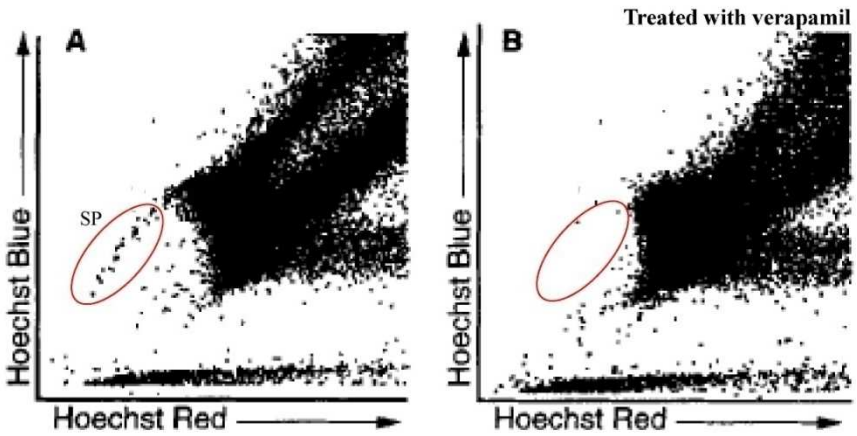

Figure 5-1: Murine bone marrow side population.
(A) shows the Hoechst efflux side population (red circle) which was inhibited by verapamil in (B) accounting for 0.1% of the total population. Taken from (Goodell, Brose, Paradis et al. 1996).

Cells with a SP phenotype were identified in the adult mouse lung by Summer *et. al.* Enzyme digested mouse lung suspension was stained with Hoechst 33342 dye before flow cytometry analysis, and a SP representing 0.03-0.07% of all cells was

present: the efflux was inhibited by verapamil (Summer, Kotton, Sun et al. 2003). To examine the additional phenotypic characteristics of this SP, various antibodies were also used to stain the cells after Hoechst incubation. It was observed that the SP was heterogeneous consisting of 65-75% CD45-positive cells (an HSC marker): these cells co-expressed the endothelial marker CD31. However, the CD45-positive and C45-negative populations expressed Sca-1. To further characterise the origin of the SP, an antibody against α-smooth muscle actin (α-SMA) was used to immunostain the SP, but no detected expression was observed. Giangreco *et. al.* then investigated the hypothesis that intrapulmonary conducting airways contain a verapamil-sensitive Hoechst-effluxing population that is enriched with lung-specific epithelial stem cells (Giangreco, Shen and Reynolds 2004). Enzyme-dissociated mouse lung cell suspensions contained a SP comprising 0.09% of CD45-positive cells and 0.87% CD45-negative population. CD45-negative SP cells were also positive for stem cell antigen (Sca)-1. CD45 is a transmembrane protein present on all known differentiated haematopoietic cells except for erythrocytes and plasma cells, and is considered as a reliable HSC marker.

Bone marrow SP contains 60–70% CD45-positive cells and 30–40% CD45–negative cells (Liang, Summer, Sun *et al.* 2005). It was concluded that the CD45-negative lung SP includes two populations: one with mesenchymal characteristics, and another with airway epithelial characteristics (shown by positive staining with an antibody against clara cell secretory protein, CCSP). Summer *et. al.* then set out to examine the origin of the lung SP cells and characterise the difference between the CD45-negative and CD-45 positive subsets. They showed that these two distinct subsets have different roles in lung

tissue homeostasis (Summer, Kotton, Sun et al. 2004). SP, comprising 0.09% of cells and containing both CD45-negative and CD-45 positive cells, were identified where most of the former was seen to be derived from the host pulmonary tissues and the latter originated from bone marrow. They also showed that the CD45-positive lung SP cells were cytokeratin positive/α-SMA positive while CD45-negative SP cells were cytokeratin negative but α-SMA positive. More recently, in an attempt to identify and isolate SP cells from human tracheobronchial epithelium, it was found that CD45-negative SP cells comprised 0.12% of the total epithelial population in normal lung but 0.4% of the epithelium from asthmatic subjects, providing evidence of a dysregulated epithelium in asthmatics and suggesting a role for progenitor cells, if not stem cells, in repair mechanisms in the asthmatic epithelium (Hackett, Shaheen, Johnson et al. 2008). Moreover, these investigators observed that a very small number (< 100) of CD45-negative SP was sufficient to proliferate and differentiate into a pseudostratified epithelium when grown *in vitro* at ALI, compared to the need for up to 5 x 10^6 non-SP cells to form the differentiated multi-layer in culture. It is also worth noting that the Hoechst-effluxing SP has been shown to be an enriched source of lung tumour-initiating cells with stem cell properties (Ho, Ng, Lam *et al.* 2007).

5.1.3 How and why do these cells efflux Hoechst 33342 dye ?

Now that it has been determined that SP have the ability to efflux the DNA binding dye, Hoechst 33345, at a greater rate than other cell types in the tissue, it is necessary to understand what initiates this efflux.

Hoechst 33342 stain has been used as an index of DNA content and chromatin conformation (Arndt-Jovin and Jovin 1977), and it binds to the A-T regions of the minor groove (Lalande and Miller 1979). The ability of Hoechst dye efflux to be used as a stem cell isolation method resides in the ability of the dye to be effluxed by the ATP-binding cassette (ABC) transporter superfamily, in particular the multidrug resistance 1 (MDR1) and breast cancer resistance protein 1 (Bcrp1), also referred to as ABCG2 (Zhou, Schuetz, Bunting *et al.* 2001). The ABCG2 gene was first isolated from human tumour cell lines and has been shown to play a role in drug resistance. It has also been noted that the activity of this membrane transporter is blocked by the calcium channel inhibitor, verapamil. When Zou *et. al.* disrupted murine mdr1a and mdr1b genes (homologues of the human MDR1), they saw no difference in the SP cell number, whilst the expression of ABCG2 was highly conserved in primitive stem cells from a variety of tissues (Zhou, Schuetz, Bunting et al. 2001). This was further confirmed by observing a higher number of Hoechst-effluxing SP cells when enforced expression of ABCG2 was applied to bone-marrow cells, with the protein directly correlating to the SP phenotype. (Maliepaard, van Gastelen, de Jong *et al.* 1999). ABCG2 expression has been observed to be a widely conserved marker for Hoechst-dye-effluxing stem cells (Zhou, Schuetz, Bunting et al. 2001).

Many possibilities have been suggested as to why SP use these efflux pumps. It has been proposed that these pumps provide a protective function, since stem cells reside in the adult body over a lifetime (Scharenberg, Harkey and Torok-Storb 2002). ABCG2 could help maintain and regulate these unique stem cells (Bunting, Galipeau, Topham *et al.* 1998). Another possibility could be that ABCG2 expression interferes with stem cell homing and thus leads to

engraftment defects , possibly by conferring a toxic effect on stem-cell metabolism leading to an increase in apoptosis, as well as influencing stem cell-microenvironment interactions (Zhou, Schuetz, Bunting et al. 2001). However, the mechanism of ABCG2 and its relation to SP cells remains to be determined.

5.2 Objectives

The aim of the present study was to identify and if possible isolate distinct side populations from human bronchial epithelial cells grown *in vitro*, either in an undifferentiated or a differentiated (ALI) state. The approaches used included single cell cloning, either using FACS or limited dilution cloning, and the FACS-based Hoechst efflux method of SP isolation. Epithelial cell biopsies were expanded in culture to compliment the use of commercially available epithelial cells, and in order to establish a model to evaluate the comparison of diseased and normal samples in the future. Single cell sorting was also carried out in order to investigate the clonogenic potential of epithelial cells *in vitro*. This could be useful in reaching a better level of understanding of stem cell populations using an *in vitro* HBEC model, with the potential of studying diseased samples in this context.

5.3 Methods

Single cell sorting was carried out on undifferentiated HBEC at p3 following the protocols in section 2.1.3, using either FACS or limited dilution. Digital images were captured using a Nikon Diaphot epifluorescence microscope with a mercury lamp with SPOTCam software.

The FACS-based Hoechst efflux method detailed in section 2.3 was carried out on differentiated HBEC (p4) and undifferentiated HBEC (p3) from donor 1 only to investigate SP. The SP sorting gate was established as follows: after collecting around 250 000 events, a gate was defined using forward vs. side scatter to exclude dead cells. Both Hoechst Red and Blue fluorescence were then shown on a linear scale. A gate was defined around the SP which consisted of small cells with the lowest fluorescence profile and which disappeared with the verapamil control. When a verapamil control was not included, it was difficult to identify the SP, however, a gate was put around the very smallest cells with low fluorescence profile. Examples of the gates are shown in the results following this section.

Immunofluorescence techniques were employed as described in section 2.2.1 to characterize the epithelial cells expanded from biopsies by investigating the expression of CD44 and CCSP.

5.4 Results

5.4.1 Isolated single human airway epithelial cells from undifferentiated HBEC cultures do not have the ability to grow *in vitro* in the standard culture environment

One characteristic of many stem cell populations is their ability to expand in culture from a single cell. Therefore, single cell sorting of undifferentiated HBEC was carried out using dilution cloning (section 2.1.3) and FACS, into 96-well plates to assess the clonogenic and differentiation potential of individual cells. Single cells were observed in some wells of the plates but did not survive long on plastic in serum-free BEGM. After ten days, all cells were seen to be granulated and dead. Wells were checked for cells usually 3 days after seeding, and then at 10 day intervals for formation of colonies. Figure 5-2 below is representative of 3 experiments using dilution cloning, and shows wells early after seeding (3 days), and 10 days post-seeding. Attempts were also made to isolate single cells sorted using FACS (n=3 plates) since it would be less time consuming, but the majority of wells became infected early in the culture period due to the difficulty in maintaining sterility following FACS, and hence this approach was not pursued.

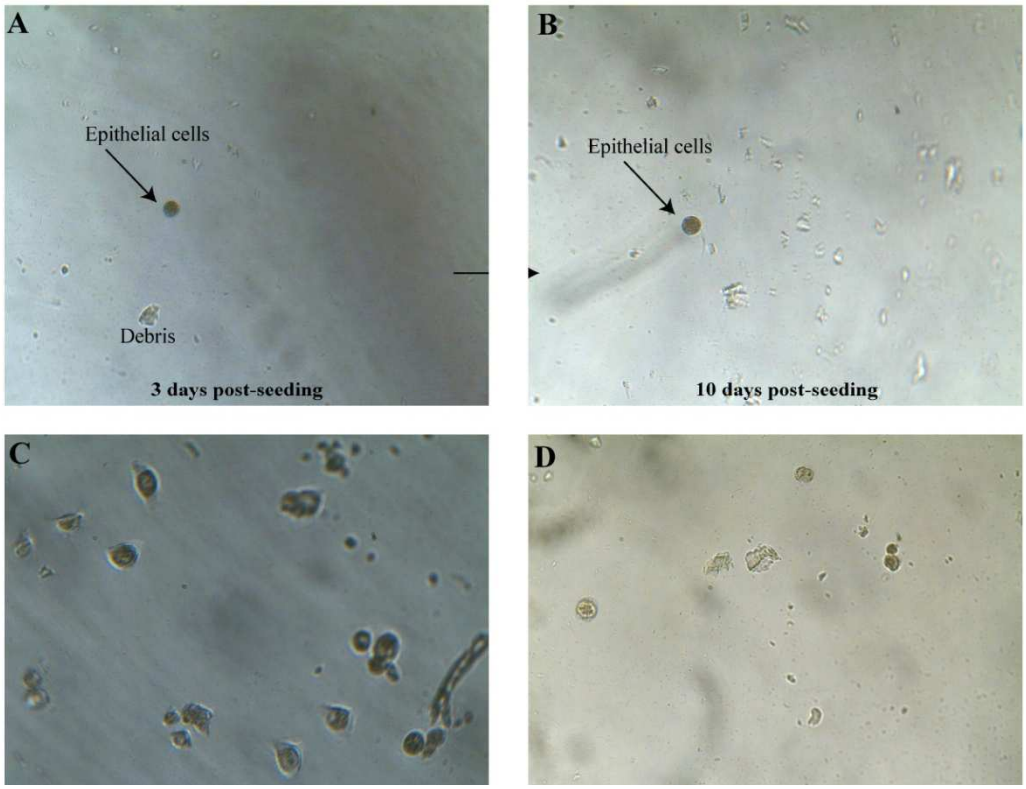

Figure 5-2: Epithelial single cell sorting using dilution cloning.
Images of random fields from 96-well plates showing a single cell 3 days post seeding (A, arrow) and 10 days post-seeding (B, arrow), with no cell division occurring. In some wells following dilution cloning, more than one cell was found (C): these wells were excluded from further analysis. Most cells looked granulated and dead when left in culture for 10 days (D). These images are representative of 3 experiments each performed in a single 96-well plate, Images are shown at a magnification of x20.

5.4.2 Side population in undifferentiated HBEC

Given that with single cells isolated from growing undifferentiated cultures (without first sorting into populations), enriching for a stem cell population failed to give rise to clonal cultures, attempts were next made to determine if a side population of cells was present, using the Hoechst-efflux method described above. SP cells were identified on the basis of verapamil-sensitive Hoechst-efflux p3 cell suspensions were incubated with 5 µg/ml Hoechst 33342 for 90 min (as described in 2.3). In a total of seven experiments, SP cells were identified in three, accounting for 0.05-1.15% of all cells present in these positive experiments.

Figure 5-3 represents SP characteristics with inhibition by verapamil of Hoechst efflux, in cultured undifferentiated HBEC.

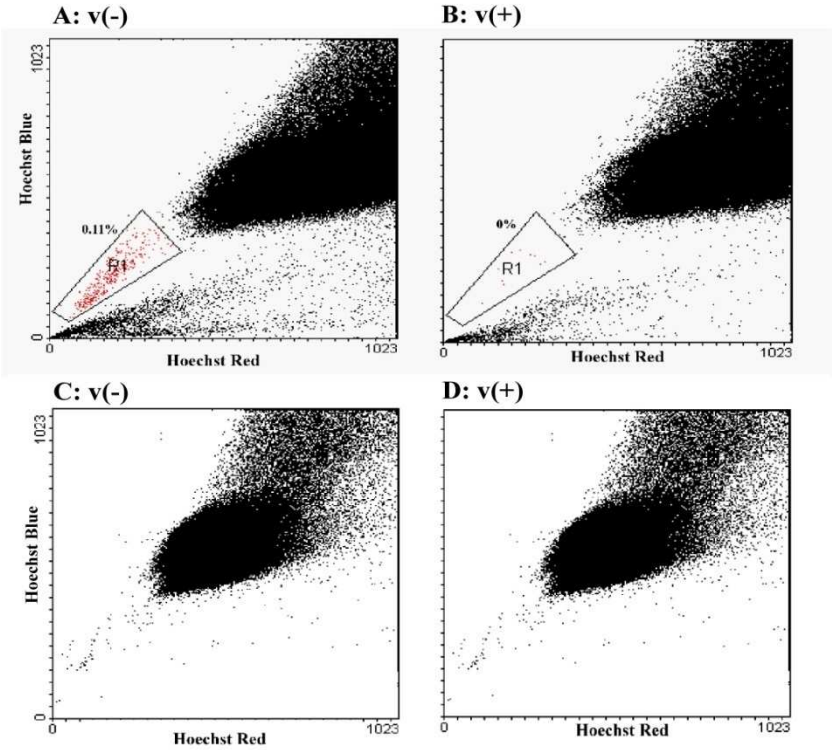

Figure 5-3: FACS analysis of SP present in cultured undifferentiated HBEC at p3.
(A) shows a representative positive culture showing presence of SP, detected at dual wavelength of Hoechst excitation and emission at 670/30-nm band pass and 450/65-nm band-pass filters. Hoechst efflux was inhibited with verapamil (B). (C) is a negative example of cultures with no SP where in (D) pre-treatment with verapamil was also carried out. Experiments were repeated 7 times with 3 positive cultures for SP.

Having demonstrated the presence of SP in at least some populations of primary human airway epithelial cell cultures, attempts were then made to investigate whether the number of SP cells was increased in response to injury in a single experiment. Cultured undifferentiated HBEC were wounded (as described in section 2.1.1.7) and then analysed for the presence of SP. In these wounded cultures, a SP was identified and efflux was inhibited by both verapamil and another ABCG2 inhibitor, Fumitremorgan C (FTC) (Rabindran, Ross, Doyle *et*

al. 2000) (Figure 5-4), with 2-fold higher number compared to the unwounded cultures (0.06% vs. 0.03% of total cells, respectively). However, for reasons which are unclear, the potential SP in the unwounded cultures was inhibited by FTC but not verapamil. Given the lack of a marked increase in the size of the SP in the undifferentiated cultures despite wounding, I proceeded to try and investigate this SP in differentiated epithelial cell cultures.

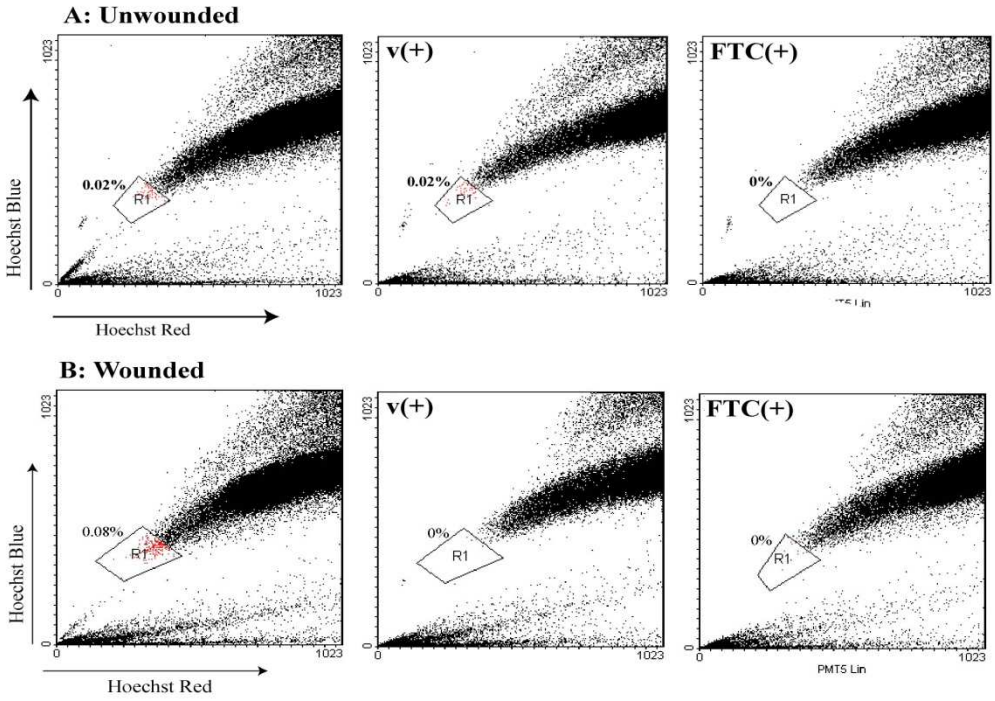

Figure 5-4: FACS analysis of SP in wounded undifferentiated HBEC.
(A) shows FACS analysis data for undifferentiated HBEC with 0.02% SP inhibited by only fumitremorgin C but not verapamil. This SP was 4 fold higher in wounded undifferentiated HBEC 24 hrs post-wounding (B) accounting for 0.08% of total cells in culture and inhibited by both verapamil and FTC. This experiment was carried out once.

5.4.3 SP in cultured differentiated HBEC grown at ALI

Since a SP was identified in some cultures of undifferentiated HBEC, the FACS-based Hoechst-efflux method of stem cell purification was then carried out to try and identify SP in differentiated HBEC cultures grown at ALI. This was repeated

five times with a SP identified in one experiment comprising 0.14% SP. Figure 5-5 shows the identified SP where the efflux was inhibited by verapamil, and an example of cultures that had no SP.

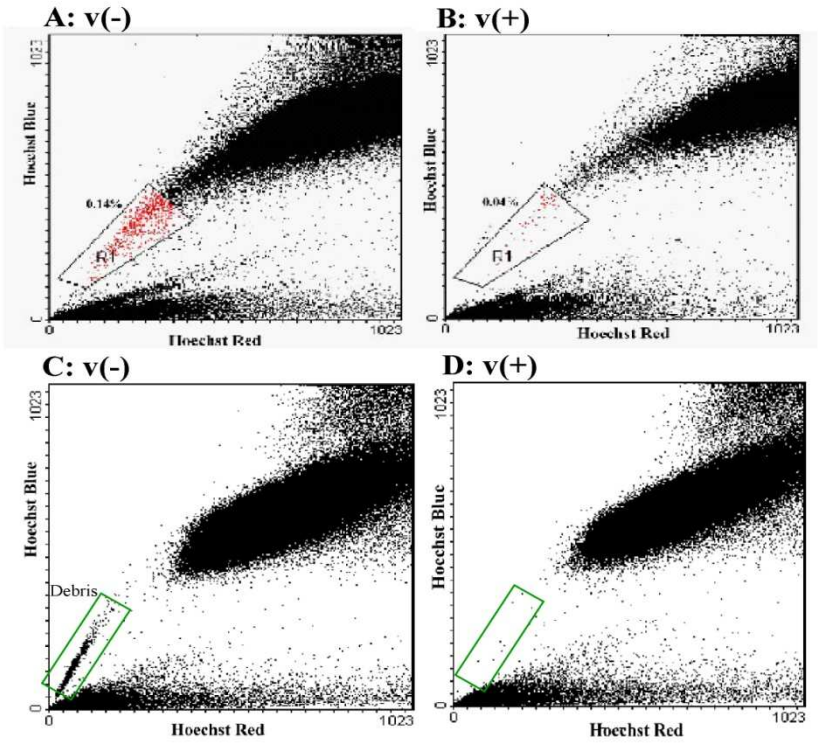

Figure 5-5: FACS analysis of SP in differentiated HBEC grown at ALI.
The SP was identified once out of five experiments, accounting for 0.14% of the cells present (A) and was inhibited by verapamil (B). A representative negative result is presented where no SP was seen (C) and with (D) pre-treatment with verapamil. Apparent cells gated in green (C+D) were observed to be debris according to PI staining.

5.4.4 SP in epithelial cells expanded form lung biopsies

During the course of these studies, it was possible to perform FACS based Hoechst efflux experiment using tracheal epithelial cells expanded from cells isolated from bronchial biopsies from a normal individual. These biopsies were carried out by Dr. Claudia Ceresa as described in section 2.1.2. After epithelial cells were obtained in culture, they were characterised to determine the phenotype of the cells. These expanded cells had an epithelial morphology in culture

(Spindle-shaped cuboidal, Figure 5-6), and stained positive for basal and Clara epithelial markers expression (CD44 and CCSP, Figure 5-7). Biopsy epithelial cells characterisation was only carried out once since there were not sufficient cells for repeat characterisations and FACS analysis of Hoechst dye efflux ability.

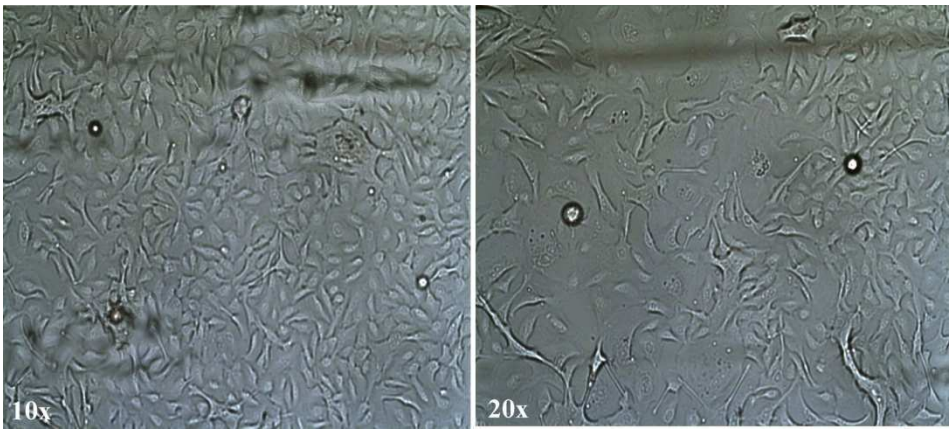

Figure 5-6: Brightfield images of epithelial cells grown from lung biospsies.
Both images show a cuboidal spindle-like epithelial phenotype. Random fields were captured at 10x and 20x magnifications.

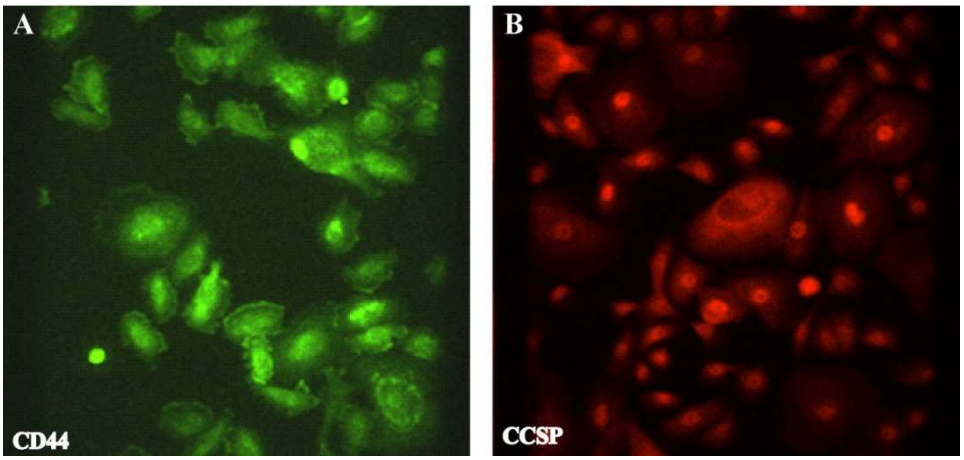

Figure 5-7: Immunofluorescence images of epithelial cells expanded from lung biopsies.
(A) shows positive expression of CD44 (an epithelial basal cell marker, green), and (B) shows positive expression of clara cell secretory protein (Clara cell marker, red). Images were taken at x20 magnification and are representative of 4 random fields captured from the single cultured cell population described.

Hoechst-efflux analysis of SP was then carried out on the harvested cells at p1; and a SP was identified accounting for 0.15% of all cells (Figure 5-8 A). Because of the limited number of cells which could be expanded from this biopsy, it was not possible to perform either the verapamil control or a repeat of the experiment during the time course of this study. A further experiment was performed on cells at a latter passage (p4) and again a SP was observed accounting for 0.04% of all cells (Figure 5-8 B). By p4 sufficient cells were available to include a verapamil control (Figure 5-8 B and C), and as would be expected, Hoechst exclusion was inhibited by verapamil. As a preliminary conclusion, it seems therefore that SP numbers are higher when the cells are expanded straight from biopsies than when cultured for a few passages in culture, and this could explain why SP identification in cultured HBEC using late passaged cells is less robust.

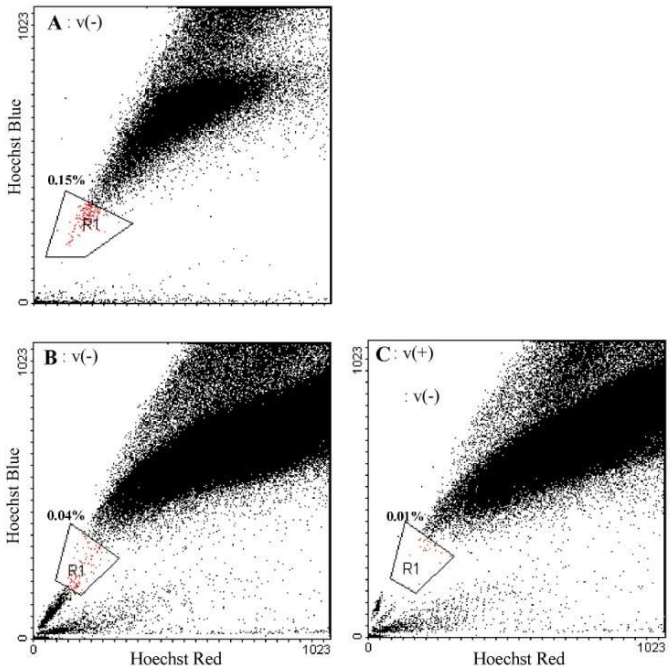

Figure 5-8: FACS analysis SP from epithelial cells derived from lung biopsies.
(A) shows FACS analysis data with 0.15% of SP from epithelial cells at passage 1 (no verapamil control was carried out due to insufficient cell numbers). (B) shows a FACS analysis of SP (0.04%) when the cells are passaged further (passage4), inhibited by verapamil (C, 0.01%).

5.5 Discussion

This chapter describes a series of experiments where the identification of potential progenitor cell populations, in human airway epithelial models, was attempted. Epithelial single cell cloning was first carried out from commercially obtained human bronchial epithelial cells (HBEC). However, it did not prove feasible to expand these single cells in culture on plastic using serum free BEGM. The cells looked granulated and were non-viable early after culture (10days) in all experiments. Therefore, identification of a side population (SP) as previously used in studies in other cell types was then pursued in order to look for the presence of potential progenitor cells in this HBEC model.

A SP was identified in at least some cultures, accounting for 0.1-1% in commercially purchased cultured HBEC (undifferentiated and differentiated at ALI), and also in epithelial cell populations expanded from lung biopsies. It proved very difficult to grow these SP cells in culture and maintain sterility of FACS-separated cells, and on the two occasions where the isolation was successful, infections were seen in resultant cultures.

As mentioned above, a SP was also seen in epithelial cells expanded from lung biopsies, when passaged *in vitro* in culture media. Adequate number of cells to perform FACS analysis was only obtained once since the supply of biopsies was limited and the number of cells to start with was very low: in one other experiment, epithelial cell cultures were obtained but expansion in culture was inadequate to undertake FACS studies. Similar results have been recently reported using human tracheobronchial epithelium, where SP investigation was done on fresh cells isolated from transplant donor lungs by protease digestion, with 0.12%

±0.01 SP present (Hackett, Shaheen, Johnson et al. 2008), similar to the SP percentage observed in our cultures when it was present. Although these results have to be considered preliminary in nature, they suggest that SP are present in early cell culture but appear to decline in number with repeated cell passage.

The observation that epithelial cells could be isolated from biopsies and expanded in culture is of interest and provides a potential model for future studies. These epithelial cells from lung biopsies were characterised by the expression of the basal cell marker CD44 and Clara cell marker CCSP. The cells were also differentiated at ALI as described in chapter 2 and a multi-layered epithelium was generated, where mucus production on the surface of cultures was observed. This was carried out only once during the course of this study, since there were not many biopsies available. However, this could be useful in the future to allow the study of cells from different disease states such as asthma and COPD, by comparing differentiation potential of disease and normal samples.

Technical limitations emerged during the course of these experiments; infections were often seen in SP experiments and single cell cloning in the cultures early post-seeding. Moreover, it proved difficult to carry out single cell manipulation of epithelial cells using our culture conditions. Most previously published work to investigate the clonogenic potential of epithelial cells was done in xenograft animal models *in vivo* or using feeder cell layers (Hong, Reynolds and Watkins 2004) (Hitoshi Kitamura 1993). It may be worth trying these approaches, or using a potentially suitable substratum such as collagen in the future.

The main value in identifying SP in biopsy derived cultures would be to allow the study of progenitor cell biology in the context of disease. Moreover, SP has been observed to be a more general feature of malignant disease than previously

thought (Hirschmann-Jax, Foster, Wulf *et al.* 2004), (Ho, Ng, Lam et al. 2007), and thus the approaches described here could provide a model for the further understanding of lung cancer.

It has previously been observed when investigating SP activity that this population is associated with the expression of stem cell antigen 1 (sca-1), for example in mouse mammary gland (Welm, Tepera, Venezia *et al.* 2002), mouse heart (Oh, Bradfute, Gallardo *et al.* 2003), and mouse liver (Bryon E. Petersen 2003). Sca-1 is an 18-kDa mouse glycosyl phosphatidylinositol-anchored cell surface protein of the *Ly6* gene family which has been associated with tissue-resident stem and progenitor cells (Holmes and Stanford 2007). Sca-1 and SP relationship has been reported in the lung (Summer, Kotton, Sun et al. 2003) (Giangreco, Shen and Reynolds 2004), however, it was not seen to be present in the airway epithelium or alveolar type II cells, both of which are suspected to exhibit progenitor activity. On the other hand, sca-1^+ broncheoalveolar cells with *in vitro* multilineage differentiation capacity have been isolated from murine lung (Kim, Jackson and Woolfenden 2005). Although an ortholog for sca-1 has not yet been identified in humans, the data identified in sca-1 null mice demonstrate a number of important concepts in stem cell biology including: the association of degenerative diseases and altered stem cell pool, the importance of stem cell responses to tissue damage and maintenance. Thus identifying a human sca-1 and understanding its function and pathways will potentially facilitate the understanding and manipulation of resident stem/progenitor cell populations in order to apply new therapies and regenerative medicine applications.

In summary, therefore, it appears that a SP is present in at least some culture model systems of primary human airway epithelial cells. These cultures proved

technically demanding to undertake, but with further development, this approach holds considerable promise for the study of airway epithelial repair.

The SP has been identified in several other organs including the heart, limbal epithelium. Cardiac SP have been identified in adult mouse heart with the ability to efflux the Hoechst 33342 and expression of ABCG2, containing both "vascular" and "non-vascular" cells; and were observed to differentiate into cardiomyocyte-like cells with spontaneous contraction (Yamahara, Fukushima, Coppen *et al.* 2008).

This could be implicated in myocardial regeneration and in the pathogenesis of cardiac diseases. Moreover, a SP has also been identified in the human limbal epithelium (0.2%), with the expression of ABCG2 in the limbal basal epithelial cells, although they were not consistently distributed (Watanabe, Nishida, Yamato *et al.* 2004). These SP findings could be exploited for new tissue engineering approaches to try and reconstruct damaged surfaces, including the eye, heart, and lung epithelium.

Chapter 6. **Summary and Conclusions**

As the first contact with the outer environment, the airway epithelium is constantly susceptible to damage from a wide range of inhaled toxins and particles. As described in chapter 1, the airway epithelium has a number of specific functions to ensure lung homeostasis either in health or under disease conditions. In the studies described in this thesis, two main functions of the airway epithelium were highlighted. First I concentrated on identifying the role of resident epithelial stem/progenitor cells thought to be involved in wound healing (described in chapter 3 and chapter 5 respectively). Secondly, I investigated the potential role of these epithelial cells in regulating inflammation (discussed in chapter 4). The main objective of this study was to reach a better understanding of the role of epithelial cell involvement in wound repair. This is particularly important given the observation that the epithelium is seen to be subject to inappropriate repair cycles in a number of lung diseases for example, epithelial dysfunction is considered to be a feature underlying asthma and COPD (Holgate 2008) (Puchelle, Zahm, Tournier et al. 2006).

6.1.1 Human bronchial epithelial cell (HBEC) wound repair model

As discussed in chapter 3, although a number of *in vitro* and *in vivo* models of both human and animal airway epithelium have been developed over the years (Table 3-1 and Table 3-2), relatively little is known about the control of airway epithelium repair mechanisms, due in part to the complexity of the respiratory tree, and the lack of appropriate models to mimic wound repair of the human

airway epithelium *in vitro*. I adapted a human bronchial epithelial cell (HBEC) model (Dupuit, Gaillard, Hinnrasky et al. 2000) to allow the study of repair mechanisms following wounding. Initially, I characterised this model using differentiation markers for the epithelial cell types present. HBEC were grown on polyester porous membranes using specialised bronchial epithelial growth and differentiation media. The cells were differentiated for three weeks at air liquid interface (ALI). It was observed that the model contained basal, ciliated, and secretory cells *in vitro*. Differentiated epithelia demonstrated mucus production and ciliated cells expressed beating cilia, much like the airway epithelium *in vivo* (see section 3.4.1). Having established a multi-cellular functional epithelium *in vitro*, epithelial disruption was studied by scrape wounding the cell layer using a sterile p200 pipette tip, to mimic the epithelial dysfunction that might occur in the adult body during daily exposure to inhaled toxins and pathogens resulting in epithelial desquamation, as well as the damage seen to the epithelium in respiratory diseases such as asthma and COPD. The scrape-wound was monitored *in vitro* in both undifferentiated and differentiated HBEC by measuring the wound area over a 48 hrs time period. It was observed that differentiated HBEC repaired more rapidly than undifferentiated cells. By 20 hrs post-wounding, the wound was completely healed in all differentiated cultures, whereas the wound was 87% healed in undifferentiated cells by 48 hrs post-wounding (see section 3.4.2). These studies were followed by the investigation of the underlying wound repair mechanism in this model. It has previously been shown that dedifferentiation and migration of cells are the first events that take place after injury, followed by proliferation of new cells to compromise for the loss of cells, then de-differentiation and re-epithelisation (Puchelle 2000). It has also been previously

observed that migration does occur shortly after injury in this HBEC model; this was apparent both by light microscopy and also by studies where lamellopedia were seen at the edge of cells migrating to close the wound (Wadsworth, Nijmeh and Hall 2006). This migration is a separate event from proliferation where the latter occurred at a distant site from the wound edge. In the studies described in this thesis, proliferation was monitored using the marker Ki-67. It was observed that the number of Ki-67 positive cells was significantly higher in differentiated wounded HBEC compared to unwounded cells at 24 hrs post-wounding, suggesting an increase in proliferation at that time point after injury, which was after the wound was completely healed (section 0). Interestingly, this was not the case with undifferentiated wounded and unwounded HBEC, where no significant difference was seen between both. The explanation for this is unclear but may be due to the lack of relevant pro-proliferative features released by differentiated but not undifferentiated cell types. Moreover, slower rates of proliferation/migration in the undifferentiated model (as seen by the delayed wound closure as well), might be another reason for the described observation. It was also observed that Ki-67 positive cell numbers were significantly higher in wounded cultures at 0hrs post-wounding compared to unwounded cells. The reason remains unclear and needs further investigation.

It was important to then move on and address which cell types might be involved in this wound repair mechanism. It has previously been proven that resident stem or progenitor cells are involved in repair events of the respiratory epithelium (Emura 1997). The cells classically suspected to be the stem or progenitor cells are basal and mucus-secretory cells of the trachea and bronchi, Clara cells of the bronchioles, and alveolar type II cells in the alveoli (Otto 2002) (Bishop 2004). In

this differentiated HBEC model, cells were immunofluorescently stained with Ki-67 and a number of epithelial-cell specific markers, to try and identify which cell type(s) are proliferating after injury. Immediately after wounding (0-4 hrs), an increase in CD44 staining was seen at wound edges compared to the rest of the layer (section 3.4.4). Moreover, all Ki-67 positive cells were also CD44 and CK14 positive and were seen to be present in the basal layer. As CD44 and CK14 are markers for basal cells, this provided strong evidence that basal cells contain the subpopulation of progenitor cells responsible for re-epithelisation (section 3.4.4). Interestingly, CD44 has previously been seen to be increased in the airway epithelium of subjects suffering from asthma (Leir, Baker, Holgate et al. 2000), suggesting a role for CD44 in disease pathology. When images of the Clara cell marker CC-26 were captured, the positive cells (i.e. secretory cells) were not the same as the cells seen to be proliferating following wounding; these cells were seen (as would be expected) to localize to the apical layer of the surface (section 3.4.4). On the other hand, previous findings (at least in this HBEC model) showed ciliated cells to be responsible for wound repair of murine airway epithelium (Park, Wells, Zorn et al. 2006). After mice were treated with naphthalene (resulting in selective injury of non-ciliated cells), it was observed that ciliated cells were capable of remarkable plasticity, and were responsible for the repair of the bronchial epithelium. When CD44 mRNA relative expression was measured post-wounding from HBEC cDNA, no significant difference was evident between wounded and unwounded cells, which suggests that the increase in CD44 staining was not due to new synthesis of the protein (section 3.4.5).

Although the data presented in this thesis all relate to using the HBEC wound model to study repair of the acute wound, it has also proven possible to repeatedly

injur the epithelium *in vitro*, mimicking a chronic wound such as the damage seen in asthma and COPD, following repeated inflammatory insults (Wadsworth, Nijmeh and Hall 2006).

6.1.2 Secretory profile of wounded human bronchial epithelial cells (HBEC)

Wound healing is a complex process, but what is known thus far is that it involves the three overlapping events of an inflammatory reaction, proliferation, and remodelling. The clinical conditions, asthma and COPD, both involve a disruption of these three processes (discussed in more detail in sections 1.2.1.1 and 1.2.1.2). In COPD, both inflammation and structural changes have been observed in small airways and lung parenchyma, contributing to the development of airway obstruction. Increased release of pro-inflammatory mediators has been seen in the lungs of patients with COPD. Infiltration of the small airway wall by $CD8^+$ and $CD68^+$ T cells takes place, as well as an increase in macrophages in airway and alveolar lumen (Saetta, Di Stefano, Turato *et al.* 1998). This leads to fibrosis and emphysema, thickening of the airway wall, luminal narrowing, and an increase in smooth muscle mass (Kuwano, Bosken, Pare *et al.* 1993), which are all present in some COPD patient's airways. Similarly, infiltration of $CD4^+$ Th2 cells and eosinophils has been demonstrated in the small airways and surrounding alveolar walls of patients suffering from asthma (Hamid, Song, Kotsimbos *et al.* 1997). As well as inflammation, asthma is characterized by mucous metaplasia, an increase of wall thickness (due in part to increase in mass of smooth muscle cells) especially in the large airways (Carroll, Elliot, Morton *et al.* 1993), and an increase in the thickness of the reticular basement membrane. One of the major roles of the epithelium is the production of a wide range of cytokines and other

mediators including chemokines and growth factors. In airway disease however, inappropriate secretion of certain cytokines and chemokines by epithelial cells of subjects suffering from asthma and COPD can be seen (reviewed in (Chung, Barnes. 1999) (Chung 2001)). Thus, inappropriate activation and recruitment of a number of inflammatory cells such as neutrophils and eosinophils takes place to the epithelial layer, resulting in a cycle of inflammatory cell recruitment and airway damage.

The secretory profile of the wounded HBEC model was investigated in this study in two ways. Initial experiments concentrated on measurement of a number of key cytokines and chemokines involved in airway diseases in supernatants collected from the *in vitro* HBEC model where two donors were used. Secondly the relative expression of mRNA for the cytokines and chemokines that were of interest at the protein level was assessed. The results are discussed in detail in section 4.4.1 and 4.5. Briefly, it was observed that IL-6, IL-8, ENA-78, G-CSF, RANTES, IL-1β, and MIP-1β secretions were increased in wounded HBEC cultures especially at 72 hrs post-wounding. This was reflected at the mRNA level for IL-6, IL-8, ENA-78, and G-CSF potentially at 24 hrs post-wounding. Finally, no clear difference was seen in IP-10 secretion between wounded and unwounded HBEC. A comparison of the epithelial cytokine secretion in asthma, COPD, and this HBEC wound model is presented in Table 4-18.

Interestingly, IL-8 and ENA-78 are key chemokines for neutrophils (Engelhardt, Toksoy, Goebeler *et al.* 1998). An increased concentration of IL-8 as well as the number of neutrophils have been observed in the sputum of patients suffering from COPD compared to normal and asthmatic subjects (Keatings, Collins, Scott *et al.* 1996) (Yamamoto, Yoneda, Yoshikawa *et al.* 1997). IL-8 has also been

observed to be secreted by epithelial cells, attracting neutrophils which in turn produce neutrophil elastase. Neutrophil elastase induces IL-8 gene expression by epithelial cells (Nakamura, Yoshimura, McElvaney *et al.* 1992), leading to an 'inflammatory cycle' which may in part participate in the airway obstruction in both asthma and COPD. IL-6 is also involved in inflammation, in part *via* inducing an increase in circulating neutrophil numbers, (Benjamini E. 2000). IL-6 has also been observed to be produced by epithelial cells (Stadnyk 1994) and has been observed to be elevated in sputum from patients with frequent exacerbations of COPD compared to those with stable disease (Bhowmik, Seemungal, Sapsford *et al.* 2000).

Similarly asthma is characterised by eosinophilia and neutrophilia in the airways, releasing mediators that cause bronchial epithelial damage and airway obstruction. Eosinophils have been proven to have a central role in the inflammation seen in asthmatic airways, with the number of eosinophils correlating with the severity of the disease. However, this cell type has proven to be insufficient by itself in explaining all the inflammation occurring in the asthmatic airway (Macdowell and Peters 2007). Additionally, neutrophils may play a role in the pathogenesis of asthma, but this remains controversial Neutrophil numbers were not observed to be increased in biopsies obtained from patients suffering from asthma compared to normal subjects (monitored by neutrophil elastase positive cells (Azzawi, Bradley, Jeffery *et al.* 1990). On the other hand, there is evidence suggesting that neutrophils are not only associated with acute asthma exacerbations but are found to be present in high numbers in the airways of patients suffering from chronic severe asthma (Sampson 2000). It is likely that neutrophils are involved in wound healing, chronic inflammation,

and the remodelling events seen in asthma (Wenzel 2001), however their overall importance remains unclear. IL-8 also plays a role in asthma by attracting not only neutrophils but also eosinophils to the epithelium, as observed in one study where IL-8 was measured in the sputum of patients suffering from either COPD or asthma (Yamamoto, Yoneda, Yoshikawa et al. 1997). Another eosinophil chemoattractant is RANTES: Berkman and colleagues have observed an increase in RANTES mRNA expression when they investigated bronchial biopsy and BAL cells from patients with mild asthma (Berkman, Krishnan, Gilbey et al. 1996), thus supporting a role for RANTES in normal and asthmatic airways.

In addition, the granulocyte colony-stimulating factor (G-CSF) is a survival factor for granulocytes, promoting their growth (Benjamini E. 2000). G-CSF has been observed to be produced by T cells and monocytes, as well as epithelial cells, and it has been observed that induced expression of G-CSF by airway cells constantly exposed to bacteria (as seen in cystic fibrosis (CF)) promoted the growth and survival of leukocytes (Saba, Soong, Greenberg et al. 2002). G-CSF has been particularly used in the past to treat neutropenia arising from for example chemotherapy, *via* escalating the rate of natural growth of haematopoietic cell lineages (Benjamini E. 2000).

Inflammation is a complex process initiated by tissue damage caused by a wide range of factors. Asthmatic inflammation for example is induced at least in part by allergens including airborne pollens, dust, viral and bacterial infections, as well as various irritant chemicals. Shedding of the epithelial layer has also been observed in some patients suffering from asthma (Goldie, Fernandes, Rigby *et al.* 1988). Thus, although the HBEC model investigated in this study, employed a physical injury and is not a fully appropriate representation of asthma and COPD,

the cytokines secreted by the epithelial cells correlated with the important factors that have previously been seen in airway disease. This could be taken further by exposure of the HBEC model to various other insults such as chemical injuries, biologic injuries (e.g. infection by microorganisms), and immunologic injuries (e.g. exposure to lipopolysaccharide(LPS)), followed by investigating the secretory profile of the epithelium. Moreover, the HBEC model contains only epithelial cells, and as described earlier, asthma and COPD are diseases involving a range of cell types, characterised by complex events involving for example the vascular endothelium, fibrocytes, and smooth muscle cells. This could be taken further, however, by trying to attempt co-culture containing epithelial cultures grown on inserts and monolayer cultures of for example airway myofibroblasts or inflammatory cells.

6.1.3 Identification of Potential Airway Epithelial Cell Progenitors

In order to reach a better understanding of the epithelial progenitor cell populations in airway repair, the *in vitro* HBEC wounding model was investigated using single cell cloning, and a FACS-based method to attempt and isolate putative progenitor/stem cells. Airway epithelial cells were also expanded from lung biopsies *in vitro*, to assess their differentiation potential, and identify if a side population (SP) was present. Single cell cloning failed to identify a true stem cell population in our standard conditions. A SP was identified in some cultures accounting for a small percentage of the total cells. These cells might be the transient amplifying cells rather than the more primitive stem cells. To really be sure this SP represented stem cells, one would want to show their ability to expand and self-renew indefinitely in culture and exhibit further markers (such as

the ability to differentiate into all epithelial cell lineages). However, this was technically difficult to study and despite extensive attempts I was unable to clarify these issues. The major difficulties encountered were as follows. First, it was very difficult to keep the cultures free from infection at the times when the SP was identified due to problems mainitaing sterility during cell handling with FACS. Second, due to the very small percentage of the SP and the small number of cells available from a single biopsy, it was difficult to generate sufficient cell numbers perform all the studies one would ideally pursue. One possible solution for that is trying to obtain bronchial brushings (where a high sufficient number of cells could potentially be available) followed by isolation of SP and their ability for expansion and differentiation. Finally, it is also possible that these cultures might not actually contain true stem cells, and the re-epithelialisation seen *in vivo* could be due to circulating stem cells as some previous reports have suggested (discussed in section 1.3.2.2). Moreover, this injury model might not provide a suitable stimulus for the stem cells to expand in culture: for example they may require the presence of additional growth factors derived from other cell types present in the airways but absent from the culture model.

The role of epithelial stem cells in the lung has been discussed in section 1.3.2, and the cells classically thought to have stem cell properties are subpopulations of basal cells, Clara cells, and alveolar type II cells. Two putative stem cell niches in the bronchioles have been identified thus far (see Figure 1-7), albeit in mice models where chemical injury by naphthalene was carried out. The first resided in close proximity to neuroepithelial bodies (NEB). Proliferative populations were found, expressing-CCSP and were termed variant CCSP-expressing Clara cells (vCE) (Reynolds, Giangreco and Power 2000) (Reynolds, Hong and Giangreco

2000). The second microenvironment seen to replace the naphthalene-depleted Clara cells was observed to be located near the broncheoalveolar duct junction (BADJ), where proliferative cells were present co-expressing CCSP and SPC (alveolar type II marker) (Giangreco, Reynolds and Stripp 2002) (Hong, Reynolds and Giangreco 2001). These were also seen to be positive for stem cell antigen-1 (Sca-1) and CD34. This led to the conclusion that those cells had the capacity to differentiate into cell populations which could promote the epithelial elements in both the bronchioles and alveoli, and these were therefore called broncheoalveolar stem cells (BASC) (Kim, Jackson and Woolfenden 2005). Thus far, however, there have not been any studies comparing the features of vCE and BASC populations and hence the relationship between them remains uncertain. A recent report by Hacket *et. al.* (Hackett, Shaheen, Johnson et al. 2008) described a SP in human tracheobronchial epithelium with proliferative potential and the ability to generate a differentiated epithelium *in vitro*. They also observed a higher percentage of SP in asthmatic airways, potentially providing evidence that the SP is altered during disease. These data suggest that the stem cell population in asthmatic airways is expanded possibly to enable enhanced repair following airway epithelial damage. The non-hematopoietic SP cells exhibited epithelial cell markers: cytokeratin (CK)-5, E-cadherin, the tight junctional protein ZO-1, tissue factor (TF), CD151, and p63, but were negative for the mesenchymal marker vimentin. One future direction to study these questions would be to try to differentiate epithelial cells obtained from bronchial biopsies from normal or diseased patients and use these as model to characterise stem cell/side population derived cells. These experiments will undoubtedly prove technically difficult but with further development, this approach holds promise for

the study of airway epithelial repair, especially if it proves possible to expand epithelial cells from biopsies obtained from patients suffering from asthma and COPD, after which comparison to normal samples could provide more in-sight into the pathophysiology of these diseases.

The application and values of identifying stem cells in the lung and their potential application in disease treatment was discussed in section 1.4. The concept that the airway epithelium is maintained though multiple resident stem/progenitor cell populations, suggests that a more in-depth knowledge of their behaviour in normal and diseased states could shed light into understanding the mechanisms behind common respiratory diseases. To achieve this, further work is required. First, basic knowledge of the airway progenitor cell behaviour needs to be obtained, followed by clearly defining the molecular signature of these cells and their response to injury. Moreover, identifying a stem cell population in the lung could prove useful in developing *in vitro* culture models (such as those used in the studies described in this thesis). These models could be used to investigate the mechanism of action of existing and novel therapies.

An interesting recent piece of work by investigators in Spain and the UK described how they were able to produce a cellular, tissue-engineered airway with normal properties and functions, and transplant it back to a patient with severe bronchial/tracheal disease, without the risk of rejection (Macchiarini P. 2008). Briefly, they were able to colonize recipient's epithelial cells and chondrocyte mesenchymal stem cells onto a donor matrix which was hence matched for HLA expression. This matrix was used to prepare an airway graft and transplanted back to the patient who was suffering from left main bronchus malacia. Interestingly, the epithelial and chondrocytes were observed to be deeply embedded in the

matrix by 24 hrs, suggesting the matrix provided an ideal environment for these cells. 100% adherence was observed after 24 hrs, with the cells functioning appropriately *in vivo* as well. These observations provide new evidence that autologous cells and the use of appropriate matrices provide potential functional solutions for serious clinical disorders.

These observations raise the question of whether or not the approaches described in this thesis could be adapted for tissue regeneration approaches such as this. It is likely that if it proves possible to isolate populations of airway epithelial cells enriched for stem cells (perhaps from side population) this would facilitate this kind of approach. At present, the need for manufactured airways such as this is limited, being reserved for rare cases of tracheal or bronchial malacia, although bronchial grafts could potentially be useful to manage bronchial stenosis (e.g. such as these seen in some pulmonary vasculitis cases) or for reconstructive surgery following tumour resection.

In summary, the *in vitro* differentiated human bronchial epithelial cell wounding model described in this thesis should prove a valuable tool in the field of respiratory research. Reaching a better understanding of airway epithelial injury and repair mechanisms, both by defining the progenitor cell populations involved, and the key cytokines secreted could lead to a better understanding of airway diseases, and provide models for potential therapeutic applications in regenerative medicine, tissue engineering, and cell-based therapies.

6.1.4 Future directions

Future work will include an attempt to co-culture differentiated epithelial cells with a number of other cell types such as smooth muscle cells, macrophages,

fibroblasts, etc. Moreover, epithelial cells from biopsies are currently being used instead of commercially bought cells since they are more physiologically relevant. This will include investigating intrinsic and extrinsic differences between epithelial cells obtained from asthma patients compared to normal samples. An attempt to differentiate these cells into a pseudostratified epithelium will also be carried out, followed by investigating the wound repair mechanisms in both asthma and normal samples, looking into migration, proliferation and differentiation potential of both samples.

The secretory profile of the airway epithelium will also be investigated again using other stimuli that are more relevant to lung diseases. LPS, cigarette smoke extracts, and bacteria are examples of the different stimuli that can be used to treat the ALI cultures, which are thought to be some of the major risk factors for diseases such as asthma and COPD, since the physical model used in this study does not completely portray the damage occurring in asthma and COPD.

Finally, SP studies will be followed up by trying to investigate their presence in asthma and normal samples and if there are portrayed differently in those two samples. Differences between SP and non-SP groups will be investigated to see if there are any potential gene differences between both which might facilitate their isolation.

.

Appendix A: Sources of materials and chemicals

T25 and T75 cell culture flasks	Costar, Corning, SchipholRijk, Netherlands
1 kb DNA ladder	Invitrogen, cat# 15615-016
12-well cell culture plates with polyester inserts (0.4µm pore size)	Costar, Corning, SchipholRijk, Netherlands
Agarose	Fischer Scientific, Loughborough, UK
All trans retinoic acid (RA)	Sigma-Aldrich, Gillingham, UK
bisBenzimide H 33342 trihydrochloride (Hoechst 33342)	Sigma-Aldrich, Gillingham, UK
Bovine serum albumin (BSA)	Sigma-Aldrich, Gillingham, UK
Bronchial epithelial cell basal media (BEBM) and singlequots bulletkits	Cambrex, Lonza, Wokingham, UK
Calcium chloride ($CaCl_2$)	Fischer Scientific, Loughborough, UK
Cell culture plates (96, 24-well plates)	Corning, SchipholRijk, Netherlands
Cryovials	Nunc, Fisher Scientific, Loughborough, UK
Diethylpyrocarbonate (DEPC)-treated water	Invitrogen, Paisley, UK
Dimethyl sulphoxide (DMSO)	Sigma-Aldrich, Gillingham, UK
Dulbecco's modified eagle medium (DMEM)	Sigma-Aldrich, Gillingham, UK
Ethanol (100%)	Fisher, Loughborough, UK
Ethidium bromide (EBr)	Invitrogen, Paisley, UK
Fetal Calf serum (FCS)	Sigma-Aldrich, Gillingham, UK
Formaldehyde (37%)	Phillip Harris, Cheshire, UK
Glacial acetic acid	Fischer Scientific, Loughborough, UK
Goat serum	Sigma-Aldrich, Gillingham, UK
Hank's balanced salt solution (HBSS)	Gibco, Invitrogen, Paisley, UK
L-glutamine	Sigma-Aldrich, Gillingham, UK
Magnesium chloride (MgCl2)	Sigma-Aldrich, Gillingham, UK

N-2-Hydroxyethylpiperazine-N'-2-ethanesulfonic acid (HEPES)	Sigma-Aldrich, Gillingham, UK
Orange G loading dye	Sigma-Aldrich, Gillingham, UK
Phosphate buffered saline (PBS)	Oxoid, Hampshire, UK
Primers	Invitrogen, Paisley, UK
Procarta® Cytokine Assay Kit	Panomics, cat# PC1028 Vignate-Milano, Italy
Propidium iodide (PI)	Sigma-Aldrich, Gillingham, UK
QIAshredder	Qiagen, Cat# 79654, UK
RNase-Free DNase Set	Qiagen Cat# 79254, UK
RNeasy Mini Kit	Qiagen, cat# 74104, UK
Soybean trypsin inhibitor (0.5 mg/ml)	Invitrogen, Paisley, UK
ß-mercaptoethanol	Sigma-Aldrich, Gillingham, UK
Superscript 1st Strand System	Fischer Scientific, Invitrogen, Loughborough, UK, (Cat# VX11904018)
Taqman Probes	Eurogentec, Hampshire, UK
Taqman® PCR Universal Master mix	Applied Biosystems Cat# 4304437, Warrington, UK
Triton X-100	Sigma-Aldrich, Gillingham, UK
Trypsin-EDTA (10x)	Sigma-Aldrich, Gillingham, UK
vaccum filtration system,	Millipore (P/M MAVM0960R and WP6111560),
Verapamil hydrochloride	Sigma-Aldrich, Gillingham, UK

Appendix B: Raw data of Luminex experiment

Time	EXPERIMENT 1																
	Wounded								Unwounded								Negative control
	0		24		48		72		0		24		48		72		
IL-8	95.96	94.46	2946.5	2664	4398.5	4180.9	OOR>	18663	155.03	132.85	1618.8	926.91	1696	1648	5887.3	6856.7	0.12
IL-6	OOR<	OOR<	25.28	OOR<	47.68	52.06	187.7	121.3	OOR<	OOR<	OOR<	OOR<	OOR<	OOR<	62.72	113.84	0.27
IL-1β	OOR<	OOR<	OOR<	OOR<	OOR<	OOR<	0.46	0.19	OOR<	OOR<	OOR<	OOR<	OOR<	OOR<	OOR<	OOR<	0.03
ENA78	OOR<	OOR<	68.12	OOR<	233.3	151.34	1899.2	515.93	OOR<	OOR<	OOR<	OOR<	OOR<	OOR<	31.76	115.77	OOR<
G-CSF	OOR<	OOR<	47.65	17.74	35.66	27.09	402.71	182.48	OOR<	OOR<	OOR<	OOR<	OOR<	OOR<	90.31	170.83	OOR<
RANTES	OOR<	OOR<	OOR<	OOR<	OOR<	12.22	38.48	24.27	OOR<	OOR<	OOR<	OOR<	OOR<	OOR<	OOR<	OOR<	0
IP-10	OOR<	OOR<	0.29	0.58	3.21	3.58	47.11	13.81	0	0.01	0.19	0.09	0.19	0.23	2.47	101.25	0.03
VEGF	28.31	22.49	272.8	282.78	440.48	429.16	1158.1	796.95	41.69	44.44	289.07	294.32	332.69	376.45	664.53	883.01	OOR<
MCP-1	OOR<	OOR<	OOR<	OOR<	OOR<	OOR<	20.61	5.12	OOR<	OOR<	OOR<	OOR<	OOR<	OOR<	OOR<	OOR<	OOR<
IL-2	OOR<	OOR<	OOR<	OOR<	OOR<	OOR<	OOR<	OOR<	OOR<	OOR<	OOR<	OOR<	OOR<	OOR<	OOR<	OOR<	OOR<
IL-4	OOR<	22.99	OOR<	OOR<	OOR<	OOR<	OOR<	OOR<	OOR<	OOR<	OOR<	OOR<	OOR<	OOR<	OOR<	OOR<	0.31
IL-5	OOR<	OOR<	OOR<	OOR<	OOR<	OOR<	OOR<	OOR<	OOR<	OOR<	OOR<	OOR<	OOR<	OOR<	OOR<	OOR<	OOR<
IL-7	OOR<	OOR<	OOR<	OOR<	OOR<	0	0.21	0.04	OOR<	OOR<	OOR<	OOR<	OOR<	OOR<	0	OOR<	OOR<
IL-10	OOR<	OOR<	OOR<	OOR<	OOR<	OOR<	OOR<	OOR<	OOR<	OOR<	OOR<	OOR<	OOR<	OOR<	OOR<	OOR<	OOR<
IL-12 P40	OOR<	OOR<	OOR<	OOR<	OOR<	OOR<	9.57	9.57	OOR<	OOR<	OOR<	OOR<	OOR<	OOR<	OOR<	OOR<	0.11
IL-12 IL70	OOR<	OOR<	OOR<	OOR<	OOR<	OOR<	OOR<	OOR<	OOR<	OOR<	OOR<	OOR<	OOR<	OOR<	OOR<	OOR<	OOR<
IL-13	OOR<	OOR<	OOR<	OOR<	OOR<	OOR<	OOR<	OOR<	OOR<	OOR<	OOR<	OOR<	OOR<	OOR<	OOR<	OOR<	OOR<
IL-17	OOR<	OOR<	OOR<	OOR<	OOR<	OOR<	OOR<	OOR<	OOR<	OOR<	OOR<	OOR<	OOR<	OOR<	OOR<	OOR<	OOR<
FGF-basic	OOR<	OOR<	OOR<	OOR<	OOR<	OOR<	OOR<	OOR<	OOR<	OOR<	OOR<	OOR<	OOR<	OOR<	OOR<	OOR<	3.2
NGF	OOR<	OOR<	OOR<	OOR<	OOR<	OOR<	OOR<	OOR<	OOR<	OOR<	OOR<	OOR<	OOR<	OOR<	OOR<	OOR<	0.09
Leptin	OOR<	OOR<	OOR<	OOR<	OOR<	OOR<	OOR<	OOR<	OOR<	OOR<	OOR<	OOR<	OOR<	OOR<	OOR<	OOR<	0.01
Eotaxin	OOR<	OOR<	OOR<	OOR<	OOR<	OOR<	OOR<	OOR<	OOR<	OOR<	OOR<	OOR<	OOR<	OOR<	OOR<	OOR<	0.02
MIP-1β	OOR<	OOR<	OOR<	OOR<	OOR<	OOR<	OOR<	OOR<	OOR<	OOR<	OOR<	OOR<	OOR<	OOR<	OOR<	OOR<	0.15
MIP-1α	OOR<	OOR<	OOR<	OOR<	OOR<	OOR<	57.2	OOR<	OOR<	OOR<	OOR<	OOR<	OOR<	OOR<	OOR<	OOR<	OOR<
TNFβ	OOR<	OOR<	OOR<	OOR<	OOR<	OOR<	OOR<	OOR<	OOR<	OOR<	OOR<	OOR<	OOR<	OOR<	OOR<	OOR<	
TNFα	OOR<	OOR<	OOR<	OOR<	OOR<	OOR<	OOR<	OOR<	OOR<	OOR<	OOR<	OOR<	OOR<	OOR<	OOR<	OOR<	OOR<
GM-CSF	OOR<	OOR<	OOR<	OOR<	OOR<	OOR<	OOR<	OOR<	OOR<	OOR<	OOR<	OOR<	OOR<	OOR<	OOR<	OOR<	OOR<
IFN-gamma	OOR<	OOR<	OOR<	OOR<	OOR<	OOR<	OOR<	OOR<	OOR<	OOR<	OOR<	OOR<	OOR<	OOR<	OOR<	OOR<	OOR<

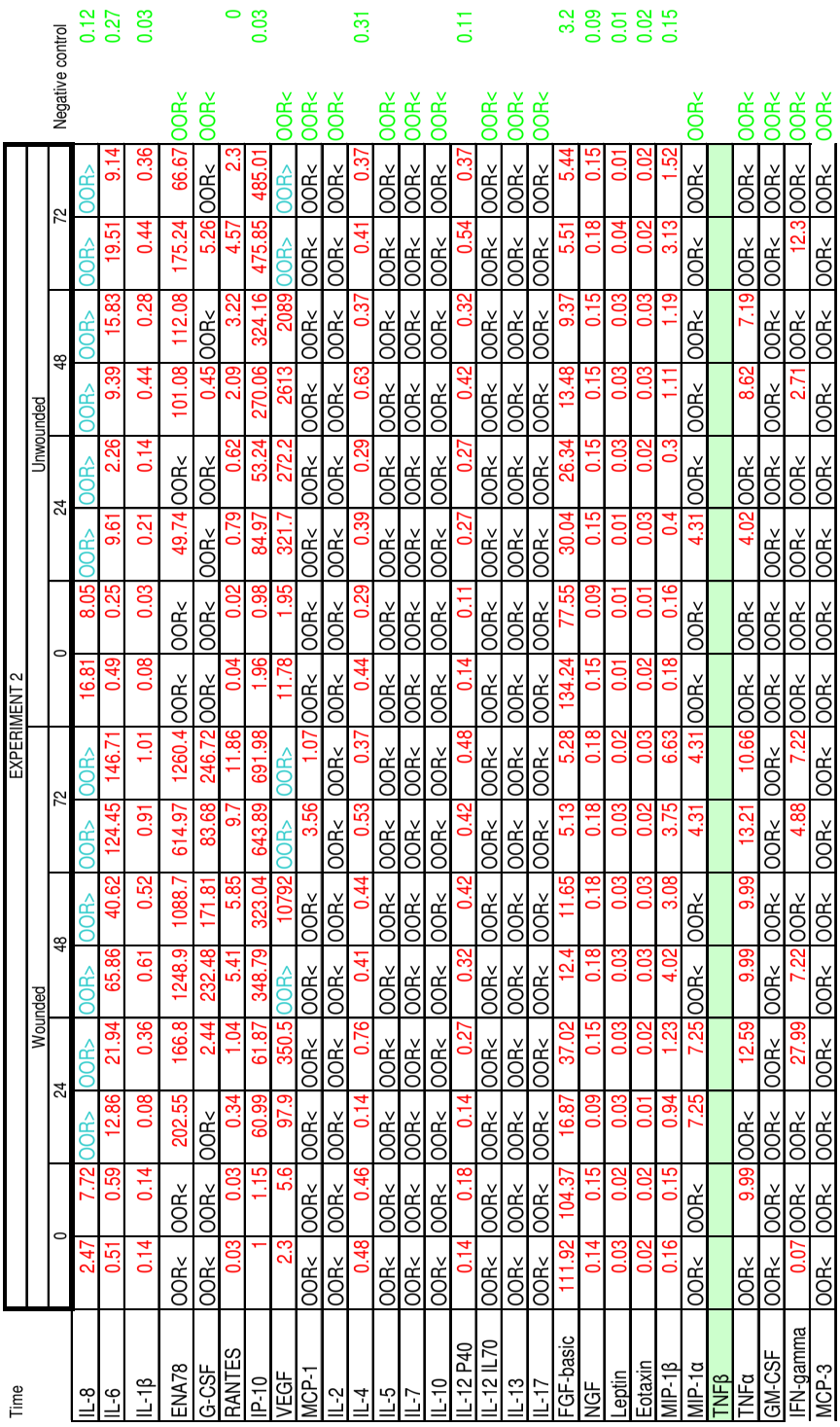

Time	EXPERIMENT 2																								Negative control
	Wounded									Unwounded															
	0		24		48		72			0		24		48		72									
IL-8	2.47	7.72	OOR>	OOR>	OOR>	OOR>	OOR>	16.81	8.05	OOR>	OOR>	OOR>	OOR>	OOR>	OOR>										0.12
IL-6	0.51	0.59	12.86	21.94	65.86	40.62	124.45	146.71	0.49	0.25	9.61	2.26	9.39	15.83	19.51	9.14									0.27
IL-1β	0.14	0.14	0.08	0.36	0.61	0.52	0.91	1.01	0.08	0.03	0.21	0.14	0.44	0.28	0.44	0.36									0.03
ENA78	OOR<	OOR<	202.55	166.8	1248.9	1088.7	614.97	1260.4	OOR<	OOR<	49.74	OOR<	101.08	112.08	175.24	66.67	OOR<								
G-CSF	OOR<	OOR<	OOR<	2.44	232.48	171.81	83.68	246.72	OOR<	OOR<	OOR<	OOR<	0.45	OOR<	5.26	OOR<	OOR<								
RANTES	0.03	0.03	0.34	1.04	5.41	5.85	9.7	11.86	0.04	0.02	0.79	0.62	2.09	3.22	4.57	2.3									0
IP-10	1	1.15	60.99	61.87	348.79	323.04	643.89	691.98	1.96	0.98	84.97	53.24	270.06	324.16	475.85	485.01									0.03
VEGF	2.3	5.6	97.9	350.5	OOR>	10792	OOR>	OOR>	11.78	1.95	321.7	272.2	2613	2089	OOR>	OOR>	OOR<								
MCP-1	OOR<	OOR<	OOR<	OOR<	OOR<	OOR<	3.56	1.07	OOR<	OOR<	OOR<	OOR<	OOR<	OOR<	OOR<	OOR<	OOR<								
IL-2	OOR<	OOR<	OOR<	OOR<	OOR<	OOR<	OOR<	OOR<	OOR<	OOR<	OOR<	OOR<	OOR<	OOR<	OOR<	OOR<	OOR<								
IL-4	0.48	0.46	0.14	0.76	0.41	0.44	0.53	0.37	0.44	0.29	0.39	0.29	0.63	0.37	0.41	0.37									0.31
IL-5	OOR<	OOR<	OOR<	OOR<	OOR<	OOR<	OOR<	OOR<	OOR<	OOR<	OOR<	OOR<	OOR<	OOR<	OOR<	OOR<	OOR<								
IL-7	OOR<	OOR<	OOR<	OOR<	OOR<	OOR<	OOR<	OOR<	OOR<	OOR<	OOR<	OOR<	OOR<	OOR<	OOR<	OOR<	OOR<								
IL-10	OOR<	OOR<	OOR<	OOR<	OOR<	OOR<	OOR<	OOR<	OOR<	OOR<	OOR<	OOR<	OOR<	OOR<	OOR<	OOR<	OOR<								
IL-12 P40	0.14	0.18	0.14	0.27	0.32	0.42	0.42	0.48	0.14	0.11	0.27	0.27	0.42	0.32	0.54	0.37									0.11
IL-12 IL70	OOR<	OOR<	OOR<	OOR<	OOR<	OOR<	OOR<	OOR<	OOR<	OOR<	OOR<	OOR<	OOR<	OOR<	OOR<	OOR<	OOR<								
IL-13	OOR<	OOR<	OOR<	OOR<	OOR<	OOR<	OOR<	OOR<	OOR<	OOR<	OOR<	OOR<	OOR<	OOR<	OOR<	OOR<	OOR<								
IL-17	OOR<	OOR<	OOR<	OOR<	OOR<	OOR<	OOR<	OOR<	OOR<	OOR<	OOR<	OOR<	OOR<	OOR<	OOR<	OOR<	OOR<								
FGF-basic	111.92	104.37	16.87	37.02	12.4	11.65	5.13	5.28	134.24	77.55	30.04	26.34	13.48	9.37	5.51	5.44									3.2
NGF	0.14	0.15	0.09	0.15	0.18	0.18	0.18	0.18	0.15	0.09	0.15	0.15	0.15	0.15	0.18	0.15									0.09
Leptin	0.03	0.02	0.03	0.03	0.03	0.03	0.03	0.02	0.01	0.01	0.01	0.03	0.03	0.03	0.04	0.01									0.01
Eotaxin	0.02	0.02	0.01	0.02	0.03	0.03	0.02	0.03	0.02	0.01	0.03	0.02	0.03	0.03	0.02	0.02									0.02
MIP-1β	0.16	0.15	0.94	1.23	4.02	3.08	3.75	6.63	0.18	0.16	0.4	0.3	1.11	1.19	3.13	1.52									0.15
MIP-1α	OOR<	OOR<	7.25	7.25	OOR<	OOR<	4.31	4.31	OOR<	OOR<	4.31	OOR<	OOR<	OOR<	OOR<	OOR<	OOR<								
TNFβ																									
TNFα	OOR<	9.99	OOR<	12.59	9.99	9.99	13.21	10.66	OOR<	OOR<	4.02	OOR<	8.62	7.19	OOR<	OOR<	OOR<								
GM-CSF	OOR<	OOR<	OOR<	OOR<	OOR<	OOR<	OOR<	OOR<	OOR<	OOR<	OOR<	OOR<	OOR<	OOR<	OOR<	OOR<	OOR<								
IFN-gamma	0.07	OOR<	OOR<	27.99	7.22	OOR<	4.88	7.22	OOR<	OOR<	OOR<	OOR<	2.71	OOR<	12.3	OOR<	OOR<								
MCP-3	OOR<	OOR<	OOR<	OOR<	OOR<	OOR<	OOR<	OOR<	OOR<	OOR<	OOR<	OOR<	OOR<	OOR<	OOR<	OOR<	OOR<								

Figure 6-1: Tables above represent the raw data obtained from the the luminex experiment. The numbers represent mean concentration (pg/mls) .of the duplicates carried out in two separate HBEC cultures. Negative control concentrations are also presented in green. The highlighted mediator was investigated only in this experiment. Each table represent two experiments giving a total of n=4 values for data analysis. The highlighted mediator was only investigated in the first luminex assay due to the restrictions of the purchased kits.

Bibliography

Aarbiou, J., M. Ertmann, S. van Wetering*, et al.* (2002). "Human neutrophil defensins induce lung epithelial cell proliferation in vitro." J Leukoc Biol **72**(1): 167-174.

Aarbiou, J., R. M. Verhoosel, S. van Wetering*, et al.* (2004). "Neutrophil Defensins Enhance Lung Epithelial Wound Closure and Mucin Gene Expression In Vitro." Am. J. Respir. Cell Mol. Biol. **30**(2): 193-201.

Aggarwal, S. and M. F. Pittenger (2005). "Human mesenchymal stem cells modulate allogeneic immune cell responses." Blood **105**(4): 1815-1822.

Aikawa, T., S. Shimura, H. Sasaki*, et al.* (1992). "Marked goblet cell hyperplasia with mucus accumulation in the airways of patients who died of severe acute asthma attack." Chest **101**(4): 916-921.

Altraja, A., A. Laitinen, I. Virtanen*, et al.* (1996). "Expression of laminins in the airways in various types of asthmatic patients: a morphometric study." Am J Respir Cell Mol Biol **15**(4): 482-8.

Altschul, S. F., T. L. Madden, A. A. Schaffer*, et al.* (1997). "Gapped BLAST and PSI-BLAST: a new generation of protein database search programs." Nucleic Acids Res **25**(17): 3389-402.

Alvi, A., H. Clayton, C. Joshi*, et al.* (2003). "Correction: Functional and molecular characterisation of mammary side population cells." Breast Cancer Res **5**(1): E1.

Arndt-Jovin, D. J. and T. M. Jovin (1977). "Analysis and sorting of living cells according to deoxyribonucleic acid content." J. Histochem. Cytochem. **25**(7): 585-589.

Atkinson, J. J., H. M. Toennies, K. Holmbeck*, et al.* (2007). "Membrane type 1 matrix metalloproteinase is necessary for distal airway epithelial repair and keratinocyte growth factor receptor expression after acute injury." Am J Physiol Lung Cell Mol Physiol **293**(3): L600-610.

Avril-Delplanque, A., I. Casal, N. Castillon*, et al.* (2005). "Aquaporin-3 Expression in Human Fetal Airway Epithelial Progenitor Cells." Stem Cells **23**(7): 992-1001.

Azzawi, M., B. Bradley, P. K. Jeffery*, et al.* (1990). "Identification of activated T lymphocytes and eosinophils in bronchial biopsies in stable atopic asthma." Am Rev Respir Dis **142**(6 Pt 1): 1407-13.

Bals, R., C. Beisswenger, S. Blouquit*, et al.* (2004). "Isolation and air-liquid interface culture of human large airway and bronchiolar epithelial cells." J Cyst Fibros **3 Suppl 2**: 49-51.

Benjamini E., C. R., Sunshine G. (2000). Immunology, John Whiley & Sons, Inc.

Bergeron, C. and L. P. Boulet (2006). "Structural changes in airway diseases: characteristics, mechanisms, consequences, and pharmacologic modulation." Chest **129**(4): 1068-87.

Berkman, N., V. L. Krishnan, T. Gilbey*, et al.* (1996). "Expression of RANTES mRNA and protein in airways of patients with mild asthma." Am. J. Respir. Crit. Care Med. **154**(6): 1804-1811.

Berthiaume, Y., G. Voisin and A. Dagenais (2006). "The alveolar type I cells: the new knight of the alveolus?" J Physiol **572**(Pt 3): 609-10.

Bhowmik, A., T. A. Seemungal, R. J. Sapsford*, et al.* (2000). "Relation of sputum inflammatory markers to symptoms and lung function changes in COPD exacerbations." Thorax **55**(2): 114-20.

Bishop, A. E. (2004). Pulmonary epithelial stem cells. **37:** 89-96.

Boers, J. E., A. W. Ambergen and F. B. Thunnissen (1998). "Number and proliferation of basal and parabasal cells in normal human airway epithelium." Am. J. Respir. Crit. Care Med. **157**: 2000.

Borger, P., M. Tamm, J. L. Black*, et al.* (2006). "Asthma: is it due to an abnormal airway smooth muscle cell?" Am J Respir Crit Care Med **174**(4): 367-72.

Borish, L. C. and J. W. Steinke (2003). "2. Cytokines and chemokines." Journal of Allergy and Clinical Immunology **111**(2, Supplement 2): 460-475.

Borok, Z., C. Li, J. Liebler*, et al.* (2006). "Developmental pathways and specification of intrapulmonary stem cells." Pediatr Res **59**(4 Pt 2): 84R-93R.

Borthwick, D. W., M. Shahbazian and Q. T. Krantz (2001). "Evidence for stem-cell niches in the tracheal epithelium." Am. J. Respir. Cell Mol. Biol. **24**: 662.

Bosson J. , S. N., Bucht A., Helleday R., Pourazar J., Holgate S. T., Kelly F. J., Sandström T., Wilson S.,. Frew A. J., Blomberg A. (2003). "Ozone-induced bronchial epithelial cytokine expression differs between healthy and asthmatic subjects." Clinical & Experimental Allergy **33**(6): 777-782.

Bove, P. F., Hristova, M., Wesley, U.V., *et al.* (2008). "Inflammatory Levels of Nitric Oxide Inhibit Airway Epithelial Cell Migration by Inhibition of the Kinase ERK1/2 and Activation of Hypoxia-inducible Factor-1{alpha}." J. Biol. Chem. **283**(26): 17919-17928.

Bove, P. F., Wesley, U.V., Greul, A-K, *et al.* (2007). "Nitric Oxide Promotes Airway Epithelial Wound Repair through Enhanced Activation of MMP-9." Am. J. Respir. Cell Mol. Biol. **36**(2): 138-146.

Petersen, B. E, Grossbard, B., Hatch, E., *et. al.* (2003). "Mouse A6-positive hepatic oval cells also express several hematopoietic stem cell markers." Hepatology **37**(3): 632-640.

Budak, M. T., O. S. Alpdogan, M. Zhou, *et al.* (2005). "Ocular surface epithelia contain ABCG2-dependent side population cells exhibiting features associated with stem cells." J Cell Sci **118**(Pt 8): 1715-24.

Buisson, A., Zahm, J., Polette, M., Pierrot, D., Bellon, G., Puchelle, E., Birembaut, P., Tournier, J. (1996). "Gelatinase B is involved in the in vitro wound repair of human respiratory epithelium." Journal of Cellular Physiology **166**(2): 413-426.

Buisson AC, G. C., Polette M, Zahm JM, Birembaut P, Tournier JM. (1996). "Wound repair-induced expression of a stromelysins is associated with the acquisition of a mesenchymal phentype in human respiratory epithlial cells." Lab Investigation **74**(3): 658-69.

Bunting, K. D., J. Galipeau, D. Topham, *et al.* (1998). "Transduction of Murine Bone Marrow Cells With an MDR1 Vector Enables Ex Vivo Stem Cell Expansion, but These Expanded Grafts Cause a Myeloproliferative Syndrome in Transplanted Mice." Blood **92**(7): 2269-2279.

Capelli, A., A. Di Stefano, I. Gnemmi, *et al.* (1999). "Increased MCP-1 and MIP-1beta in bronchoalveolar lavage fluid of chronic bronchitics." Eur Respir J **14**(1): 160-165.

Carroll, N., J. Elliot, A. Morton, *et al.* (1993). "The structure of large and small airways in nonfatal and fatal asthma." Am Rev Respir Dis **147**(2): 405-10.

Chang, J. C., R. Summer and X. Sun (2005). "Evidence that bone marrow cells do not contribute to the alveolar epithelium." Am. J. Respir. Cell Mol. Biol. **33**: 335.

Cheng, S. L., H. C. Wang, C. J. Yu, *et al.* (2008). "Increased expression of placenta growth factor in COPD." Thorax **63**(6): 500-506.

Chevillard, M., J. Hinnrasky, D. Pierrot, *et al.* (1993). "Differentiation of human surface upper airway epithelial cells in primary culture on a floating collagen gel." Epithelial Cell Biol **2**(1): 17-25.

Choe, M. M., A. A. Tomei and M. A. Swartz (2006). "Physiological 3D tissue model of the airway wall and mucosa." Nat. Protocols **1**(1): 357-362.

Chopra D P. , Sullivan, J., Wille J. J. , Siddiqui K. M. (1987). "Propagation of differentiating normal human tracheobronchial epithelial cells in serum-free medium." Journal of Cellular Physiology **130**(2): 173-181.

Chung K. , Barnes, P. (1999). "Cytokines in Asthma." Thorax **54**(9): 825–857.

Chung, K. F. (2001). "Cytokines in chronic obstructive pulmonary disease." European Respiratory Journal **18**: 50S-59S.

Coraux, C., R. Hajj, P. Lesimple, *et al.* (2005). "In vivo models of human airway epithelium repair and regeneration." EUROPEAN RESPIRATORY REVIEW **14**(97): 131-136.

Coraux, C., B. Nawrocki-Raby, J. Hinnrasky, *et al.* (2005). Embryonic Stem Cells Generate Airway Epithelial Tissue. **32:** 87-92.

Cox G, G. J., Jordana M. (1992). "Bronchial epithelial cell-derived cytokines (G-CSF and GM-CSF) promote the survival of peripheral blood neutrophils in vitro." American Journal of Respiratory Cell and Molecular Biology **7**(5): 507-513.

Crapo JD, B. B., Gehr P, Bachofen M, Weibel ER. (1982). "Cell number and cell characteristics of the normal human lung." The American Review of Respiratory Disease **125**(6): 740-745.

Crystal, R. G., S. H. Randell, J. F. Engelhardt*, et al.* (2008). "Airway Epithelial Cells: Current Concepts and Challenges." Proc Am Thorac Soc **5**(7): 772-777.

Danahay, H., H. Atherton, G. Jones*, et al.* (2002). "Interleukin-13 induces a hypersecretory ion transport phenotype in human bronchial epithelial cells." Am J Physiol Lung Cell Mol Physiol **282**(2): L226-236.

De Boer, W. I. (2002). "Cytokines and therapy in COPD: a promising combination?" Chest **121**(5 Suppl): 209S-218S.

de Jong, P. M., M. A. van Sterkenburg, S. C. Hesseling*, et al.* (1994). "Ciliogenesis in human bronchial epithelial cells cultured at the air- liquid interface." Am. J. Respir. Cell Mol. Biol. **10**(3): 271-277.

de Kok, J. B., R. W. Roelofs, B. A. Giesendorf*, et al.* (2004). "Normalization of gene expression measurements in tumor tissues: comparison of 13 endogenous control genes." Lab Invest **85**(1): 154-159.

Delplanque, A., C. Coraux, R. Tirouvanziam*, et al.* (2000). "Epithelial stem cell-mediated development of the human respiratory mucosa in SCID mice." J Cell Sci **113**(5): 767-778.

Devalia, J. L., A. M. Campbell, R. J. Sapsford*, et al.* (1993). "Effect of nitrogen dioxide on synthesis of inflammatory cytokines expressed by human bronchial epithelial cells in vitro." American Journal of Respiratory Cell and Molecular Biology ; Vol/Issue: 9:3: Pages: 271-278.

Di Stefano, A., A. Capelli, M. Lusuardi*, et al.* (1998). "Severity of Airflow Limitation Is Associated with Severity of Airway Inflammation in Smokers." Am. J. Respir. Crit. Care Med. **158**(4): 1277-1285.

DiCosmo, B. F., D. Picarella and R. A. Flavell (1994). "Local production of human IL-6 promotes insulitis but retards the onset of insulin-dependent diabetes mellitus in non-obese diabetic mice." Int Immunol **6**(12): 1829-37.

Dirk Adriaensen, D. W. S. (1993). "Neuroendocrine cells and nerves of the lung." The Anatomical Record **236**(1): 70-86.

Donninger, H., R. Glashoff, H.-M. Haitchi, *et al.* (2003). "Rhinovirus Induction of the CXC Chemokine Epithelial-Neutrophil Activating Peptide-78 in Bronchial Epithelium." The Journal of Infectious Diseases **187**(11): 1809-1817.

Duan, D., A. Sehgal and J. Yao (1998). "Lef1 transcription factor expression defines airway progenitor cell targets for in utero gene therapy of submucosal gland in cystic fibrosis." Am. J. Respir. Cell Mol. Biol. **18**: 750.

Dupuit, F., D. Gaillard, J. Hinnrasky, *et al.* (2000). Differentiated and functional human airway epithelium regeneration in tracheal xenografts. **278:** L165-176.

Eglitis, M. A. and E. Mezey (1997). "Hematopoietic cells differentiate into both microglia and macroglia in the brains of adult mice." Proc Natl Acad Sci U S A **94**(8): 4080-5.

Ehrhardt, C., B. Forbes and K.-J. Kim (2008). In Vitro Models of the Tracheo-Bronchial Epithelium. Drug Absorption Studies**:** 235-257.

Ehrhardt, C., C. Kneuer, J. Fiegel, *et al.* (2002). "Influence of apical fluid volume on the development of functional intercellular junctions in the human epithelial cell line 16HBE14o-: implications for the use of this cell line as an in vitro model for bronchial drug absorption studies." Cell Tissue Res **308**(3): 391-400.

Elias, J. A., Z. Zhu and G. Chupp (1999). "Airway remodeling in asthma." J. Clin. Invest. **104**: 1001.

Emura, M. (1997). "Stem cells of the respiratory epithelium and their in vitro cultivation." In Vitro Cell Dev Biol Anim **33**(1): 3-14.

Engelhardt, E., A. Toksoy, M. Goebeler, *et al.* (1998). "Chemokines IL-8, GROalpha, MCP-1, IP-10, and Mig are sequentially and differentially expressed during phase-specific infiltration of leukocyte subsets in human wound healing." Am J Pathol **153**(6): 1849-60.

Engelhardt, J. F. (2001). Stem Cell Niches in the Mouse Airway. **24:** 649-652.

Engelhardt, J. F., H. Schlossberg, J. R. Yankaskas, *et al.* (1995). "Progenitor cells of the adult human airway involved in submucosal gland development." Development **121**(7): 2031-2046.

Engelhardt, J. F., J. R. Yankaskas and J. M. Wilson (1992). "In vivo retroviral gene transfer into human bronchial epithelia of xenografts." J Clin Invest **90**(6): 2598-607.

Evans MJ, V. W. L., Fanucchi MV, Plopper CG (2001). "Cellular and molecular characteristics of basal cells in airway epithelium." Experimental Lung Research **27**(5): 401-415.

Ferrari, G., G. Cusella, D. Angelis*, et al.* (1998). "Muscle Regeneration by Bone Marrow-Derived Myogenic Progenitors." Science **279**(5356): 1528-1530.

Fixman, E. D., A. Stewart and J. G. Martin (2007). "Basic mechanisms of development of airway structural changes in asthma." Eur Respir J **29**(2): 379-389.

Folkard, S. G., J. Westwick and A. B. Millar (1997). "Production of interleukin-8, RANTES and MCP-1 in intrinsic and extrinsic asthmatics." Eur Respir J **10**(9): 2097-2104.

Forbes, B. (2000). "Human airway epithelial cell lines for in vitro drug transport and metabolism studies." Pharmaceutical Science & Technology Today **3**(1): 18-27.

Foresi, A., G. Bertorelli, A. Pesci*, et al.* (1990). "Inflammatory markers in bronchoalveolar lavage and in bronchial biopsy in asthma during remission." Chest **98**(3): 528-535.

Gerdes, J. (1990). "Ki-67 and other proliferation markers useful for immunohistological diagnostic and prognostic evaluations in human malignancies." Semin Cancer Biol **1**(3): 199-206.

Giangreco, A., K. R. Groot and S. M. Janes (2007). "Lung cancer and lung stem cells: strange bedfellows?" Am J Respir Crit Care Med **175**(6): 547-53.

Giangreco, A., S. D. Reynolds and B. R. Stripp (2002). "Terminal bronchioles harbor a unique airway stem cell population that localizes to the bronchoalveolar duct junction." Am J. Pathol. **161**: 173.

Giangreco, A., H. Shen and S. D. Reynolds (2004). "Molecular phenotype of airway side population cells." Am. J. Physiol. Lung Cell Mol. Physiol. **286**: L624.

Goldie, R. G., L. B. Fernandes, P. J. Rigby*, et al.* (1988). "Epithelial dysfunction and airway hyperreactivity in asthma." Prog Clin Biol Res **263**: 317-29.

Goodell, M. A., K. Brose, G. Paradis*, et al.* (1996). "Isolation and functional properties of murine hematopoietic stem cells that are replicating in vivo." J Exp Med **183**(4): 1797-806.

Gosney, J. R., M. C. Sissons and R. O. Allibone (1988). "Neuroendocrine cell populations in normal human lungs: a quantitative study." Thorax **43**(11): 878-882.

Gray, T. E., K. Guzman, C. W. Davis*, et al.* (1996). "Mucociliary differentiation of serially passaged normal human tracheobronchial epithelial cells." Am J Respir Cell Mol Biol **14**(1): 104-12.

Green, K. J. and J. C. Jones (1996). "Desmosomes and hemidesmosomes: structure and function of molecular components." FASEB J. **10**(8): 871-881.

Gruenert, D. C., W. E. Finkbeiner and J. H. Widdicombe (1995). "Culture and transformation of human airway epithelial cells." Am J Physiol **268**(3 Pt 1): L347-60.

Guo, F. H., S. A. A. Comhair, S. Zheng*, et al.* (2000). "Molecular Mechanisms of Increased Nitric Oxide (NO) in Asthma: Evidence for Transcriptional and Post-Translational Regulation of NO Synthesis." J Immunol **164**(11): 5970-5980.

Hackett, T. L., F. Shaheen, A. Johnson*, et al.* (2008). "Characterization of Side Population Cells from Human Airway Epithelium." Stem Cells: 2008-0171.

Hajj, R., T. Baranek, R. Le Naour*, et al.* (2007). "Basal Cells of the Human Adult Airway Surface Epithelium Retain Transit-Amplifying Cell Properties." Stem Cells **25**(1): 139-148.

Hakonarson, H., C. Kim, R. Whelan*, et al.* (2001). "Bi-directional activation between human airway smooth muscle cells and T lymphocytes: role in induction of altered airway responsiveness." J Immunol **166**(1): 293-303.

Hall, I. P. (2000). "Second messengers, ion channels and pharmacology of airway smooth muscle." Eur Respir J **15**(6): 1120-7.

Hamid, Q., Y. Song, T. C. Kotsimbos*, et al.* (1997). "Inflammation of small airways in asthma." J Allergy Clin Immunol **100**(1): 44-51.

Hirschmann-Jax, C., A. E. Foster, G. G. Wulf*, et al.* (2004). "A distinct "side population" of cells with high drug efflux capacity in human tumor cells." Proceedings of the National Academy of Sciences **101**(39): 14228-14233.

Hitoshi Kitamura, T. E. G. A. M. J. Y. I. P. N. (1993). "Enhanced Growth Potential of Cultured Rahbit Tracheal Epithelial Cells Following Exposure to N-Methyl-N'-nitro-N-nitrosoguanidine." Cancer Science **84**(11): 1113-1119.

Ho, M. M., A. V. Ng, S. Lam*, et al.* (2007). "Side population in human lung cancer cell lines and tumors is enriched with stem-like cancer cells." Cancer Res **67**(10): 4827-33.

Holgate (2000). "Epithelial damage and response." Clinical & Experimental Allergy **30**(s1): 37-41.

Holgate, S. T. (2007). "Epithelium dysfunction in asthma." J Allergy Clin Immunol **120**(6): 1233-44; quiz 1245-6.

Holgate, S. T. (2008). "The airway epithelium is central to the pathogenesis of asthma." Allergol Int **57**(1): 1-10.

Holgate, S. T., D. E. Davies, S. Puddicombe*, et al.* (2003). "Mechanisms of airway epithelial damage: epithelial-mesenchymal interactions in the pathogenesis of asthma." Eur Respir J **22**(44_suppl): 24S-29.

Holmes, C. and W. L. Stanford (2007). "Concise Review: Stem Cell Antigen-1: Expression, Function, and Enigma." Stem Cells **25**(6): 1339-1347.

Hong, K. U., S. D. Reynolds and A. Giangreco (2001). "Clara cell secretory protein-expressing cells of the airway neuroepithelial body microenvironment include a label-retaining subset and are critical for epithelial renewal after progenitor cell depletion." Am. J. Respir. Cell Mol. Biol. **24**: 671.

Hong, K. U., S. D. Reynolds and S. Watkins (2004). "Basal cells are a multipotent progenitor capable of renewing the bronchial epithelium." Am. J. Pathol. **164**: 577.

Hong, K. U., S. D. Reynolds and S. Watkins (2004). "In vivo differentiation potential of tracheal basal cells: evidence for multipotent and unipotent subpopulations." Am. J. Physiol. Lung Cell Mol. Physiol. **286**: L643.

Hook, G. E. R., A. R. Brody, G. S. Cameron*, et al.* (1987). "Repopulation of Denuded Tracheas by Clara Cells Isolated from the Lungs of Rabbits." Experimental Lung Research **12**(4): 311 - 329.

Hoshino, M., M. Takahashi and N. Aoike (2001). "Expression of vascular endothelial growth factor, basic fibroblast growth factor, and angiogenin immunoreactivity in asthmatic airways and its relationship to angiogenesis." Journal of Allergy and Clinical Immunology **107**(2): 295-301.

Howat, W. J., J. A. Holmes, S. T. Holgate*, et al.* (2001). "Basement membrane pores in human bronchial epithelium: a conduit for infiltrating cells?" Am J Pathol **158**(2): 673-80.

Jeffery, P. K. (1992). "Pathology of asthma." Br Med Bull **48**(1): 23-39.

Jeffery, P. K. (1998). "Structural and inflammatory changes in COPD: a comparison with asthma." Thorax **53**(2): 129-36.

Jeffery, P. K. (2000). "Comparison of the Structural and Inflammatory Features of COPD and Asthma Giles F. Filley Lecture." Chest **117**(90051): 251S-260.

Jeffery, P. K. (2001). "Remodeling in Asthma and Chronic Obstructive Lung Disease." Am. J. Respir. Crit. Care Med. **164**(10): 28S-38.

Jeffery, P. K. and D. Li (1997). "Airway mucosa: secretory cells, mucus and mucin genes." Eur Respir J **10**(7): 1655-1662.

Joan Gil, E. R. W. (1971). "Extracellular lining of bronchioles after perfusion-fixation of rat lungs for electron microscopy." The Anatomical Record **169**(2): 185-199.

Jorissen, M., B. Van der Schueren, J. Tyberghein*, et al.* (1989). "Ciliogenesis and coordinated ciliary beating in human nasal epithelial cells cultured in vitro." Acta Otorhinolaryngol Belg **43**(1): 67-73.

Kalluri, R. and E. G. Neilson (2003). "Epithelial-mesenchymal transition and its implications for fibrosis." J Clin Invest **112**(12): 1776-84.

Kawaguchi, M., F. Kokubu, S. Matsukura*, et al.* (2003). "Induction of C-X-C Chemokines, Growth-Related Oncogene {alpha} Expression, and Epithelial Cell-Derived Neutrophil-Activating Protein-78 by ML-1 (Interleukin-17F) Involves Activation of Raf1-Mitogen-Activated Protein Kinase Kinase-Extracellular Signal-Regulated Kinase 1/2 Pathway." J Pharmacol Exp Ther **307**(3): 1213-1220.

Keatings, V. M., P. D. Collins, D. M. Scott*, et al.* (1996). "Differences in interleukin-8 and tumor necrosis factor-alpha in induced sputum from patients with chronic obstructive pulmonary disease or asthma." Am J Respir Crit Care Med **153**(2): 530-4.

Keenan, K., J. Combs and E. McDowell (1983). "Regeneration of hamster tracheal epithelium after mechanical injury." Virchows Archiv B Cell Pathology Zell-pathologie **42**(1): 193-214.

Khair, O. A., J. L. Devalia, M. M. Abdelaziz*, et al.* (1994). "Effect of Haemophilus influenzae endotoxin on the synthesis of IL-6, IL-8, TNF-alpha and expression of ICAM-1 in cultured human bronchial epithelial cells." Eur Respir J **7**(12): 2109-2116.

Kicic, A., E. N. Sutanto, P. T. Stevens*, et al.* (2006). "Intrinsic Biochemical and Functional Differences in Bronchial Epithelial Cells of Children with Asthma." Am. J. Respir. Crit. Care Med. **174**(10): 1110-1118.

Kikuchi, T., J. D. Shively, J. S. Foley*, et al.* (2004). "Differentiation-dependent responsiveness of bronchial epithelial cells to IL-4/13 stimulation." Am J Physiol Lung Cell Mol Physiol **287**(1): L119-26.

Kim, C. F. (2007). "Paving the road for lung stem cell biology: bronchioalveolar stem cells and other putative distal lung stem cells." Am J Physiol Lung Cell Mol Physiol: 00015.2007.

Kim, C. F., E. L. Jackson and A. E. Woolfenden (2005). "Identification of bronchioalveolar stem cells in normal lung and lung cancer." Cell **121**: 823.

Kim, J. S., V. S. McKinnis, A. Nawrocki*, et al.* (1998). "Stimulation of migration and wound repair of guinea-pig airway epithelial cells in response to epidermal growth factor." Am J Respir Cell Mol Biol **18**(1): 66-74.

Knight, D. A. and S. T. Holgate (2003). "The airway epithelium: structural and functional properties in health and disease." Respirology **8**(4): 432-46.

Knight, D. A., C. L. Lane and S. M. Stick (2004). "Does aberrant activation of the epithelial-mesenchymal trophic unit play a key role in asthma or is it an unimportant sideshow?" Current Opinion in Pharmacology **4**(3): 251-256.

Korinek, V., N. Barker, P. Moerer*, et al.* (1998). "Depletion of epithelial stem-cell compartments in the small intestine of mice lacking Tcf-4." Nat Genet **19**(4): 379-383.

Kotton, D. N. and A. Fine (2008). "Lung stem cells." Cell Tissue Res **331**(1): 145-56.

Krause, D. S., N. D. Theise, M. I. Collector*, et al.* (2001). "Multi-organ, multi-lineage engraftment by a single bone marrow-derived stem cell." Cell **105**(3): 369-77.

Kuwano, K., C. H. Bosken, P. D. Pare*, et al.* (1993). "Small airways dimensions in asthma and in chronic obstructive pulmonary disease." Am Rev Respir Dis **148**(5): 1220-5.

Lackie PM, B. J., Günthert U, Holgate ST (1997). "Expression of CD44 isoforms is increased in the airway epithelium of asthmatic subjects." American Journal of Respiratory Cell and Molecular Biology **16**(1): 14-22.

Lalande, M. E. and R. G. Miller (1979). "Fluorescence flow analysis of lymphocyte activation using Hoechst 33342 dye." J. Histochem. Cytochem. **27**(1): 394-397.

Lane, B. P., S. L. Miller and E. J. Drummond (1976). "Use of tracheal organ cultures in toxicity testing." Environ Health Perspect **16**: 89-98.

Lawson, G. W., L. S. Van Winkle, E. Toskala*, et al.* (2002). "Mouse Strain Modulates the Role of the Ciliated Cell in Acute Tracheobronchial Airway Injury-Distal Airways." Am J Pathol **160**(1): 315-327.

Lechner, J. F., A. Haugen, H. Autrup*, et al.* (1981). "Clonal growth of epithelial cells from normal adult human bronchus." Cancer Res **41**(6): 2294-304.

Lechner, J. F., A. Haugen, I. A. McClendon*, et al.* (1982). "Clonal growth of normal adult human bronchial epithelial cells in a serum-free medium." In Vitro **18**(7): 633-42.

Legrand, C., C. Gilles, J.-M. Zahm*, et al.* (1999). "Airway Epithelial Cell Migration Dynamics: MMP-9 Role in Cell–Extracellular Matrix Remodeling." J. Cell Biol. **146**(2): 517-529.

Leir, S.-H., J. E. Baker, S. T. Holgate*, et al.* (2000). Increased CD44 expression in human bronchial epithelial repair after damage or plating at low cell densities. **278:** L1129-1137.

Leir, S. H., S. T. Holgate and P. M. Lackie (2003). "Inflammatory cytokines can enhance CD44-mediated airway epithelial cell adhesion independently of CD44 expression." Am J Physiol Lung Cell Mol Physiol **285**(6): L1305-11.

Liang, S. X., R. Summer, X. Sun*, et al.* (2005). "Gene expression profiling and localization of Hoechst-effluxing CD45- and CD45+ cells in the embryonic mouse lung." Physiol. Genomics **23**(2): 172-181.

Lin, H., H. Li, H. J. Cho*, et al.* (2007). "Air-liquid interface (ALI) culture of human bronchial epithelial cell monolayers as an in vitro model for airway drug transport studies." J Pharm Sci **96**(2): 341-50.

Lopez-Souza, N., P. C. Avila and J. H. Widdicombe (2003). "Polarized cultures of human airway epithelium from nasal scrapings and bronchial brushings." In Vitro Cell Dev Biol Anim **39**(7): 266-9.

Lukacs, N. W., C. M. Hogaboam, S. L. Kunkel*, et al.* (1998). "Mast cells produce ENA-78, which can function as a potent neutrophil chemoattractant during allergic airway inflammation." J Leukoc Biol **63**(6): 746-751.

Lukacs, N. W., T. J. Standiford, S. W. Chensue*, et al.* (1996). "C-C chemokine-induced eosinophil chemotaxis during allergic airway inflammation." J Leukoc Biol **60**(5): 573-578.

Lumsden, A. B., A. McLean and D. Lamb (1984). "Goblet and Clara cells of human distal airways: evidence for smoking induced changes in their numbers." Thorax **39**(11): 844-9.

M. R. Sears, P. M. R. S. (1993). "The definition and diagnosis of asthma." Allergy **48**(s17): 12-16.

Macchiarini P., J. P., Go T., Asnaghi M.A., Rees L.E., Cogan T.A., Dodson A., Martorell J., Bellini S., Parnigotto P.P., Dickinson S.C , Hollander A.P., Mantero S., Conconi M.T. and Birchall M.A. (2008). "Clinical

transplantation of a tissue-engineered airway " The Lancet **8**(Early Online Publication).

Macdowell, A. L. and S. P. Peters (2007). "Neutrophils in asthma." Curr Allergy Asthma Rep **7**(6): 464-8.

Macpherson, H., P. Keir, S. Webb*, et al.* (2005). "Bone marrow-derived SP cells can contribute to the respiratory tract of mice in vivo." J Cell Sci **118**(Pt 11): 2441-50.

Maliepaard, M., M. A. van Gastelen, L. A. de Jong*, et al.* (1999). "Overexpression of the BCRP/MXR/ABCP Gene in a Topotecan-selected Ovarian Tumor Cell Line." Cancer Res **59**(18): 4559-4563.

Marhaba, R. and M. Zöller (2004). "CD44 in Cancer Progression: Adhesion, Migration and Growth Regulation." Journal of Molecular Histology **35**(3): 211-231.

Marini, M., E. Vittori, J. Hollemborg*, et al.* (1992). "Expression of the potent inflammatory cytokines, granulocyte-macrophage-colony-stimulating factor and interleukin-6 and interleukin-8, in bronchial epithelial cells of patients with asthma." Journal of Allergy and Clinical Immunology **89**(5): 1001-1009.

Marshall, L. J., B. Perks, T. Ferkol*, et al.* (2001). "IL-8 released constitutively by primary bronchial epithelial cells in culture forms an inactive complex with secretory component." J Immunol **167**(5): 2816-23.

Mason, R. J. (2006). "Biology of alveolar type II cells." Respirology **11 Suppl**: S12-5.

Masubuchi, T., S. Koyama, E. Sato*, et al.* (1998). "Smoke Extract Stimulates Lung Epithelial Cells to Release Neutrophil and Monocyte Chemotactic Activity." Am J Pathol **153**(6): 1903-1912.

Masui, T., L. M. Wakefield, J. F. Lechner*, et al.* (1986). "Type beta transforming growth factor is the primary differentiation-inducing serum factor for normal human bronchial epithelial cells." Proc Natl Acad Sci U S A **83**(8): 2438-42.

Mathias, N. R., F. Yamashita and V. H. L. Lee (1996). "Respiratory epithelial cell culture models for evaluation of ion and drug transport." Advanced Drug Delivery Reviews **22**(1-2): 215-249.

Mattoli, S., M. A. Stacey, G. Sun, *et al.* (1997). "Eotaxin Expression and Eosinophilic Inflammation in Asthma." Biochemical and Biophysical Research Communications **236**(2): 299-301.

Mattsson, J., M. Jansson, A. Wernerson, *et al.* (2004). "Lung epithelial cells and type II pneumocytes of donor origin after allogeneic hematopoietic stem cell transplantation." Transplantation **78**(1): 154-7.

McDowell, E. M., P. J. Becci, W. Schurch, *et al.* (1979). "The respiratory epithelium. VII. Epidermoid metaplasia of hamster tracheal epithelium during regeneration following mechanical injury." J Natl Cancer Inst **62**(4): 995-1008.

McGuire, J. K., Q. Li and W. C. Parks (2003). "Matrilysin (Matrix Metalloproteinase-7) Mediates E-Cadherin Ectodomain Shedding in Injured Lung Epithelium." Am J Pathol **162**(6): 1831-1843.

Medoff, B. D., A. Sauty, A. M. Tager, *et al.* (2002). "IFN-{gamma}-Inducible Protein 10 (CXCL10) Contributes to Airway Hyperreactivity and Airway Inflammation in a Mouse Model of Asthma." J Immunol **168**(10): 5278-5286.

Mimeault, M., R. Hauke and S. K. Batra (2007). "Stem cells: a revolution in therapeutics-recent advances in stem cell biology and their therapeutic applications in regenerative medicine and cancer therapies." Clin Pharmacol Ther **82**(3): 252-64.

Mio, T., D. J. Romberger, A. B. Thompson, *et al.* (1997). "Cigarette smoke induces interleukin-8 release from human bronchial epithelial cells." Am. J. Respir. Crit. Care Med. **155**(5): 1770-1776.

Miotto, D., P. Christodoulopoulos, R. Olivenstein, *et al.* (2001). "Expression of IFN-[gamma]-inducible protein; monocyte chemotactic proteins 1, 3, and 4; and eotaxin in TH1- and TH2-mediated lung diseases." Journal of Allergy and Clinical Immunology **107**(4): 664-670.

Morrison, D., R. M. Strieter, S. C. Donnelly, *et al.* (1998). "Neutrophil chemokines in bronchoalveolar lavage fluid and leukocyte-conditioned medium from nonsmokers and smokers." Eur Respir J **12**(5): 1067-1072.

Myerburg, M. M., J. D. Latoche, E. E. McKenna, *et al.* (2007). "Hepatocyte growth factor and other fibroblast secretions modulate the phenotype of

human bronchial epithelial cells." Am J Physiol Lung Cell Mol Physiol **292**(6): L1352-1360.

Nakamura, H., K. Yoshimura, N. G. McElvaney*, et al.* (1992). "Neutrophil elastase in respiratory epithelial lining fluid of individuals with cystic fibrosis induces interleukin-8 gene expression in a human bronchial epithelial cell line." J Clin Invest **89**(5): 1478-84.

Naylor, B. (1962). "**The Shedding of the Mucosa of the Bronchial Tree in Asthma**." Thorax **17**(1): 69-72.

Neugebauer, P., H. Endepols, A. Mickenhagen*, et al.* (2003). "Ciliogenesis in submersion and suspension cultures of human nasal epithelial cells." Eur Arch Otorhinolaryngol **260**(6): 325-30.

Neuringer, I. and S. Randell (2004). "Stem cells and repair of lung injuries." Respiratory Research **5**(1): 6.

Neurohr, C., S. L. Nishimura and D. Sheppard (2006). "Activation of Transforming Growth Factor-beta by the Integrin {alpha}vbeta8 Delays Epithelial Wound Closure." Am. J. Respir. Cell Mol. Biol. **35**(2): 252-259.

Nocker, R. E., D. F. Schoonbrood, E. A. van de Graaf*, et al.* (1996). "Interleukin-8 in airway inflammation in patients with asthma and chronic obstructive pulmonary disease." Int Arch Allergy Immunol **109**(2): 183-91.

Oh, H., S. B. Bradfute, T. D. Gallardo*, et al.* (2003). "Cardiac progenitor cells from adult myocardium: Homing, differentiation, and fusion after infarction." Proceedings of the National Academy of Sciences of the United States of America **100**(21): 12313-12318.

Ohkawara Y, Y. K., Tanno Y, Tamura G, Ohtani H, Nagura H, Ohkuda K, Takishima T. (1992). "Human lung mast cells and pulmonary macrophages produce tumor necrosis factor-alpha in sensitized lung tissue after IgE receptor triggering." American Journal of Respiratory Cell and Molecular Biology **7**(4): 385-392.

Ohuchi, E., K. Imai, Y. Fujii*, et al.* (1997). "Membrane Type 1Matrix Metalloproteinase Digests Interstitial Collagens and Other Extracellular Matrix Macromolecules." J. Biol. Chem. **272**(4): 2446-2451.

Otto, W. R. (2002). "Lung epithelial stem cells." J. Pathol. **197**: 527.

Paine, R. d., M. W. Rolfe, T. J. Standiford, *et al.* (1993). "MCP-1 expression by rat type II alveolar epithelial cells in primary culture." J Immunol **150**(10): 4561-4570.

Park, K. S., J. M. Wells, A. M. Zorn, *et al.* (2006). "Transdifferentiation of ciliated cells during repair of the respiratory epithelium." Am J Respir Cell Mol Biol **34**(2): 151-7.

Patel, I. S., N. J. Roberts, S. J. Lloyd-Owen, *et al.* (2003). "Airway epithelial inflammatory responses and clinical parameters in COPD." Eur Respir J **22**(1): 94-99.

Petersen, B. E., W. C. Bowen, K. D. Patrene, *et al.* (1999). "Bone marrow as a potential source of hepatic oval cells." Science **284**(5417): 1168-70.

Petit, I., M. Szyper-Kravitz, A. Nagler, *et al.* (2002). "G-CSF induces stem cell mobilization by decreasing bone marrow SDF-1 and up-regulating CXCR4." Nat Immunol **3**(7): 687-694.

Pilewski, J. M., J. D. Latoche, S. M. Arcasoy, *et al.* (1997). "Expression of integrin cell adhesion receptors during human airway epithelial repair in vivo." Am J Physiol Lung Cell Mol Physiol **273**(1): L256-263.

Pilewski JM, P. R. J., Kaiser LR, Albelda SM. (1994). "Expression of endothelial cell adhesion molecules in human bronchial xenografts." American Journal of Respiratory and Critical Care Medicine **150**(3): 195801.

Pollak, M. N., H. T. Huynh and S. P. Lefebvre (1992). "Tamoxifen reduces serum insulin-like growth factor I (IGF-I)." Breast Cancer Res Treat **22**(1): 91-100.

Puchelle, E. (2000). "Airway epithelium wound repair and regeneration after injury." Acta Otorhinolaryngol Belg **54**(3): 263-70.

Puchelle, E., J.-M. Zahm, J.-M. Tournier, *et al.* (2006). "Airway Epithelial Repair, Regeneration, and Remodeling after Injury in Chronic Obstructive Pulmonary Disease." Proc Am Thorac Soc **3**(8): 726-733.

Rabindran, S. K., D. D. Ross, L. A. Doyle, *et al.* (2000). "Fumitremorgin C Reverses Multidrug Resistance in Cells Transfected with the Breast Cancer Resistance Protein." Cancer Res **60**(1): 47-50.

Randell, S. H. (1992). "Progenitor-Progeny Relationships in Airway Epithelium." Chest **101**(3_Supplement): 11S-16.

Rawlins, E. L. (2008). "Lung Epithelial Progenitor Cells: Lessons from Development." Proc Am Thorac Soc **5**(6): 675-681.

Rennard, S. I., K. A. Rickard, J. R. Spurzem*, et al.* (1992). "Airways Inflammation." Chest **101**(3_Supplement): 30S-32.

Reynolds, S. D., A. Giangreco and J. H. Power (2000). "Neuroepithelial bodies of pulmonary airways serve as a reservoir of progenitor cells capable of epithelial regeneration." Am. J. Pathol. **156**: 269.

Reynolds, S. D., K. U. Hong and A. Giangreco (2000). "Conditional Clara cell ablation reveals a self-renewing progenitor function of pulmonary neuroendocrine cells." Am. J. Physiol. Lung Cell Mol. Physiol. **278**: L1256.

Roche, W. R. M., S. Baker, J. Holgate, S. T. (1993). "Cell Adhesion Molecules and the Bronchial Epithelium."_____

American Review OF Respiratory Disease **149**(6): S79.

Rogers, A. V., A. Dewar, B. Corrin*, et al.* (1993). "Identification of serous-like cells in the surface epithelium of human bronchioles." Eur Respir J **6**(4): 498-504.

Rothenberg, M. E. (2004). "VEGF obstructs the lungs." Nat Med **10**(10): 1041-1042.

Rusznak, C., P. R. Mills, J. L. Devalia*, et al.* (2000). "Effect of Cigarette Smoke on the Permeability and IL-1beta and sICAM-1 Release from Cultured Human Bronchial Epithelial Cells of Never-Smokers, Smokers, and Patients with Chronic Obstructive Pulmonary Disease." Am. J. Respir. Cell Mol. Biol. **23**(4): 530-536.

Saba, S., G. Soong, S. Greenberg*, et al.* (2002). "Bacterial Stimulation of Epithelial G-CSF and GM-CSF Expression Promotes PMN Survival in CF Airways." Am. J. Respir. Cell Mol. Biol. **27**(5): 561-567.

Sacco, O., M. Silvestri, F. Sabatini*, et al.* (2004). "Epithelial cells and fibroblasts: structural repair and remodelling in the airways." Paediatr Respir Rev **5 Suppl A**: S35-40.

Saetta, M., A. Di Stefano, G. Turato*, et al.* (1998). "CD8+ T-Lymphocytes in Peripheral Airways of Smokers with Chronic Obstructive Pulmonary Disease." Am. J. Respir. Crit. Care Med. **157**(3): 822-826.

Saetta, M., M. Mariani, P. Panina-Bordignon*, et al.* (2002). "Increased Expression of the Chemokine Receptor CXCR3 and Its Ligand CXCL10 in Peripheral Airways of Smokers with Chronic Obstructive Pulmonary Disease." Am. J. Respir. Crit. Care Med. **165**(10): 1404-1409.

Sampson, A. P. (2000). "The role of eosinophils and neutrophils in inflammation." Clin Exp Allergy **30 Suppl 1**: 22-7.

Sauty, A., M. Dziejman, R. A. Taha*, et al.* (1999). "The T Cell-Specific CXC Chemokines IP-10, Mig, and I-TAC Are Expressed by Activated Human Bronchial Epithelial Cells." J Immunol **162**(6): 3549-3558.

Scharenberg, C. W., M. A. Harkey and B. Torok-Storb (2002). "The ABCG2 transporter is an efficient Hoechst 33342 efflux pump and is preferentially expressed by immature human hematopoietic progenitors." Blood **99**(2): 507-512.

Schoch, K. G., A. Lori and K. A. Burns (2004). "A subset of mouse tracheal epithelial basal cells generates large colonies in vitro." Am. J. Physiol. Lung Cell Mol. Physiol. **286**: L631.

Shaykhiev, R., J. Behr and R. Bals (2008). "Microbial patterns signaling via Toll-like receptors 2 and 5 contribute to epithelial repair, growth and survival." PLoS ONE **3**(1): e1393.

Shigemura, N., M. Okumura, S. Mizuno*, et al.* (2006). "Autologous transplantation of adipose tissue-derived stromal cells ameliorates pulmonary emphysema." Am J Transplant **6**(11): 2592-600.

Shimizu, T., P. Nettesheim, F. C. Ramaekers*, et al.* (1992). "Expression of "cell-type-specific" markers during rat tracheal epithelial regeneration." Am J Respir Cell Mol Biol **7**(1): 30-41.

Shoji, S., K. A. Rickard, R. F. Ertl, *et al.* (1989). "Lung fibroblasts produce chemotactic factors for bronchial epithelial cells." Am J Physiol Lung Cell Mol Physiol **257**(2): L71-79.

Sigurdson, L., T. Sen, L. Hall Iii, *et al.* (2003). "Possible Impedance of Luminal Reepithelialization by Tracheal Cartilage Metalloproteinases." Arch Otolaryngol Head Neck Surg **129**(2): 197-200.

Soloperto, M., V. L. Mattoso, A. Fasoli, *et al.* (1991). "A bronchial epithelial cell-derived factor in asthma that promotes eosinophil activation and survival as GM-CSF." Am J Physiol Lung Cell Mol Physiol **260**(6): L530-538.

Sousa, A. R., S. J. Lane, J. A. Nakhosteen, *et al.* (1996). "Expression of interleukin-1 beta (IL-1beta) and interleukin-1 receptor antagonist (IL-1ra) on asthmatic bronchial epithelium." Am. J. Respir. Crit. Care Med. **154**(4): 1061-1066.

Spencer, H., D. Rampling, P. Aurora, *et al.* (2005). "Transbronchial biopsies provide longitudinal evidence for epithelial chimerism in children following sex mismatched lung transplantation." Thorax **60**(1): 60-62.

Spurrell, J. C. L., S. Wiehler, R. S. Zaheer, *et al.* (2005). "Human airway epithelial cells produce IP-10 (CXCL10) in vitro and in vivo upon rhinovirus infection." Am J Physiol Lung Cell Mol Physiol **289**(1): L85-95.

Stadnyk, A. W. (1994). "Cytokine production by epithelial cells." FASEB J **8**(13): 1041-7.

Stellato, C., L. A. Beck, G. A. Gorgone, *et al.* (1995). "Expression of the chemokine RANTES by a human bronchial epithelial cell line. Modulation by cytokines and glucocorticoids." J Immunol **155**(1): 410-418.

Strauer, B. E., M. Brehm, T. Zeus, *et al.* (2001). "[Intracoronary, human autologous stem cell transplantation for myocardial regeneration following myocardial infarction]." Dtsch Med Wochenschr **126**(34-35): 932-8.

Stripp, B. R. (2008). "Hierarchical Organization of Lung Progenitor Cells: Is there An Adult Lung Tissue Stem Cell?" Proc Am Thorac Soc **5**(6): 695-698.

Stripp, B. R. and S. D. Reynolds (2008). "Maintenance and repair of the bronchiolar epithelium." Proc Am Thorac Soc **5**(3): 328-33.

Sugahara, K., J. Tokumine, K. Teruya*, et al.* (2006). "Alveolar epithelial cells: differentiation and lung injury." Respirology **11 Suppl**: S28-31.

Summer, R., D. N. Kotton, X. Sun*, et al.* (2004). "Origin and phenotype of lung side population cells." Am J Physiol Lung Cell Mol Physiol **287**(3): L477-483.

Summer, R., D. N. Kotton, X. Sun*, et al.* (2003). "Side population cells and Bcrp1 expression in lung." Am J Physiol Lung Cell Mol Physiol **285**(1): L97-104.

Ten Have-Opbroek, A. A., J. R. Benfield, J. H. van Krieken*, et al.* (1997). "The alveolar type II cell is a pluripotential stem cell in the genesis of human adenocarcinomas and squamous cell carcinomas." Histol Histopathol **12**(2): 319-36.

Terunuma, A., K. L. Jackson, V. Kapoor*, et al.* (2003). "Side Population Keratinocytes Resembling Bone Marrow Side Population Stem Cells Are Distinct From Label-Retaining Keratinocyte Stem Cells." **121**(5): 1095-1103.

Tetley, T. D. (2005). "Inflammatory cells and chronic obstructive pulmonary disease." Curr Drug Targets Inflamm Allergy **4**(6): 607-18.

Thannickal, V. J., G. B. Toews, E. S. White*, et al.* (2004). "Mechanisms of pulmonary fibrosis." Annu Rev Med **55**: 395-417.

Umemoto, T., M. Yamato, K. Nishida*, et al.* (2006). "Limbal Epithelial Side-Population Cells Have Stem Cell-Like Properties, Including Quiescent State." Stem Cells **24**(1): 86-94.

Vachier, I., G. Chiappara, Antonio M. Vignola*, et al.* (1998). "Glucocorticoid Receptors in Bronchial Epithelial Cells in Asthma." Am. J. Respir. Crit. Care Med. **158**(3): 963-970.

Van Scott, M. R., S. Hester and R. C. Boucher (1987). "Ion transport by rabbit nonciliated bronchiolar epithelial cells (Clara cells) in culture." Proceedings of the National Academy of Sciences of the United States of America **84**(15): 5496-5500.

Vaughan, M. B., R. D. Ramirez, W. E. Wright, *et al.* (2006). "A three-dimensional model of differentiation of immortalized human bronchial epithelial cells." Differentiation **74**(4): 141-148.

Velden, V. H. and H. F. Versnel (1998). "Bronchial epithelium: morphology, function and pathophysiology in asthma." Eur Cytokine Netw **9**(4): 585-97.

Viallard, J. F., J. L. Pellegrin, V. Ranchin, *et al.* (1999). "Th1 (IL-2, interferon-gamma (IFN-gamma)) and Th2 (IL-10, IL-4) cytokine production by peripheral blood mononuclear cells (PBMC) from patients with systemic lupus erythematosus (SLE)." Clin Exp Immunol **115**(1): 189-95.

Wadsworth, S., H. Nijmeh and I. A. N. Hall (2006). "Glucocorticoids Increase Repair Potential in a Novel in vitro Human Airway Epithelial Wounding Model." Journal of Clinical Immunology **26**(4): 376-387.

Wagers, A. J., R. I. Sherwood, J. L. Christensen, *et al.* (2002). "Little Evidence for Developmental Plasticity of Adult Hematopoietic Stem Cells." Science **297**(5590): 2256-2259.

Wang C. Z., E. M. J., Cox R. A., Burke A. S, Qingiyan ZHU, Herndon D. N., Barrow R. E. (1992). "Morphologic changes in basal cells during repair of tracheal epithelium." The American journal of pathology **141**(3): 753–759.

Wang, C. Z., M. J. Evans, R. A. Cox, *et al.* (1992). "Morphologic changes in basal cells during repair of tracheal epithelium." Am J Pathol **141**(3): 753-9.

Watanabe, K., K. Nishida, M. Yamato, *et al.* (2004). "Human limbal epithelium contains side population cells expressing the ATP-binding cassette transporter ABCG2." FEBS Lett **565**(1-3): 6-10.

Weiss, D. J., M. A. Berberich, Z. Borok, *et al.* (2006). "Adult Stem Cells, Lung Biology, and Lung Disease." Proc Am Thorac Soc **3**(3): 193-207.

Welm, B. E., S. B. Tepera, T. Venezia, *et al.* (2002). "Sca-1(pos) cells in the mouse mammary gland represent an enriched progenitor cell population." Dev Biol **245**(1): 42-56.

Wenzel, S. E. (2001). "The significance of the neutrophil in asthma." Clinical & Experimental Allergy Reviews **1**(2): 89-92.

Williams, M. C. (2003). "ALVEOLAR TYPE I CELLS: Molecular Phenotype and Development." Annual Review of Physiology **65**(1): 669-695.

Witherden, I. R., E. J. Vanden Bon, P. Goldstraw*, et al.* (2004). "Primary Human Alveolar Type II Epithelial Cell Chemokine Release: Effects of Cigarette Smoke and Neutrophil Elastase." Am. J. Respir. Cell Mol. Biol. **30**(4): 500-509.

Woolhouse, I. S., D. L. Bayley and R. A. Stockley (2002). "Sputum chemotactic activity in chronic obstructive pulmonary disease: effect of {alpha}1-antitrypsin deficiency and the role of leukotriene B4 and interleukin 8." Thorax **57**(8): 709-714.

Yamahara, K., S. Fukushima, S. R. Coppen*, et al.* (2008). "Heterogeneic nature of adult cardiac side population cells." Biochemical and Biophysical Research Communications **371**(4): 615-620.

Yamamoto, C., T. Yoneda, M. Yoshikawa*, et al.* (1997). "Airway inflammation in COPD assessed by sputum levels of interleukin-8." Chest **112**(2): 505-10.

Yu, F. X., J. Guo and Q. Zhang (1998). "Expression and distribution of adhesion molecule CD44 in healing corneal epithelia." Invest. Ophthalmol. Vis. Sci. **39**(5): 710-717.

Yuhgetsu, H., Y. Ohno, N. Funaguchi*, et al.* (2006). "Beneficial effects of autologous bone marrow mononuclear cell transplantation against elastase-induced emphysema in rabbits." Exp Lung Res **32**(9): 413-26.

Zahm, J. M., H. Kaplan, A. L. Herard*, et al.* (1997). "Cell migration and proliferation during the in vitro wound repair of the respiratory epithelium." Cell Motil Cytoskeleton **37**(1): 33-43.

Zepeda, M. L., M. R. Chinoy and J. M. Wilson (1995). "Characterization of stem cells in human airway capable of reconstituting a fully differentiated bronchial epithelium." Somat Cell Mol Genet **21**(1): 61-73.

Zhou, S., J. D. Schuetz, K. D. Bunting*, et al.* (2001). "The ABC transporter Bcrp1/ABCG2 is expressed in a wide variety of stem cells and is a molecular determinant of the side-population phenotype." Nat Med **7**(9): 1028-1034.

Zhu, J. I. E., Y. S. Qiu, S. Majumdar*, et al.* (2001). "Exacerbations of Bronchitis . Bronchial Eosinophilia and Gene Expression for Interleukin-4,

Interleukin-5, and Eosinophil Chemoattractants." Am. J. Respir. Crit. Care Med. **164**(1): 109-116.